Doctoral Dissertation
National Doctoral Program in
DEFENSE AGAINST NATURAL RISKS AND ECOLOGICAL TRANSITION OF THE BUILT ENVIRONMENT (38th Cycle)

Seismic assessment and strengthening of monumental masonry structures, with a particular focus on churches

Behrad Ghaffarpasand

Department of Civil Engineering and Architecture
University of Catania

Department of Civil, Chemical and Environmental Engineering
University of Genoa

This dissertation is submitted for the degree of

Doctor of Philosophy

May 2026

Supervisors:

Prof. Sergio Lagomarsino - Department of Civil, Chemical, and Environmental Engineering (DICCA), University of Genoa, Via Montallegro 1, 4 16145 Genoa, Italy

Prof. Stefania Degli Abbati - Department of Civil, Chemical, and Environmental Engineering (DICCA), University of Genoa, Via Montallegro 1, 4 16145 Genoa, Italy

Prof. Daniele Malomo - Department of Civil Engineering, McGill University, 817 Sherbrooke Street West, Montreal, QC, H3A 0C3, Canada

External Reviewers:

Prof. Gianmarco de Felice - Department of Civil Engineering, Computer Science and Aeronautical Technologies Roma Tre University, Italy

Prof. Arun Menon - Department of Civil Engineering, IIT Madras, India

Doctoral Examination Committee:

Prof. Mauro Corrado - Department of Structural, Building and Geotechnical Engineering (DISEG), Politecnico di Torino, Italy

Prof. Anastasia Athanasiou - Department of Civil and Environmental Engineering, Bauhaus-Universität Weimar, Weimar, Germany

Prof. Antonella di Luggo - Department of Architecture, University of Napoli Federico II, Naples, Italy

National Doctoral Program in
DEFENSE AGAINST NATURAL RISKS AND ECOLOGICAL TRANSITION OF THE BUILT ENVIRONMENT
XXXVIII Cycle

I hereby declare that the contents and organization of this dissertation constitute my own original work and does not compromise in any way the rights of third parties, including those relating to the security of personal data.

Behrad Ghaffarpasand Genoa, April 06, 2026

Summary

This thesis investigates the seismic assessment and strengthening of monumental masonry structures, with a particular focus on unreinforced masonry (URM) churches. It frames churches as vulnerable heritage structures due to their complex and irregular configurations, weak connections among macro-elements, and brittle materials. These characteristics lead to frequent susceptibility to out-of-plane (OOP) local mechanisms rather than a global box-like behavior. The thesis highlights key research gaps, such as the choice of an appropriate modeling strategy, the trade-off between accuracy and computational cost in analysis methods, the lack of a practitioner-oriented framework that links global and local responses, and the need for retrofit decision-support for vulnerable secondary elements.

After reviewing the available seismic assessment procedures for URM churches in the literature, the thesis adopts the Church of Nostra Signora delle Grazie e Sant'Egidio in Bussana Vecchia, Italy, as the case study. Using this case study, the thesis compares three numerical modeling strategies, namely finite element model (FEM), discrete element model (DEM), and equivalent frame model (EFM), to assess their ability in reproducing modal properties, pushover response, and damage mechanisms.

Following that comparison, the thesis proposes a practitioner-oriented seismic assessment framework that combines modal pushover analysis on a global FE model with nonlinear kinematic analysis of local mechanisms. This method is for URM churches whose behavior lies between full global behavior and full independent macro-element responses, allowing the engineers to account for both the structural interactions and post-peak local collapse development. The procedure is then applied on the case study, focusing on the OOP mechanism of façade and nave wall.

Finally, the thesis moves from the assessment problem toward retrofit design decision-support, with a particular focus on bell gables as vulnerable secondary elements. It develops a multi-objective optimization procedure to compare retrofit solutions in terms of seismic effectiveness, ductility, and implementation costs.

Overall, the draft presents a research path from vulnerability understanding, to comparative assessment of modeling strategies, to an integrated assessment framework, and finally to retrofit optimization, contributing scientifically and practically to seismic assessment of historic masonry churches.

Acknowledgment

First and foremost, I would like to express my profound gratitude to my supervisors, Prof. Sergio Lagomarsino, Prof. Stefania Degli Abbati, and Prof. Daniele Malomo, for their unwavering guidance, encouragement, and support throughout my PhD studies. Their mentorship and expertise have been invaluable in shaping my research direction and helping me to develop my skills as a researcher. I am truly grateful for the countless hours they dedicated to reading and commenting on my work, and for their constructive feedback and suggestions, which have greatly improved the quality of this thesis. Without their expert knowledge, patience, and dedication, this work would not have been possible.

My deepest thanks go to my family for their unwavering love, encouragement, and support throughout my academic journey. I would especially like to thank my parents, who have always been my biggest cheerleaders. Even during the hardships they faced, including war, they never stopped supporting me. Without their constant love and sacrifice, I would not have been able to complete this journey.

I am also grateful to my colleagues and friends for their support, feedback, and encouragement during this challenging but rewarding experience. They have provided me with a sense of community, and their feedback on my work has been instrumental in improving the quality of this thesis.

Thank you all for your support, encouragement, and inspiration.

I dedicate this work to all those who sacrificed their lives to bring light into the darkness. Their courage, sacrifice, and hope will never be forgotten.

Contents

1. Introduction and research context 1
1.1 Background 1
1.2 Research Gaps 3
1.3 Objectives and Open Issues 4
1.4 Layout of the Thesis 6
2. Seismic Assessment of Masonry Churches 8
2.1 Introduction 8
2.2 Vulnerable Elements and Post-Earthquake Seismic Behavior 9
2.1.1 Key architectural and structural features of churches 9
2.1.3 Structural vulnerabilities identified in historical churches 10
2.1.4 Structural strengthening or upgrading 14
2.3 Seismic Assessment Approaches for URM Churches 16
2.2.1 Territorial-scale assessment procedures 17
2.2.2 Local assessment procedures 32
2.2.3 Numerical approaches at the building scale 41
2.4 Conclusions 45
3. The case study of Bussana Vecchia ruined church 47
3.1 Introduction 47
3.2 Historical Background 48
3.3 The 1887 Earthquake and Observed Damage 48
3.4 Structural Features of the Church 49
3.5 Conclusions 51
4. Comparative modeling strategies for churches: EFM vs FEM vs DEM 52
4.1 Introduction 52

4.2 Basis of Adopted Numerical Models 54
4.2.1 Continuum models 54
4.2.2 Equivalent frame models 56
4.2.3 Discontinuum models 59
4.3 Cross-calibration and Comparison of Modal Response 61
4.3.1 Parameter cross-calibration and elastic alignment.....61
4.3.2 Modal comparison: MAC index 65
4.4 Comparative Seismic Analysis.....67
4.4.1 Global capacity comparison: Pushover curves 67
4.4.2 Failure mechanisms and damage patterns 72
4.5 Conclusions 85
5. A practitioner-oriented seismic assessment framework for churches (modal pushover + nonlinear kinematics).....88
5.1 Introduction 88
5.2 Review of Available Methodologies and Challenges 89
5.2.1 Open issues on modelling and analysis methods.....89
5.2.2 Overview of procedures for the seismic assessment available in the literature and codes.....92
5.3 Adopted Procedure for the Seismic Assessment of Churches and Its Field of Applicability 94
5.3.1 Decision Tree (When to Use What).....94
5.3.2 Proposed procedure.....97
5.4 Application to the Case Study: the Church of Nostra Signora delle Grazie e Sant'Egidio in Bussana 101
5.4.1 The numerical model of the church 101
5.4.2 Modal analysis and load pattern definition.....101
5.4.3 Results of the modal pushover analysis.....103
5.4.4 Integration with nonlinear kinematic analysis 105
5.5.5 Results of the seismic assessment.....108

5.5 Conclusions 111

6. Retrofit design and decision-support for vulnerable components: multi-objective optimization for bell gables 113

6.1 Introduction 113

6.2 Out-of-Plane Seismic Performance 115

6.3 Adopted Procedure and Optimization Algorithm 118

6.4 Results of the Application to Church Bell Gables 121

6.4.1 Case study description 121

6.4.2 Selection and evaluation of retrofitting scenarios 122

6.4.3 Results of nonlinear kinematic analysis and algorithm performance 124

6.5 Conclusions 127

7. Conclusions and future work 128

7.1 Main Findings of the Thesis 128

7.2 Limitations of the Research and Future Work 131

8. References 133

9. Appendix A 157

List of Figures

Figure 1: The common damage observed in past-earthquakes; a & b) the OOP response of the façade (Borri et al. 2019; Ferracuti et al. 2022), c) the collapse of the bell tower (Brandonisio et al. 2013), d & e) the OOP response of lateral walls (Penna et al. 2019; Ferracuti et al. 2022), and f) the detachment of the apse from the structure (Giresini 2016) 14

Figure 2: Seismic hazard in Liguria (MPS04, http://zonesismiche.mi.ingv.it/). The star indicates the location of the Bussana village. 49

Figure 3: Current plan, aerial, and sectional views of the Church of Nostra delle Grazie e S. Egidio (Italy) 50

Figure 4: (a) 3D FEM of the church and (b) mesh sensitivity 55

Figure 5: Adopted constitutive law for URM in FEM 56

Figure 6: (a) The 3D view of the EFM of the church, (b) The 3D view of the meshed model, (c) and (d) mesh modifications of the façade to include 3D-pier elements (red elements) 58

Figure 7: (a) The 3D view of the EFM-equivalent model, (b) Introducing boundary elements and eliminating intersections, and (c) The final DEM model of the church 60

Figure 8: Adopted constitutive law for URM in DEM 61

Figure 9: The effects of tensile strength and strain on the FEM pushover curves in the X direction 63

Figure 10: Comparison of the first four mode shapes obtained from EFM, FEM, and DEM of the church 64

Figure 11: The base shear-displacement (pushover) curves of EFM, FEM, and DEM in the a & c) X direction and b & d) Y direction. 69

Figure 12: The pushover curves in the longitudinal direction considering control nodes on the critical macro-elements 70

Figure 13: The pushover curves in the transversal direction considering control nodes on the critical macro-elements 71

Figure 14: Performance levels on the longitudinal pushover curves of FEM and DEM 74

Figure 15: Performance levels on the transversal pushover curves of FEM and DEM.....78

Figure 16: Performance levels on the +X and +Y directions of EFM 82

Figure 17: The considered mechanisms and their corresponding mode shapes 102

Figure 18: The results of the MPA based on mode 3 in terms of the a) deformed shape of the configuration, b) damage pattern, c) modal pushover curve, and d) transformed SDOF capacity curve.....104

Figure 19: The results of the MPA based on mode 7 in terms of the a) deformed shape of the configuration, b) damage pattern, c) modal pushover curve, and d) transformed SDOF capacity curve.....105

Figure 20: The a) considered block for the NLKA and b) NLKA-based capacity curve.....106

Figure 21: The a) considered block for the NLKA and b) NLKA-based capacity curve.....107

Figure 22: The final capacity curve for the blocks located at the top of the a) longitudinal wall and b) façade.....107

Figure 23: The considered point of the macro-element for calculating FRS, the modes' contribution, and the final FRS for a) the longitudinal wall and b) the façade 110

Figure 24: Comparison of the capacity curve and demand spectrum for the a & c) longitudinal wall, and b & d) façade 111

Figure 25: The effect of a) the vertical tie-rods on the capacity curve of the bell gables, b) frictional resistances on the capacity curve of the facade 116

Figure 26: The flowchart of the multi-objective hybrid NSGAII-SA algorithm 120

Figure 27: a) Schematic view of the considered bell gable; b-c) Example of a bell gable retrofitted with vertical tie-rods. 122

List of Tables

Table 1. Overview of LV1 applications to URM churches in the literature. ..20

Table 2. Overview of LV0 applications to masonry churches in the literature. 26

Table 3. Overview of DPMs applications to URM churches in the literature 29

Table 4: Overview of LV2 applications to URM churches in the literature ...34

Table 5: Overview of nonlinear kinematic analysis analysis applications to URM churches in the literature.....38

Table 6. The adopted URM mechanical properties in FEM 55

Table 7: The properties of the Mohr-Coulomb model used in DEM with linear softening constitutive law 61

Table 8: The natural periods for the first four modes of the DEM of the church 63

Table 9:The natural periods for the first four modes of EFM, FEM, and DEM and the percentage error of each model computed with respect to the mean period value for each mode. 64

Table 10: MAC matrices for FEM, DEM, and EFM (The MAC indexes are in percentage).....65

Table 11: Adopted criteria for defining performance levels in FEM, DEM, and EFM 73

Table 12: Damage and failure mechanisms at DL, SD, and NC performance levels in +X direction.....75

Table 13: Damage and failure mechanisms at DL, SD, and NC performance levels in -X direction.....76

Table 14: Damage and failure mechanisms at DL, SD, and NC performance levels in +Y direction.....79

Table 15: Damage and failure mechanisms at DL, SD, and NC performance levels in -Y direction.....80

Table 16: Damage and failure mechanisms at DL, SD, and NC performance levels of EFM in the +X direction 83

Table 17: Damage and failure mechanisms at DL, SD, and NC performance levels of EFM in the +Y direction 84

Table 18: First ten vibration modes and their periods, modal participations, and involved macro-elements 101

Table 19: The geometrical properties of the block located at the top of the wall and the results of the NLKA 106

Table 20: The geometrical properties and the NLKA results of the block located at the top of the facade 106

Table 21: Modal properties and their relative contribution to the FRS for the upper block of the longitudinal wall 109

Table 22: Modal properties and relative contribution to the FRS for the upper block of the facade 109

Table 23: The optimal retrofitting solutions for the bell gable 125

Table 24: The categories of the results and their range of variation 126

Table 25: Parameters used to calculate the PFA 126

Table 26: Evaluation of the local mechanism for each retrofitting scenario 126

Chapter 1

Introduction and research context

1.1 Background

A significant portion of the world's architectural and historical heritage were made of unreinforced masonry (URM), and churches are one of its most representative classes (De Lorenzis et al. 2007; Meoni et al. 2019). These buildings are not just constructions; they are strongly tied to the memory, identity, ritual, and collective history, making them central to the culture and continuity of local communities. Therefore, safeguarding churches against natural hazards means protecting irreplaceable historic heritage and places with high social significance, attracting the interest of several engineering practitioners and applied researchers in the last decades (Casolo et al. 2000; Lourenço 2002; Kappos et al. 2008; Lagomarsino and Cattari 2015a; Jiménez-Pacheco et al. 2022; Vuoto et al. 2022).

Among URM structures, churches have shown more seismic vulnerability than other ordinary buildings. This comes first from the nature of masonry, which is a material characterized by negligible tensile strength, brittle post-peak behavior, and low ductility. In contrast with other materials used in modern buildings, masonry is not able to sustain large inelastic deformations, and damage may progress much faster after the crack initiation, which becomes critical when masonry is subjected to cyclic horizonal loads, such as earthquakes.

Another source of vulnerability of URM churches is their historical construction methods. Most historical churches were erected before seismic codes were developed, having mostly been designed for gravity. This typically results in

the absence of seismic detailing and lack of box-behavior when subjected to horizontal loads (Lagomarsino 2012; Sorrentino et al. 2014; Penna et al. 2019; Preciado et al. 2020; Mishra et al. 2022). URM churches are also often characterized by prominent architectural and non-engineered structural features, which tend to exacerbate their seismic vulnerability: slender unrestrained components (spires, parapets, gables), spacious halls (increased non-supported length of diaphragm's members), tall columns, and flexible diaphragms. Consequently, their seismic response is seldom governed by in-plane (IP) modes. Instead, the main issue lies in the out-of-plane (OOP) failures through local mechanisms involving different macro-elements (de Felice et al. 2022b). Furthermore, irregularities in plan and elevation, often introduced by elements such as bell towers, create asymmetric mass and stiffness distribution, which can induce torsional effects and trigger progressive damage in URM churches (Penna et al. 2019; Briceño et al. 2021). The abovementioned aspects, in addition to the challenges associated with identifying the residual mechanical properties of older materials, make the structural analysis of monumental churches particularly difficult (Ciocci et al. 2018).

The consequences of this vulnerability are not limited only to structural damage. Earthquake damage to churches can be a threat to human lives through sudden brittle failures, even when the structure strength has not yet reached to its threshold of global collapse. Local OOP mechanisms can involve heavy and big portions of masonry, non-structural elements, false vaults, decorative elements, and attached components. Therefore, in the case of URM churches, it may not be sufficient to just verify their lateral capacity and resistance; it is needed to have an understanding of how local OOP mechanisms affect and govern the behavior and seismic response, how interactions among the structural elements affect OOP mechanisms, and how to take into account OOP mechanisms in the seismic verification process.

These considerations explain why the seismic assessment of URM churches, despite of extensive research available in the literature, is still a challenging task. Existing methods cover a wide spectrum, ranging from territorial, empirical, and simplified approaches to refined and detailed numerical ones. Each has advantages and disadvantages when applied to monuments and historical heritage, highlighting the need for a case-by-case trade-off between accuracy and computational cost.

1.2 Research Gaps

The first motivation of this thesis is the need to protect cultural heritage in seismic-prone areas. In European countries, particularly Italy, historical URM churches are significantly widespread and often exposed to moderate-to-high seismic hazards, as documented in the literature (Lagomarsino 2012; Sorrentino et al. 2014; Penna et al. 2019). In addition, the churches, due to having elongated structural elements, weak connections, flexible diaphragms, and irregular configurations, often show a behavior that is more complicated than other URM buildings, remaining difficult to interpret through standard methodologies. Even when recurrent damage patterns are known, predicting which macro-element will govern the response and how it will interact with the rest of the structure is not straightforward. This highlights the need for an assessment methodology and procedure more tailored to these types of URM structures.

Historically, URM churches were designed with a primary focus on vertical loads, mainly dead loads, which resulted in relatively satisfactory performance under vertical forces. Therefore, since they were erected before the development of any seismic codes, they often cannot have a satisfactory performance against horizontal loads, such as wind and seismic forces. Additionally, due to their irregular configurations and architectural/artistic features, they are hardly expected to have a box-like behavior, in which IP mechanisms are dominant. Instead, their seismic behavior is often governed by OOP local mechanisms. The local responses can also be attributed to the absence of adequate connections between various sections of the structure and insufficient bonding of materials. Unlike materials like reinforced concrete and steel, which are ductile, URM, such as brick, stone, and adobe, are characterized as brittle. Brittle materials are unable to endure loads after undergoing yielding and exhibiting plastic deformations. Consequently, they are prone to sudden, severe, and catastrophic failures. Hence, even in the case of limited structural damage, non-structural elements might suffer significant damage. This failure mechanism does not give people enough time to escape and poses a significant risk to the safety of people. Therefore, it is highly needed to evaluate the seismic behavior of URM churches with a modeling strategy that is able to capture the potential OOP mechanisms and to verify their behavior through a framework in which OOP mechanisms are taken into account.

Moreover, there is a clear need to understand the trade-off between the computational cost and the accuracy of the results in modeling the historical URM churches. Highly detailed and refined models can provide detailed representations

of the churches' behavior but, due to their high computational efforts, they can become impractical for professional purposes, especially when multiple structures are required to be evaluated. On the other hand, simpler methods are more accessible and appropriate to engineers and practitioners for their engineering practices. However, their simplifications may become critical when it comes to structures whose behavior is governed by local mechanisms and is significantly affected by the interactions among macro-elements. Therefore, it is essential to understand under what conditions each modeling strategy can be reliable and beneficial.

Another motivation of this research thesis comes from the gap between the available research tools and practitioner's routine procedures. Available codes and guidelines provide general principles for seismic assessment of heritage monumental structures. However, in order to reliably assess the URM churches' seismic behavior, relying on the codes' principle may not be sufficient, and substantial engineering judgments are still required in choosing modeling assumptions, deciding whether global or local analyses should be performed, defining the seismic demand for upper-level mechanisms, and choosing an optimal retrofitting solution compatible with both the structural safety and conservation. A practitioner-oriented framework is therefore needed: one that does not oversimplify the problem, but helps engineers to make decisions within a solid framework.

Finally, the last motivation of this thesis concerns the choice of optimal retrofitting solutions for secondary elements, such as bell gables. Due to their mass, slenderness, and elevation, these elements are prone to experiencing an OOP rocking or overturning failure. Their strengthening must be designed under budget constraints and with minimal visual impact on the structure's architecture. This makes them ideal case studies for moving from the assessment of local failures to a retrofitting decision-support method, in which the structural performance and cost can be evaluated simultaneously rather than separately.

1.3 Objectives and Open Issues

In response to the abovementioned motivations, this thesis pursues a set of objectives that reflect the progression of the research from understanding the seismic behavior, to assessing it, and then to supporting intervention choices.

The first objective is to compare different modeling strategies for evaluating the seismic behavior of URM churches. This comparison focuses on three modeling strategies: continuum Finite Element Model (FEM) and discontinuum Discrete

Element Model (DEM) as refined approaches, and Equivalent Frame Model (EFM) as a simplified approach. The goal is not simply to compare their final numerical inputs, but to evaluate their capacity in representing modal properties, stiffness distributions, pushover responses, and dominant damage mechanisms through a consistent case-study setting. Through this comparison, the thesis aims to highlight their strengths, limitations, and the field of applicability of each modeling strategy for URM churches.

The second objective is to assess whether modeling strategies that are simpler and associated with lighter computational cost than more advanced and refined models can provide reliable predictions for monumental heritage structures. This includes examining their simplifying assumptions, computational advantages, and the extent to which they can provide the key features of the seismic response. Therefore, this thesis aims to address the trade-off between the computation efficiency and the accuracy of the predictions, which is a central issue of real-world engineering applications.

The third objective is to develop an assessment procedure tailored to URM churches whose response is often dominated by local mechanisms. This objective aims to link the global modal and pushover results with local nonlinear kinematic analysis of relevant macro-elements. The purpose is to build a framework to assess the range of the behavior of URM churches that lie between a fully global box-like response and fully independent macro-elements.

Finally, the last objective is to develop a rational decision-making method for retrofitting of the secondary elements of churches, with a special focus on bell gables. The thesis investigates retrofitting solutions through a multi-objective procedure that considers three main aspects: seismic and structural efficiency, ductility, and cost. The main aim is to develop a framework for intervention selection under realistic constraints that can be used by practitioners and engineers.

These objectives can be framed into the following research questions:

Q1: How is the ability of refined and simplified modeling strategies, FEM vs. DEM vs. EFM, to predict the seismic response of URM churches, with a focus on modal properties, global capacity, and damage mechanisms?

Q2: To what extent can computationally efficient and more simplified modeling strategies provide reliable results for complex URM churches, and what modifications can be applied to them to improve their predictions?

Q3: How can a seismic assessment framework be developed for URM churches whose behavior is governed by local mechanisms but significantly affected by structural interactions?

Q4: How can a retrofit intervention be designed to improve the behavior of local mechanisms through a multi-objective approach that balances the structural efficiency, ductility, and implementation cost?

1.4 Layout of the Thesis

Following this introduction chapter, Chapter 2 reviews the seismic behavior and the available seismic assessment methodologies for URM churches. It discusses their architectural and artistic features, main vulnerability sources, recurrent observed post-earthquakes damage, and the main assessment approaches available in the literature, from territorial empirical to detailed numerical ones.

Chapter 3 introduces the case-study adopted throughout the thesis, namely the Church of Nostra Signora delle Grazie e Sant'Egidio in Bussana Vecchia, Italy. This chapter presents its historical development, structural features, and the reason for choosing this case-study as the representative benchmark for investigation.

Chapter 4 discusses the comparative seismic analysis of the Bussana church through three modeling strategies: FEM, DEM, and EFM. This chapter addresses the models' assumptions, calibration choices, and the comparison of modal properties, pushover results, and predicted damage mechanism patterns. This chapter aims to answer the question of how different modeling strategies with different assumptions can perform when applied to complex URM churches.

Chapter 5 develops the integrated practitioner-oriented seismic assessment framework that combines the modal pushover analysis with nonlinear kinematic analysis. This chapter clarifies the field of application of the proposed framework, explains the logic of combining the global and local responses, and demonstrates the method through its application on the local mechanisms of the macro-elements of the Bussana church.

Chapter 6 focuses on retrofit design and decision-support method for local mechanism of vulnerable secondary elements, with specific application on the bell gable of Bussana church. By formulating this into a multi-objective problem, this chapter addresses this problem by using multi-objective algorithms and investigates how retrofitting solutions can be compared in terms of seismic activation threshold,

their ductility, and cost, thereby discussing how the optimal solution can be selected according to available resources and budget.

Finally, Chapter 7 discusses the main findings and scientific and practical contribution of this thesis, identifies the limitations faced during the research and possible future developments in the field of seismic assessment of historical URM churches.

Chapter 2

Seismic Assessment of Masonry Churches

2.1 Introduction

URM churches constitute one of the most complex and vulnerable classes within the built cultural heritage. Unlike other types of structures with straightforward designs, churches often feature elaborate architectural elements such as tall towers, vaulted ceilings, domes, and thick walls. These features create irregular and intricate configurations that impose significant structural challenges when it comes to the assessment of their seismic behavior. This complicated configuration makes them particularly susceptible to natural hazards, such as earthquakes.

Because of this complexity, a reliable assessment requires a deep understanding of their recurrent vulnerabilities, typical failure modes, and the available procedures. Over the years, several approaches were proposed, ranging from territorial and empirical methods and simplified mechanical procedures to advanced numerical techniques. Each offers limitations and strengths depending on the scale of the analysis, the level of available data, the desired accuracy, and the objectives of the assessment.

In this context, this chapter aims to review the structural characteristics, main seismic vulnerabilities, and assessment procedures for URM churches. It first discusses the structural features that govern the behavior of churches, then examines the most recurrent seismic damage mechanisms and strengthening interventions implemented on churches and reported in the literature, and finally reviews the methods currently adopted for the seismic assessment. The main goal of this chapter is to establish a state-of-the-art that the subsequent chapters are based on.

2.2 Vulnerable Elements and Post-Earthquake Seismic Behavior

2.1.1 Key architectural and structural features of churches

Historical churches are architecturally complex URM structures characterized by large dimensions and spatial volumes, plan and height irregularities, and structural discontinuities. Their primary components are apse, façade, nave, transept, vault, and domes, and bell tower, each showing distinct behavior. These components do not typically act as a single integrated structural unit; instead, they respond individually with limited mutual interactions, a feature that has been widely documented in post-earthquake surveys, particularly following the 2009 L'Aquila (da Porto et al. 2012), 2016-2017 central Italy seismic sequence (Penna et al. 2019; Canuti et al. 2021), and the 2010–2011 Canterbury earthquake sequence (Lagomarsino et al. 2019a).

The load-bearing system of URM churches typically consists of long-span vaulted roofs and vertical elements, such as columns, pillars, buttresses, walls, and bell towers. Gravity and seismic loads are transferred from roofs as horizontal flexural/shear elements to vertical components, transferring them to the foundation (Giaretton et al. 2014; Pirchio et al. 2021b). These structures usually feature timber trusses (Dal Cin and Russo 2016), wooden roofs (Longarini et al. 2022), and different types of cross vaults (barrel, groin, and timbrel vaults) (Bertolesi et al. 2019).

Depending on regions and the availability of materials, URM churches usually were made of various materials around the world. Field surveys from Italy and Portugal show that URM churches commonly were made of various types of stone masonry, including limestones such as breccia aquilana in central Italy, and regional granites and ornamental limestones (Lioz, Black Mem Martins, and Blue Sintra) in Portugal, combined with lime-based mortars (Lourenco 2005; Foraboschi 2013; Lourenço et al. 2013; Masciotta et al. 2017; Lezzerini et al. 2019; Ramirez et al. 2019; Franchi et al. 2022; Pacheco and Cachão 2024). In New Zealand, churches were often built using natural stones, clay bricks, and timbers, and the use of reinforced concrete became mandatory after the Hawke's Bay earthquake destruction (Dizhur et al. 2011; Giaretton et al. 2014; Marotta et al. 2015). Turkish URM historical structures rely on heterogeneous stone units of variable geometry and weak mortars. For instance, URM churches in Hatay and Osmaniye were constructed using irregular cut natural stones, commonly limestones, basalt, and

other sedimentary stones (Hatır et al. 2019; Bozyigit et al. 2024; Aydınalp et al. 2025).

Across Mexico, colonial churches were frequently constructed using light-weight volcanic rounded stones immersed in lime-based mortars; this type of mixture constitutes a kind of low-strength concrete (similar to cyclopean concrete), which is lighter than normal stone masonry and has a greater tensile strength than brick masonry (Meli and Sánchez-ramírez 2007; García and Meli 2008; Peña and Chávez 2016).

URM churches also contain non-structural artistic assets, such as frescos, altars, statues, holy water fonts, and bells, which can be placed either in gables or steeples, that contribute to their cultural heritage (Pianigiani et al. 2020; Davis et al. 2024).

2.1.3 Structural vulnerabilities identified in historical churches

URM churches have a long history of being affected by seismic events all around the world, leading to identifying the most vulnerable parts and multiple phases of post-earthquake reconstruction and retrofitting. Masonry is inherently brittle and prone to cracking under tension loads and can be degraded over time due to natural aging, climate change, leading to the reducing its cohesion and integrity and increasing its vulnerability. This degradation manifests itself as cracks and voids in the walls and other parts of the structure (Lourenço et al. 2012; Briceño et al. 2021).

Systematic analyses of the damage that occurred to churches during seismic events, starting with the Friuli earthquake in 1976 in Italy (Doglioni et al. 1994) and continuing through more recent events, show that the seismic behavior of churches can be interpreted by subdividing them into architectural components known as macro-elements (e.g., facades, naves, bell towers, apses) (Lagomarsino and Podestà 2004a, b; Lagomarsino 2012; Brandonisio et al. 2013). Each of these macro-elements exhibits an independent response, and their interaction during earthquakes may increase the structural vulnerabilities (da Porto et al. 2012). This issue arises primarily because churches often lack a unified, box-like structural behavior, which leads to differential movement among components. Contributing reasons are the slenderness of walls, the absence of intermediate diaphragms, poor interlocking between macro-elements, and the presence of deformable wooden roof systems (Valente and Milani 2019; Canuti et al. 2021).

A major vulnerability in URM churches is the OOP failure of masonry walls, particularly facades and longitudinal walls. These walls frequently lack adequate connections to perpendicular walls and roof structures, making them prone to overturning during seismic events. Additionally, weak connections among structural elements hinder the development of the box-like behavior required for effective seismic response. This has been notably observed in post-earthquake surveys, including the Sant'Andrea Church in Campi Alto (Borri et al. 2019; Penna et al. 2019), San Pietro di Coppito Church (Brandonisio et al. 2013), St. Francis Church in Amatrice, St. Peter and St. Paul Church in Accumoli (Ferracuti et al. 2022), and St. Gemma Church in Goriano Sicoli (De Matteis et al. 2019a) where the façade was detached due to the lack of connections between the façade and the load-bearing walls, as well as between the façade and the roof structure.

In churches with potential OOP responses of the façade, cracks typically form vertically at the junction between the façade and the longitudinal walls. These cracks often propagate from stress points, further weakening the structure and increasing the likelihood of a full OOP failure. These cracks have been observed in the San Benedetto Abate and San Fiorentino Martire damaged by the 2012 Emilia earthquake (Valente et al. 2017). In addition, various boundary conditions imposed on facades by other components, such as bell towers or the quality of their connections with perpendicular walls or roof systems, may lead to their partial OOP response, in which the whole façade was not involved in the mechanism. This mechanism was observed in the San Silvestro Church after the 2009 L'Aquila earthquake (Brandonisio et al. 2013) and San Leonardo Limosino Church (Sorrentino et al. 2014).

In addition to OOP responses, walls are also susceptible to in-plane (IP) responses, often resulting from shear loads. This damage mechanism typically manifests as diagonal cracks across the walls. Such cracking is frequently observed in lateral walls, bell towers, and domes, especially when these elements are constructed with poor-quality masonry. During the damage survey conducted after the 2009 L'Aquila earthquake, diagonal shear cracks were noted on the bell tower of the St. Bernardino Church, the lateral walls of the St. Eusanio Church in Sant'Eusanio Forconese and the apse of the St. Massimo and Giorgio Church in L'Aquila (De Matteis et al. 2019a), on the chapel walls and vault of Church of San Juan del Hospital in Valencia, Spain (Sangiorgio et al. 2021), and on the belfries of Church of San Juan Bautista and Church of San Francisco de Asis in Mexico (Preciado et al. 2022).

Another common damage mechanism that has been seen in churches during the earthquakes is the overturning of the apse. This failure is due to the weak connection between the apse and other parts of the structure or to the presence of wide openings, leading to the propagation of shear cracks at their junction, particularly in the upper sections near the roof and side walls, where overturning forces were concentrated. A meaningful example is the case of St. Martino church in Gagliano Aterno, where the diagonal cracks, typical of this mechanism, have been surveyed (De Matteis et al. 2019a). This mechanism was also observed in Sfintii Arhangheli Church in Romania (Mosoarca et al. 2025), St. Venerio Church located at the center of Reggiolo, Italy (Giresini 2016), and San Francisco Church and Salvador basilica in Chile (Palazzi et al. 2020).

Bell towers are particularly vulnerable to seismic forces due to their slender and tall structure, which makes them prone to total or partial collapse. The height-to-base ratio and the presence of weak masonry often contribute to their instability. In the case of San Benedetto in Norcia, the collapse of the bell tower caused significant damage to the church (Penna et al. 2019) . Similarly, in the San Pietro di Coppito Church in L'Aquila, the partial collapse of the bell tower triggered the collapse of the apse roof (Brandonisio et al. 2013). When the bell tower is attached to the façade, cracks often propagate at the point of their connection, as observed in the San Pedro Apostol Church in Andahuaylillas, Peru (Briceño et al. 2021). Additionally, vertical cracks may form on the façade due to the dynamic interaction between the two structural elements, as seen in the San Silvestro Church in L'Aquila (Brandonisio et al. 2013). The crack patterns on the bell tower have also been observed in the St. Francis Church in Campli (Ferracuti et al. 2022).

For the building structure to distribute lateral pressures efficiently, especially in the event of a seismic or wind event, a rigid diaphragm is essential, resulting in making the displacements of the walls compatible. Differential movements among walls can result from flexible roof systems, such as a timber roof system, increasing the possibility of OOP wall failure and roof collapse. In addition, many churches feature vaulted ceilings over their naves and lateral naves. These vaults were highly vulnerable to collapse during seismic activity, particularly where poor connections between the vault and walls existed. During a detailed survey conducted to assess the damage to 87 churches after the 2009 Abruzzo earthquake, in and around L'Aquila, the vault mechanisms were activated in about 70% of churches, making it one of the most common damage mechanisms (Da Porto et al., 2012). In addition, the settlement of buttresses can pull the walls outward, detaching the walls from the vaults. This can make the vaults unable to transfer horizontal thrust to the walls,

increasing the vulnerability of URM churches against earthquakes. This separation was observed in Beverley Minister, a Gothic church located in the UK (Atamturktur et al. 2011).

Furthermore, many structures in regions like New Zealand have sloping roofs with raised ties rather than bottom chords. Although this design offers an open interior appeal, the insufficient counteraction of the sloped roof's thrust weakens the structure's stability. Increased pressure is applied to the walls in the absence of a bottom chord, which increases the possibility of instability and failure (Marotta et al. 2015).

The non-structural elements of churches, including artworks and decorative features, are particularly vulnerable during seismic events. These vulnerabilities arise primarily from their attachment to structural elements and the inherent fragility of their materials. Damage occurs due to poor connections and the movement of the supporting structures. For instance, frescoes, which are directly attached to the walls, are highly susceptible to detachment, cracking, or complete collapse when the supporting wall is damaged. Their bond to the wall can be easily compromised by seismic forces, leading to significant deterioration (Pianigiani et al. 2020). Another vulnerable non-structural element is false *camorcanna* vaults, which are often found in historical churches and used to replicate the appearance of traditional, heavier vaults. Their lightweight nature makes them particularly vulnerable during seismic events. In the Abbey of Holy Mary in Montesanto, the false *camorcanna* vaults were among the most vulnerable elements observed during the post-earthquake inspection. They exhibited significant cracks and damage during the seismic events, highlighting their susceptibility to even moderate seismic forces (Ferracuti et al. 2022).

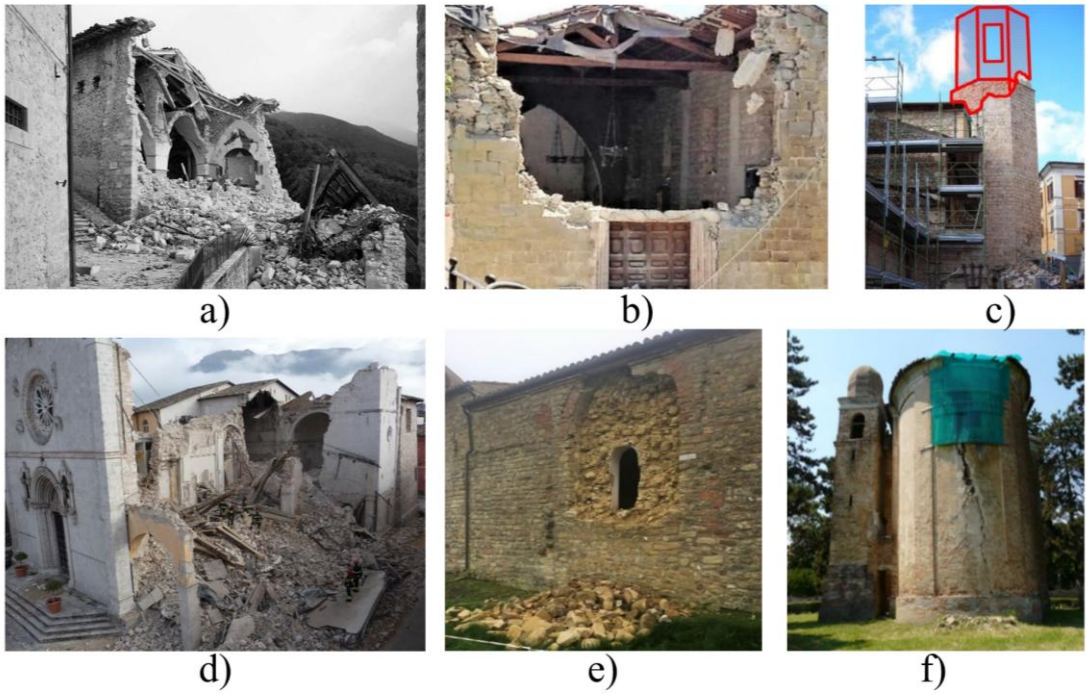

Figure 1: The common damage observed in past-earthquakes; a & b) the OOP response of the façade (Borri et al. 2019; Ferracuti et al. 2022), c) the collapse of the bell tower (Brandonisio et al. 2013), d & e) the OOP response of lateral walls (Penna et al. 2019; Ferracuti et al. 2022), and f) the detachment of the apse from the structure (Giresini 2016)

2.1.4 Structural strengthening or upgrading

The main aim of seismic retrofitting and strengthening of URM structures is to increase their load-carrying capacity and delay collapse under strong and significant external loadings, such as earthquakes. Based on the available literature, it has three main concepts: i) improving structural integrity, ii) reducing seismic demands, and iii) upgrading the existing building (Wang et al. 2018; Yavartanoo and Kang 2022; FathiAzar et al. 2024). Additionally, designing a strengthening intervention for URM structures must follow a hierarchy, as neglecting it not only can cause the designed intervention unfunctional, but also can introduce new modes of failure. In other words, designing interventions to improve the connections among macro-elements, without increasing the quality and integrity of masonry assemblage, would not be fruitful; while implementing interventions to increase the capacity of structural elements would not be helpful, if the connections of the structure were poor (Vlachakis et al. 2020).

However, there are some limitations when historical URM structures are considered, such as churches. First, their conception and architectural/artistic

features must be preserved and not altered during the implementation of retrofitting interventions. The new material for repair has to be compatible with the original material in terms of chemical, physical and mechanical properties, and the designed strengthening system has to be reversible, allowing it to be replaced without causing severe damage to the original structure, and be durable according to the life time of the monument (Valluzzi et al. 2014; Yavartanoo and Kang 2022).

The earthquake-affected churches have undergone several structural strengthening interventions, primarily aimed at enhancing their seismic resistance and addressing vulnerabilities identified during previous seismic events. In order to improve the local and global responses of churches and increase their integrity, ensuring a box-like behavior, reinforced concrete horizontal and vertical elements, known as constructional columns and ring beams, can be used to confine masonry walls at all corners and intersections. This method can increase the strength of the structure in both IP and OOP directions and improve the lateral deformation and energy dissipation (Borri et al. 2009; Okail et al. 2016).

Other retrofitting interventions aiming to increase the integrity of structures and the exhibition of box-like behavior are: injecting Epoxy resin and cement-based grout to enhance flexural and tensile strength of URM materials and fill of the voids and cracks, implemented on the church of Santiago located in the city of Jerez de la Frontera, Spain (Mayorga et al. 2018), the church of Saint George of the Bârnova Monastery located in Iasi, Romania (Onutu et al. 2024), the medieval church of Tazlau Monastery in Piatra Neamt, Romania (Spiridon et al. 2023), and the church of Panaghia Krena in Chios island, Greece (Miltiadou-fezans et al. 2024). Implementing steel tie-rods strengthens the masonry walls' lateral stability and prevents them from OOP overturning, applied on the Parrocchia S. Nicolò and Chiesa parrocchiale S. Pietro, located in Novi Ligure Municipality (Ruggieri et al. 2022), and the Cathedral of Parma in Italy (Coïsson et al. 2019). Steel tie-rods can also be used to prevent the thrust of the roof in the cases in which the roof structures do not have a bottom chord, as it can be observed in St Luke’s located in Wellington, New Zealand (Marotta et al. 2015).

Additionally, “ties” can be also implemented to increase the IP strength of different URM macro-elements. For example, steel bars embedded within the masonry of the Santa Maria delle Grazie sanctuary in Amatrice to fortify the façade and improve its IP resistance to seismic forces (Penna et al. 2019), and wooden ties were arranged continuously throughout the perimeter of the church of S. Biagio D’Amiterno damaged by the 2009 Aquila earthquake (Cianchino et al. 2023).

Reinforcing the roof by replacing timber structures with reinforced concrete is often used to improve the transverse response of buildings, as it provides better anchorage for the masonry walls. However, this approach also increases the overall mass of the structure, which can alter its behavior. For example, this method was applied to the Santa Rita Church in Norcia. While it successfully prevented the lateral failure of the longitudinal walls, the gable on the façade still collapsed (Penna et al., 2019). A similar intervention was used on the St. Salvatore Church in Acquapagana. However, during the 1997 Umbria-Marche earthquake, the increased stiffness of the concrete roof contributed to additional damage. Specifically, the roof pounded against the masonry walls, causing localized damage to the upper parts of the lateral walls and buttresses (Sferrazza Papa & Silva, 2018). Despite this, the relatively strong connections between the walls, along with the presence of buttresses, helped prevent a complete out-of-plane collapse of the lateral walls.

Another commonly used intervention, due to its low cost and the benefit of preserving the architectural appearance of churches, is grout or epoxy resin injection. This technique improves the mechanical properties of masonry, reduces the percentage of voids, and increases the IP strength of the masonry elements. It is particularly effective for addressing extensive cracks in masonry caused by earthquake activity, and it is frequently adopted in many cases. Examples of this intervention can be observed in the Oratorio Via Castello, located in Monleale Municipality, and the Santi Ruffino e Venanzio Church in Sarezzano Municipality (Ruggieri et al., 2022). Moreover, the epoxy resin has been injected to fill the cracks that have been propagated at the connection of the bell tower to the façade in the San Benedetto Abate church in Northern Italy (Valente et al., 2017).

2.3 Seismic Assessment Approaches for URM Churches

Churches are not just buildings; they carry deep cultural, historical, and social values, representing generations of heritage and identity. As discussed in the previous section, they face challenges during earthquakes. Due to their age, complex configurations, and the nature of the material they were made of, they are more vulnerable to earthquakes than ordinary buildings. Unlike modern and residential buildings, churches often feature unreinforced masonry, tall naves, complex vaults, and large components, which make them more susceptible to earthquakes. Therefore, preserving these structures for the public safety requires a deep understanding of how they may respond to seismic forces.

Seismic assessment of churches is not straightforward, since there are a lot of approaches in the literature considering various scales and levels of detail. This

review breaks down three main approaches to seismic assessment, each tackling a different purpose of the risk assessment (D'Altri et al. 2020):

1. **Empirical Assessment at a territorial scale:** Assessment at a large scale uses empirical data, such as historical earthquake damage records and regional seismic patterns, to evaluate vulnerability across a group of churches in a specific area. These large-scale approaches aim to identify the structures that are more vulnerable and need more attention, assessing policymakers in prioritizing resources and interventions at the regional scale.
2. **Simplified Mechanical and Statistical models:** Simplified approaches are useful for a having preliminary vulnerability assessment without requiring detailed, structured data. These models approximate the mechanical and statistical properties to assess failure mechanisms observed in churches, offering an efficient method of risk evaluation for a broad range of structures.
3. **Numerical Approaches at the structure level:** Numerical models, such as finite element models, provide a highly detailed assessment of structures. These approaches assist engineers in simulating a unique configuration of each case and assessing the response of each of them against seismic forces. These models require detailed structural data to simulate different parts of the churches, such as vaults, naves, façades, and lateral walls. They are more computationally demanding, but provide an accurate representation of the structural behavior.

By exploring these three types of assessments, this review aims to present a comprehensive framework that addresses both the broad regional needs and the specific, detailed requirements of individual church structures. Each approach offers unique insights, and together, they form a multi-scale methodology essential for preserving these irreplaceable heritage structures while mitigating their seismic risk effectively.

2.2.1 Territorial-scale assessment procedures

Territorial-scale methods and assessments are based on post-earthquake damage observations, qualitative data, and statistical analysis of the selected parameters. In the last decades, these methods received wide interest within the engineering community because they can be applied on a regional scale to a large number of structures, providing a broad perspective on structural vulnerability. The results obtained with these methods are nevertheless quite imprecise, mainly due to

the qualitative nature of the input data and to the problem of homogeneous classification for different kinds of structures. Finally, the observations of damage created by past earthquakes are often incomplete because they refer only to regions where seismic events took place in previous times; hence, they represent only part of the view about vulnerability in wider areas (Rosti et al. 2021; Puncello and Caprili 2023).

Among the available approaches, the main focus of this thesis is on (i) the LV1 method proposed by the Italian code, (ii) the LV0 method, and (iii) Damage Probability Matrices.

The mentioned approaches are among the score methods. These methods include techniques of evaluation where numerical values are assigned to predetermined specific attributes or criteria, which are means of assessing complex processes. This is indeed a structured approach to seismic assessment in churches regarding risk and vulnerability by considering scoring within various influencing factors. These scores are then aggregated to provide an overall risk or vulnerability rating, thus making the comparison of multiple structures possible. Three popular score methodologies currently exist in this domain, which provide a standardized procedure to prioritize buildings for retrofitting or further investigation based on their seismic risk profile.

2.2.1.1 LV1 Method

The Italian Directive for seismic risk assessment of cultural heritage (Decree of the Italian Prime Minister, 2011) proposes a multilevel framework for assessing the seismic vulnerability of existing masonry structures, organized into Levels of Valuation (LVs). Each level progressively requires more detailed information and resources. In particular, the simplest level, LV1, is dedicated to large-scale territorial assessments and enables the rapid evaluation of seismic vulnerability across a wide range of structures. This approach associates the ground motion intensities to the limit states with a vulnerability index, which requires only in-situ visual inspections to provide a broad yet effective measure of seismic risk.

LV1 is a mechanism-oriented survey in which 28 potential response mechanisms representative of the most recurrent collapse mechanisms observed in churches are considered. For each mechanism of k, LV1 assigns i) a weight ρ_k which defines the relative importance of that mechanism, ii) a vulnerability score v_{ki}, and iii) a protection score v_{kp} accounting for seismic mitigation devices, such

as tie-rods and buttresses. These terms are aggregated into a vulnerability index (Equation 1).

$$i_v = \frac{\sum_{k=1}^{28} \rho_k \left(v_{ki} - v_{kp}\right)}{6 \sum_{k=1}^{28} \rho_k} + {}^1/_2 \quad (1)$$

Once the vulnerability index is determined, the seismic capacity of the church in terms of the ground motion acceleration corresponding to the Life Safety Limit State (LSLS) is estimated through the Equation 2. A safety index is then defined as the ratio of the structure's capacity to the expected demand (Equation 3).

$$a_{g(LSLS)} = 0.025 \times 1.8^{5.1-3.44 i_v} \quad (2)$$

$$f_{a(LSLS)} = \frac{a_{g(LSLS)}}{a^*_{g(LSLS)}} \quad (3)$$

Values lower than one indicate insufficient safety under the corresponding demand and therefore have higher priorities for deeper assessment.

The practical application of the LV1 method on the seismic assessment of churches can be found in the literature. For instance, Diana et al. (2023) applied LV1 on 20 churches located in Vaud and Valais Cantons in Switzerland and 12 churches in the city of Teramo, Italy, incorporating the anti-seismic devices and reporting that a small subset of churches satisfied the LV1 safety check. In a more detailed comparative study, D'Amato et al. (2019) applied the LV1 on the Matera Cathedral (SS Maria della Bruna of Matera) and four other similar churches located in the UNESCO "Sassi of Matera." The vulnerability indices were computed for all the case studies and reported values range between 0.44-0.68. This study also compared LV1 with other simplified methods, called LV0, and a more refined method (LV2) and observed that simplified methods may overestimate the seismic performance of churches. They are useful for prioritizing and ranking, but cannot be adopted for detailed assessment and retrofit design.

Given the presence of significant numbers of LV1 applications in the literature, Table 1 reports the reviewed studies in terms of data scale and level, and the principal takeaways of this method reported by the authors.

Table 1. Overview of LV1 applications to URM churches in the literature.

References	Country/Region	Churches	Overall configurations	Data level	Most critical churches	Main takeaway/ limitation
(Onescu et al. 2025)	Romania — Banat region	6 Orthodox churches	Representative Banat Orthodox type: single central nave, rectangular plan, one bell tower centrally on main façade, rounded sanctuary/apse; massive brick/mixed masonry walls; vaults (brick or lightweight false-vault wood/plasterboard); wooden spire + pitched timber roof.	Rapid visual	Holy Spirit Descent Church (CENAD): brick masonry (70–75 cm); wooden barrel false vault with lunettes; central façade bell tower; cracks on walls + damaged plaster/paintings.	Romanian framework simpler; fewer mechanisms, lower predicted damage
(Lo Monaco et al. 2023)	Romania — Banat region (Timiș & Caraș-Severin counties)	6	Typological configuration: rectangular simple plan; single nave; barrel vaults + arches; bell tower centrally incorporated into the main façade; gable/Dutch roof recurrent; Orthodox internal sequence; material: brick	Rapid visual	Holy Spirit Descent church (Cenad) — same typology: single vaulted nave + bell tower integrated in façade.	LV1 is screening only; local mechanisms vary case-by-case.
(Mishra et al. 2022)	India — Odisha (Bhubaneswar & Cuttack twin cities)	5	Mixed typologies; explicitly described cases include masonry churches with pitched roof, buttresses, and bell tower, and a cruciform-plan church; one RC pro-cathedral with non-structural dome	Rapid visual	Church of Epiphany (Cuttack). Masonry; timber truss + madras terrace roofing, pitched roof, buttresses all around, bell tower, later-added RC narthex.	LV1 just ranks churches from rapid visual surveys
(Formisano et al. 2022)	Italy — Ischia Island (Naples gulf) and Teramo district (Central Italy)	22 total (10 Ischia + 12 Teramo)	Ischia sample: single-nave with arches + bell tower; or three internal naves + barrel vault/dome + bell tower; frequent tuff/lava masonry. Teramo sample: mostly single nave with timber trusses/gable roof, sometimes bell tower; some cases with cross vaults / transept / chapels	Rapid visual	St. Michael Archangel; tuff masonry; spherical dome; arches; transept; presbytery with domed roof. St. Lucas; unworked stone + brick fragments; single nave; timber truss roof.	LV1 correlates with damage; yet underestimate the seismic behavior.

References	Country/Region	Churches	Overall configurations	Data level	Most critical churches	Main takeaway/ limitation
(Ruggieri et al. 2022)	Italy — Piemonte (Valle Scrivia earthquake area; Province of Alessandria)	90	One-nave sample: mostly "Basilica" (≈80%), remainder Latin-cross (≈20%); few façade openings; apse present in ≈80% (circular/rectangular); bell tower in ≈70%; hut-shaped façade frequent; wooden roofs frequent (various typologies).	Rapid visual	Parrocchia SS. Antonio e Fermo, Gavi; Configuration consistent with one-nave typology (basilica/Latin-cross subset; apse + frequent bell tower)	
(Fazzi et al. 2021)	Italy — Abruzzo	11 basilica churches	Typology: rectangular body with nave + aisles separated by columns/piers and arches; mainly timber truss roofs, with a few vaulted/domed; façades often gabled/salient/crowned; bell elements vary (isolated/enclosed/bell gable).	Rapid visual + drawings/survey	S. Eusanio Martire (SEU). Configuration (from typology table): stone basilica, barrel-vaulted nave, circular dome, crowned façade, bell gable; aisles with timber/truss-type covering. Façade and apse as governing macro-elements.	LV1 used for identifying critical macro-elements
(Pirchio et al. 2021a)	Italy — Trentino, Alto Adige, Veneto, Toscana, Umbria, Lazio, Campania	72 URM churches	Broad typological spread; single-nave majority (59.8%); plan classes include single nave / basilica / Latin cross; vaulting classes: none / partial / fully vaulted	Rapid visual (+basic geometry/condition survey)	Church #33 (Toscana: "Santa Croce", Abbadia San Salvatore).	
(Betti et al. 2021)	Italy — Tuscany	13 churches	Mixed Romanesque/Basilica layouts; many single- or three-nave churches; frequent timber roofs; apses common; bell towers often present	Rapid visual	San Lorenzo a Baldigliano. Single nave, one apse; bell tower (~12 m) on left side partly enclosed; timber roof; apse with brick spherical vault; squared stone masonry.	LV1 outcomes depend on subjective scoring
(Sangiorgio et al. 2021)	Spain — Valencia Italy — Tuscany	8 churches	Single-nave Gothic churches with cross vaults/chapels; Latin-cross cathedrals with transepts; cases with domes and bell towers; Siena cathedral: Latin-cross with multiple naves/transept and cross vaults	Rapid visual + documentation	Basilica of Santa María (Elche) — Latin cross, single nave + side chapels, large dome/cross vaults; issues include façade in-plane + shear in lateral walls/chapels, few anti-seismic devices.	LV1 ignores intangible aspects

References	Country/Region	Churches	Overall configurations	Data level	Most critical churches	Main takeaway/ limitation
(Salzano et al. 2022)	Italy — Ischia Island (Casamicciola Terme, Forio, Lacco Ameno)	21	one-nave churches (4 typological variants: simple / with dome / with dome+bell tower / with bell tower)	Rapid visual (A-DC + GNDT forms	Most critical at LSLS: SPB (San Pasquale Baylon, Casamicciola Terme) + SRPM (San Rocco Pio Monte), CDA (Congrega dell'Assunta), BSR (Basilica Santa Restituta) — all in Lacco Ameno. For BSR, authors explicitly link high iv to large façade openings and high wall slenderness.	LV1 is independent of the direction; only depends on iv
(Fuentes et al. 2021)	Mexico — Oaxaca; Estado de México; Morelos	40 churches (out of 60)	Colonial typologies: mostly one rectangular nave + choir + presbytery/apse; simple façade; 1–2 bell towers or bell-gable; barrel vaults with buttresses; in Central Mexico also Latin-cross with dome over transept.	Rapid visual (A-DC form)	"IGLESIA ASUNCIÓN IXTALTEPEC" Configuration: consistent with dominant colonial type (one-nave + choir + bell element; vaulted/buttressed system).	LV1 requires complete data; missing inputs prevent iv evaluation
(De Matteis et al. 2020)	Italy — Campania, Caserta District	30 churches	Two main typologies: one-nave complex (single nave + lateral chapels) and three-nave (central nave + two aisles); layouts mostly basilica (63%) and Latin-cross (37%)	Rapid visual	Annunziata Sanctuary in Dragoni. Configuration: Latin-cross with transept + apse; thrusting roof system with barrel vaults + lunettes and dome at crossing.	iv varies in a small range for homogeneous samples
(D'Amato et al. 2018)	Italy — Matera (Basilicata)	5 churches	Plan: one-nave and three-naves. Roof: calcarenite vaulted and mixed with wood trusses in central nave.	Visual and geometic survey	San Francesco d'Assisi: one-nave church with timber truss in main nave; façade noted as affected by significant erosion	LV1 may not be conservative with respect to more detailed approaches

References	Country/Region	Churches	Overall configurations	Data level	Most critical churches	Main takeaway/ limitation
(Fuentes et al. 2019)	Italy: Matera. Chile: Calama (Chiu Chiu) + Valparaíso	3	Sant'Agostino (Matera): one-nave basilica plan; calcarenite masonry; limestone vaults. San Francisco de Chiu Chiu (Calama): one-nave basilica plan with chapels+towers; adobe; timber "par y nudillo" roof. San Francisco Barón (Valparaíso): three-nave; adobe with brick façade; wooden columns + roofing.	Visual survey	San Francisco Barón	depends on input/assumptions
(De Matteis et al. 2019b)	Italy — Abruzzi	64 churches	Three-nave churches; includes: Medieval simple timber-truss churches (LV), Post-Medieval complex with apses/transepts/vaults/domes (MV), and "Hybrid" reconstructed churches (HV)	Rapid visual	Ss. Nicandro e Marciano (SNM), Roio Piano (L'Aquila)Configuration: basilica layout without transept and apse; thin vaults in central nave; rubble-stone masonry; fragility indicators include concrete ring beams on lateral walls; few anti-seismic devices	
(Diana et al. 2017)	Switzerland — Sion (Canton Valais)	1 church	Cruciform plan; 3-bay nave + two aisles; cross vaults; raised apse; surrounding chapels; massive west bell tower; stone masonry; buttresses + metal rods; timber+slate roof over vaults	Rapid visual	Sion Cathedral: Apse roof elements; belfry; apse overturning	Key mechanisms identified by LV1 may be uncertain

Across Table 1, LV1 is primarily used for territorial screenings and prioritizations, rather than a framework for retrofitting design. However, the literature reports different LV1 outcomes; some papers only calculate the vulnerability index (Eq. 1) (Fazzi et al. 2021; Pirchio et al. 2021a; Sangiorgio et al. 2021; Mishra et al. 2022), while others convert this index into a safety (capacity/demand) factor (Eq. 3) (Diana et al. 2017, 2023; D'Amato et al. 2018, 2019; Formisano et al. 2022; Salzano et al. 2022). Thus, ranking based on

vulnerability indices may differ from the ones based on safety factors, since f_a strongly depends on the seismic hazard level (Betti et al. 2021). This can be highlighted when LV1 is applied to a homogeneous set of churches, since it is more likely that their vulnerabilities are similar, resulting in relatively similar values of a_g (Eq. 2) and a clustered i_v (De Matteis et al. 2020; Betti et al. 2021). In these situations and cases that rank based on safety factors, the level of the seismic hazard becomes dominant in the ranking processes, and LV1 behaves more like a risk screening rather than a tool ranking structures just based on their vulnerabilities.

Additionally, subjectivity and data completeness are two constraints. LV1 depends on rapid visual screening of vulnerabilities and anti-seismic devices, where operator judgments become crucial in scoring them. Pirchio et al. (2021a) adopted a conservative approach by considering best (maximum i_v) and worst (minimum i_v) scenarios for macro-elements, whose some attributes are not certain or unobservable. Fuentes et al. (2021) show that the application of LV1 can be limited when required inputs are not complete. Although a larger group of churches was surveyed, the vulnerability index can be calculated for only a subset when the data is incomplete.

Additional drawbacks reported in the literature include: (i) LV1 framework was developed according to Italian churches typologies, therefore, beyond Italy, macro-element sets, weights, survey forms, and data availability may differ, highlighting the needs of local calibration and validation (Fuentes et al. 2021; Mishra et al. 2022; Onescu et al. 2025), (ii) even when LV1 outcomes show a relatively good correlation with the surveyed damage, it still can underestimate the seismic behavior when the results are interpreted at a global scale, without verification through more refined approaches (D'Amato et al. 2018; Formisano et al. 2022; Lo Monaco et al. 2023), (iii) the standard LV1 does not consider the artistic and architectural aspects and values of churches, which motivates extensions that include them (Sangiorgio et al. 2021), and (iv) LV1 neglects the direction because it aggregates the vulnerabilities into a scalar value (Salzano et al. 2022).

While LV1 represents a more structured, score-based approach to estimate vulnerabilities for a large number of heritage structures, a simpler score-based method was also proposed in the literature—known as LV0.

2.2.1.2 LV0 Method

LV0 is a qualitative assessment methodology developed to provide a rapid overview of the seismic risk of churches, and is therefore useful to prioritize

structures for more detailed analyses in the future, without requiring on-site inspections. The approach was originally proposed by Dìaz (2016) and subsequently validated in the context of church assessment studies (D'Amato et al. 2018; Fuentes et al. 2019), where it was explicitly named "Level of Valuation 0" consistent with the Italian Directive's multi-level philosophy.

LV0 expresses risk through assigning scores to three components: hazard (H), exposure (E), and vulnerability (V). The risk score is calculated using Eq. 4.

$$R = H \times E \times V \tag{4}$$

There are three tools for assigning scores to these parameters:

- **Tool 1 (Exposure, E):** scores cultural value using conservation documents and classification systems related to the cultural significance of the site.
- **Tool 2 (Hazard, H):** assigns a hazard score based on various threats according to hazard maps. These threats can be categorized into sporadic events, such as seismic events, and continuous processes, such as rainfall erosions.
- **Tool 3 (Vulnerability, V):** assigns a seismic vulnerability score by evaluating 13 factors related to the structures' location and features. These parameters are categorized into four vulnerability classes (A, B, C, and D) based on their influence on the vulnerability of the considered structure.

The simplified form of LV0 can also be used by neglecting the exposure value, and Eq. 4 can be rewritten as follows:

$$R = (H + 1) \times V \tag{5}$$

Therefore, the risk ranking depends on Tool 2 and Tool 3 scores.

The output of LV0 is a dimensionless score, R, used for ranking churches in a portfolio region. A higher value of R indicates poorer expected performance and, subsequently, higher priority for more detailed assessments. Table 2 reports the studies that applied LV0 to a number of churches in different regions.

Table 2. Overview of LV0 applications to masonry churches in the literature.

References	Country/Region	Churches	Main purpose	Data input	Main limitation
(Lo Monaco et al. 2026)	Italy – Matera; Romania – Belinț; Bencecu de Jos; Cenad; Chizătau	8 churches	Wide-area LV0_E screening for cross-country comparison	Online large-scale maps/reports	Class results weakly differentiate; higher levels needed.
(Lo Monaco et al. 2023)	Romania – Cenad; Chizătau; Bocșa; Bencecu de Jos; Beregsău Mare; Belinț	6 Romanian Orthodox masonry churches	Pre-screening and prioritisation; define a risk-based ranking to guide LV1–LV3 effort	Existing documents	LV0 quickly ranks churches by combining hazard and vulnerability; qualitative scoring cannot resolve directionality or local failure mechanisms.
(Onescu et al. 2025)	Romania – Cenad; Chizătau; Bocșa; Bencecu de Jos; Beregsău Mare; Belinț	6 churches	make informed decisions and prioritize resources	Visual and on-site observations	Good correlation with LV1
(Formisano et al. 2022)	Italy – Teramo, Ischia Island	22 churches	Comparison and screening	Rapid visual survey	LV0 is fast and versatile but should be used only for preliminary ranking, since refined methods remain needed for intervention design
(Fuentes et al. 2019)	Italy – Matera; Chile – Calama	3 churches	Rapid pre-screening to set intervention priorities;	Threats from territorial-planning documents; Vulnerability from GNDT form; qualitative scoring	LV0 combines multi-threat hazard and building vulnerability to rank churches quickly; results depend on expert scoring and simplified threat selection.
(D'Amato et al. 2019)	Italy – Matera	5 churches	Rapid pre-screening / ranking at territorial scale; compare with LV1 and LV2	Visual and geometric surveys; original drawings; hazard and threats from published maps (e.g., "Italian Risk Map/Carta del Rischio")	LV0 enables fast comparative ranking of churches with limited data; simplified methods can overestimate real seismic performance versus refined analyses.
(Fabbrocino et al. 2019)	Italy – Teramo and Ischia	22 churches	Large-scale pre-screening; rank priorities; compare territories	Physical observations and historical research	Ignores cumulative damage from seismic sequences; ranking may shift.

LV0 applications in the literature consistently indicate that the main purpose of this method is to use a dimensionless score, R, to prioritize and organize a portfolio of churches and allocate resources for more refined assessments. This is evident both in Italian territorial studies, where LV0 is used for rapid ranking at the regional scale, and in Romanian studies, where it is explicitly applied as a pre-screening to guide subsequent multi-level assessments. A further takeaway is that LV0 can be implemented using diverse input sources, such as on-site surveys, existing documents, and online large-scale maps, making it a feasible method when detailed data are limited (Formisano et al. 2022; Lo Monaco et al. 2023, 2026).

At the same time, Table 2 highlights some limitations that should be considered when interpreting the results of LV0 applications. The main limitation is that LV0

is a qualitative score-based method whose results strongly depend on assessor judgments, especially when scores are derived from documents and maps. Secondly, LV0 cannot take into account directionality and identify critical macro-elements, highlighting the need for more refined assessment methods (Formisano et al. 2022; Lo Monaco et al. 2023). Third, the ranking results of LV0 may be different from the methods estimating the vulnerability by scoring 28 mechanisms (A-DC form and LV1), since it incorporates additional parameters (e.g., conservation state, environmental alterations, fire vulnerability) beyond seismic and structural variables (Formisano et al. 2022). Finally, LV0 neglects cumulative damage caused by seismic sequences, influencing the vulnerability of the studied structures and may vary the risk ranking. This is more evident for the LV0 method, since, contrary to other rapid assessment methods that are based on post-earthquake data, it supports territorial assessment before a real seismic event happens (Fabbrocino et al. 2019).

2.2.1.3 Damage Probability Matrices

Damage Probability Matrices (DPMs) are empirical vulnerability tools that describes, for a given seismic intensity, the probability distribution of damage grades for a set of structures. They link observed post-earthquake damage to a seismic intensity measure (macroseismic intensity or PGA), providing a basis for regional screening and vulnerability assessment of structures with similar characteristics, including URM churches.

In this method, as other score methods discussed before, a damage index is estimated by giving scores to the observed damage of each macro-element. These scores range from 0, meaning no damage, to 5, meaning complete collapse, and are used to quantify the severity of damage. In the literature, there are two ways for estimating the damage index: (i) an unweighted approach (Cescatti et al. 2020; Sisti et al. 2023b) and (ii) a weighted approach (De Matteis et al. 2016; Marotta et al. 2018; Lagomarsino et al. 2019a).

The unweighted approach considers all the macro-elements of a church equally important, and the damage index is calculated through a simple average of their assigned scores.

$$i_d = \frac{1}{5}\frac{\sum_{j=1}^{n} d_{k,j}}{n} \tag{6}$$

The weighted approach considers a weighting factor ($\rho_{k,i}$) to reflect a relative importance of different macro-elements. Higher weights are assigned to the more critical elements, such as bell towers.

$$i_d = \frac{1}{5}\frac{\sum_{k=1}^{28}\rho_{k,i}d_{k,i}}{\sum_{k=1}^{28}\rho_{k,i}} \tag{7}$$

All 28 potential mechanisms that may occur in churches are included in the weighted approach, while only the activated ones are involved in the unweighted approach. This means that the damage index obtained from the unweighted approach mainly focuses on damaged macro-elements. In contrast, the damage index derived from the weighted approach provides a more global picture of the overall seismic performance of the structure, since both the damaged and undamaged elements are included. Therefore, the weighted approach tends to yield a lower value for the damage index than the unweighted one.

The damage index is then converted to six damage levels (D) of the European Microseismic Scale (EMS98 scale) according to thresholds proposed by Lagomarsino and Podestà (2004b), and a binomial probability density function (BPDF) is used to calculate the probability of a damage level of k using the following equation:

$$p_k = \frac{5!}{k!\,(5-k)!}\left(\frac{\mu_d}{5}\right)^k\left(1-\frac{\mu_d}{5}\right)^{5-k} \tag{8}$$

Where μ_d is the mean damage level and is calculated using the following equation:

$$\mu_d = \frac{\sum_{i=1}^{n} D_{k,i}}{n} \tag{9}$$

The output of a DPM is the probability of reaching a structure to a specific damage grade for a given intensity measure. This is particularly useful for territorial assessments, since it enables damage scenario estimation for a set of churches exposed to a range of seismic intensities. Table 3 is the list of the reviewed studies that used DPMs for vulnerability assessment and scenario predictions.

Table 3. Overview of DPMs applications to URM churches in the literature

References	Earthquake / dataset	Churches	Intensity measure	Main purpose	Main takeaway/ limitation
(Sisti et al. 2023b)	Central Italy, Italy	2870	PGA	fragility derivation	Location-dependent data yield few high-PGA cases, weakening the reliability of fragility curves.
(Sisti et al. 2023a)	Central Italy, Italy	2884	PGA	fragility derivation, comparison	Wide database supports DPM for multi-level fragikity derivation
(Ceroni et al. 2022)	Central Italy, Italy	633	MCS, PGA	fragility derivation	mechanism-level DPMs extend global damage analysis
(Salzano et al. 2022)	Ischia Island, Italy	27	EMS	mean-damage prediction	Small sample; intensity uncertainty weakens DPM reliability
(Ruggieri et al. 2022)	Valle Scrivia 2003, Italy	90 one-nave	IMCS, PGA	scenario, vulnerability fitting	Low-damage sample weakens DPM–BPDF matching
(Mishra et al. 2022)	Bhubaneswar–Cuttack, India	4	MSK/EMS-based	future-damage prediction	Very small sample; predictive DPM only
(Canuti et al. 2021)	Central Italy 2016, Italy	541	MCS, PGA	scenario, vulnerability fitting, comparison	DPMs fit well at global and mechanism scale
(Fuentes et al. 2021)	Mexico 2017, Mexico	60	IMM, PGA	scenario, prediction	Preliminary damaged sample; surveys should include undamaged churches
(Cescatti et al. 2020)	Central Italy, Italy	889	MCS, PGA	fragility derivation	Large sample; limited data weakens DPM reliability
(Palazzi et al. 2020)	Maule 2010, Chile	106	PGA	fragility derivation, local and global DPMs	Whole heterogeneous sample used; insufficient data for typology-specific DPMs

References	Earthquake / dataset	Churches	Intensity measure	Main purpose	Main takeaway/ limitation
(De Matteis and Zizi 2019a)	Central Italy, Italy	68	MCS, PGA	predictive-model comparison	PGA fits the observed DPMs of non-homogeneous classes better; MCS may double-count vulnerability
(De Matteis et al. 2019a)	L'Aquila, Italy	64	MCS	scenario prediction	Binomial DPM depends only on mean damage
(De Matteis and Zizi 2019b)	Central Italy, Italy	68	MCS, PGA	predictive-model comparison	PGA fits non-homogeneous classes better than MCS
(De Matteis et al. 2019b)	L'Aquila 2009, Italy	64	MCS	calibration, prediction, fragility derivation	Good DPM fit mainly at higher intensities; low-intensity damage is less well captured
(Marotta et al. 2017)	Canterbury 2010–2011	80	NZMMI (New Zealand Modified Mercalli); similar to EMS	mean-damage prediction, comparison	the macroseismic intensity alone is not able to fully explain the observed damage, and that vulnerability factors need to be accounted for
(De Matteis et al. 2016)	L'Aquila, Italy	64	MCS	scenario prediction	Binomial DPMs support preservation and future damage prediction
(Cattari et al. 2015)	Canterbury, New Zealand	48	MMI, PGA	mean-damage prediction	Preliminary analysis

Across the reviewed literature, DPMs are used as a territorial-scale tool, primarily to describe and predict damage distribution of URM churches and also as an empirical step towards the fragility assessment. In the Italian studies, DPMs are often derived by post-earthquake damage surveys of churches damaged by specific events, such as L'Aquila 2009, Central Italy seismic sequences 2016-2017, Marche 2016, Valle Scriva 2003, and other regional datasets, and are then used either to represent damage scenarios, calibrate the vulnerability predictive models, or derive fragility curves (Cescatti et al. 2020; Canuti et al. 2021; Ceroni et al. 2022; Ruggieri et al. 2022; Sisti et al. 2023a). Therefore, the main field of the application of DPMs is not detailed damage assessment of churches, but it is assessment at the population

scale, where a large number of churches are screened and surveyed, and where decision-makers need probabilistic methods for preservation planning and retrofit intervention prioritization (De Matteis et al. 2016; Palazzi et al. 2020; Canuti et al. 2021).

A major strength of DPMs is that they are able to convert distinct observational damage into an interpretable probabilistic representation. Several studies show that observed damage of URM churches can be satisfactorily reproduced by binomial models, which makes DPMs a useful tool to link post-earthquake damage evidence to predictive scenarios according to vulnerability information. This is particularly valuable when DPMs are used as an empirical basis to generate fragility curves, as in Abruzzi (De Matteis et al. 2016), central Italy (Sisti et al. 2023b, a), and Chilean studies (Palazzi et al. 2020), where they bridged the gap between the observational damage and probabilistic seismic tools.

Moreover, DPMs can be defined for both the global damage and macro-elements or mechanisms, allowing a richer description of the behavior of churches when sufficient data is available. This makes DPMs valuable for churches, whose seismic behavior is often governed by local mechanisms rather than global response. In addition, macro-element-based DPMs are also useful to identify the critical macro-elements that deserve attention and priority for subsequent retrofit designs (Palazzi et al. 2020; Canuti et al. 2021; Sisti et al. 2023a).

The main drawback and limitation of DPMs, according to the reviewed studies, is tied to their empirical nature. The most recurrent limitation of DPMs is that they are sample-dependent. When the number of surveyed churches is small, when some intensity bins include a small number of churches, or when the sample just includes damaged churches, the DPMs' results become weak or only preliminary. This weakness of the reliability of DPMs' results can appear because of either the geographical distribution of surveyed churches, leaving few structures in high-PGA regions, or the sample is incomplete or selective (Fuentes et al. 2021; Mishra et al. 2022). In other words, DPMs are highly sample-dependent and are as strong and robust as the observational dataset behind them.

The second limitation is that DPMs may lose their accuracy when the surveyed churches are heterogeneous, or too concentrated in one or two damage grades. The study of Chilean churches shows that using a heterogeneous sample leads to preliminary and overall DPMs and prevents typology-specific damage assessment (Palazzi et al. 2020). In addition, several studies show that when the sample is dominated by low-damaged observations, the fitted binomial distribution provides

a high-damage tail better than the lower damage grades, such as D0-D2 (De Matteis et al. 2019b; Ruggieri et al. 2022). Therefore, DPMs are reliable and work better with balanced and well-populated samples of URM churches.

Overall, DPMs emerge as effective empirical tools for regional seismic assessment, empirical damage scenario, and fragility derivation, but their reliability significantly depends on the surveyed sample, the choice of the intensity measure, and the dataset homogeneity.

2.2.2 Local assessment procedures

Local assessment procedures are used when the objective of the assessment is no longer the territorial ranking a set of URM churches, but is the verification of the seismic behavior of structural portions of a structure. In the general classification of the seismic assessment methods, they belong to the local/small-scale level, where the analysis is focused on a specific portion of the structure or a single macro-element. These approaches are mainly adopted when the objective is to evaluate the behavior of structural macro-elements with greater detail than that provided by territorial methods.

These assessments are particularly relevant to churches because their response is often governed by local collapse mechanisms rather than a fully global behavior. URM churches are assemblages of macro-elements, and the OOP response of each wall strongly depends on the quality of its connections with orthogonal walls, diaphragms, and the adjacent parts. When the connections between the orthogonal walls and the roof system are poor, the church cannot behave as one unit, and the walls are not able to provide sufficient restraints for their adjacent parts (D'Ayala and Speranza 2003). In such cases, the structure should be divided into different macro-elements, each analyzed separately to evaluate its capacity and potential collapse mechanism. This lack of proper connections is particularly critical for the structural and non-structural elements located at various levels of the structure (e.g., gables, decorative statues, and chimneys) since they are subjected to the elevation-based amplified seismic input (Menon and Magenes 2011; Degli Abbati et al. 2018; Lagomarsino et al. 2023). This method, the so-called macro-element approach, was originally proposed by Doglioni et al. (1994) based on the post-earthquake damage assessment of URM churches. Instead of assessing the church as one unit, this method focuses on examining the seismic performance of its constituent parts separately.

Among the local assessment approaches, kinematic-based limit analysis approaches, whose advantages are their effectiveness and computational efficiency, are widely used. It was originally proposed by Giuffrè (1991) for masonry structures based on subdividing the structure into rigid blocks. Due to its simplicity and efficiency, it was then adopted by the Italian guidelines (NTC 2008; Circolare 2019). Linear and nonlinear kinematic analyses are commonly used in engineering projects and practices.

2.2.2.1 LV2 method: linear kinematic analysis

Within the multilevel framework proposed by the Italian guideline for the assessment of heritage structures, LV2 represents the level of local assessment of URM structures at the macro-element scale. In this method, it is necessary to identify macro-elements correctly, which requires considering the construction history and any crack patterns. In contrast to LV1, this method allows evaluating the seismic response of churches more accurately by locally assessing the response of all macro-elements and identifying the most critical ones.

This method is based on the linear kinematic analysis and requires the idealization of the selected mechanism as a kinematic chain of rigid blocks connected through hinges that were placed at the most probable crack locations. The simplified mechanical assumptions are exactly the same with the ones of kinematic limit analysis: URM is assumed to have no tensile strength, infinite compressive strength, and no sliding between the blocks (Heyman 1966).

The main result of the LV2 procedure is the activation multiplier α_0, which is the horizontal load factor associated with the onset of the mechanism. This factor is calculated by applying the theorem of virtual works to the mechanism under investigation (G.U.N.47 2011). The corresponding spectral acceleration is then calculated by referring the mechanism to an equivalent single-degree-of-freedom (SDOF) system. This capacity value can be compared with the seismic demand defined by the code, both at the damage limit state and the life-safety limit state. Therefore, LV2 provides a quantitative measure of the local seismic capacity of each considered mechanism. Table 4 reports the list of the reviewed papers that adopted LV2 for local mechanism assessment in URM churches.

Table 4: Overview of LV2 applications to URM churches in the literature

References	Case study	Macro-element studied	Collapse mechanism	Boundary conditions / interaction with adjacent elements	Limitation/remarks
(Amitrano et al. 2025)	Six churches in Sorrento, Naples	Façade, tympanum, nave side walls, transept wall, apse	Overturning and flexural local collapse mechanisms	Support conditions considered; full adjacent-element interaction not considered	Depends on wall geometry, boundary conditions, and support configuration;
(Lo Monaco et al. 2023)	Jesus Resurrection Church, Belinț, Romania	Aula arches, façade, bell tower, belfry	Arch lateral response, façade overturning, belfry overturning	Macro-block kinematics; mechanism varies with local conditions and element connections	Local mechanisms vary case by case; global screening cannot replace local analyses.
(Korkmaz et al. 2023)	Surp Sargis Church, Diyarbakır, Turkey	Front, back, left, and right façades	Overturning, vertical bending, lateral bending	Façades checked separately; first and ground stories analyzed	only façade mechanisms assessed in kinematic analysis
(Gunes 2023)	Archangeloi Church, Kumyaka, Türkiye	Perimeter walls; parts of main structure	Overturning mechanisms	Does not accounts for perpendicular wall connection details and interactions	Conservative; pre-assigned mechanisms may not reflect actual irregular church behavior
(Diana et al. 2023)	Sion Cathedral; Saint François Church, Lausanne, Switzerland	Sion: apse, central arch, south façade. Lausanne: top apse, belfry, apse, chapel, south wall	Overturning, vertical bending, horizontal bending	Based on selected macro-elements based on the quality of masonry element connections, the masonry arrangement and interlocking, and the presence of ties or ring beams.	Linear kinematic results can be over-conservative; some mechanisms excluded for lack of connection/detail information
(Formisano et al. 2022)	Four churches: one in Ischia, three in Teramo	Façades, side walls, corners, tops, gables	Simple/composite overturning, corner overturning, top overturning, horizontal/vertical bending	Ground-connected or height-constrained mechanisms considered; full interactions did not considered	Simplified methods cannot replace refined models; Local mechanisms vary by macro-element
(Contrafatto et al. 2022)	Santa Maria del Ponte di Rosarolo Church, L'Aquila	Main façade, rear façade, north lateral wall, sacristy wall	Out-of-plane overturning, bending, in-plane shear	Compared cases with/without RC beam restraint and wall interlocking	RC beam and wall interlocking strongly affect predicted mechanisms
(D'Amato and Sulla 2021)	San Rocco Church, Pisticci, Italy	Main façade, narthex, colonnade, southwest façade, bell tower, belfry	Façade overturning, colonnade longitudinal response, local bell tower corner overturning, belfry response	Mainly simplified assumptions; some cases neglect wall connections, others include restraining walls	Strongly boundary-condition dependent; requires monolithic walls; no direct LV1–LV2 correlation
(Briceño et al. 2021)	San Pedro Apostol Church, Andahuaylillas, Peru	Front façade, rear façade, longitudinal wall portions	Façade rocking; wall out-of-plane overturning	Rotation-point mechanisms; height effects	Checked only three selected mechanisms; simplified kinematic results do not capture

				included through Z/H term	the church's full damage pattern
(Betti et al. 2021)	Basilica of San Francesco, Arezzo, Italy	Façade, tympanum, nave-wall portions, Bacci Chapel wall, apse-side wall	Out-of-plane overturning of selected macro-elements	Based on masonry quality, ties, adjacent convent, construction phases, local irregularities; tie-rods in Bacci Chapel neglected	No-tension rigid-block assumptions make results conservative; Bacci Chapel tie-rod effectiveness not included
(D'Amato et al. 2020)	Five Matera churches: San Giovanni Battista, San Pietro Caveoso, San Rocco, San Francesco d'Assisi, Sant'Agostino	Façade, colonnade, triumphal arch, lateral nave, top façade, gable	Façade overturning, colonnade response, nave response, top façade, gable overturning, gable breakout	Based on visual/geometric surveys; lateral restraints neglected; no stabilizing contributions considered	LV2 neglects stabilizing contributions; likely underestimates real activation multipliers
(D'Amato et al. 2019)	SS. Maria della Bruna Cathedral, compared with four Matera churches	Façade, colonnade, triumphal arch, lateral nave, top façade, gable	Façade overturning, colonnade response, nave response, top façade, gable overturning, gable breakout	Visual-based macro-elements; stabilizing contributions and wall interactions generally neglected	Simplified LV2 underestimates real multipliers; neglected stabilizing contributions; only most vulnerable mechanisms considered
(Valente and Milani 2019)	San Paolo church, Porporana; San Pietro Apostolo church, Bondeno	Façade, tympanum, side chapels, nave walls, triumphal arch, apse, bell-tower belfry	Façade overturning, tympanum overturning, side-chapel overturning, nave-wall overturning, triumphal-arch mechanism, apse overturning, belfry mechanism	Linear kinematic analysis performed with and without the interlocking between walls	Zero-interlocking assumption is over-conservative; realistic safety strongly depends on macro-elements interlocking.
(Betti et al. 2018)	Basilica of San Francesco, Arezzo, Italy	Façade, nave walls, apse, Bacci Chapel, local wall portions	Local out-of-plane overturning of identified church macro-elements	Based on cracks, wall connections, tie-rods, adjacent buildings, construction phases	May overestimate collapse acceleration; neglects masonry texture and monolithic OOP behavior
(Laterza et al. 2017)	Six Matera churches in the Sassi UNESCO site	Façade, top façade, lateral walls, colonnade, triumphal arch, apse, bell tower	Façade overturning, top overturning, nave transverse response, apse overturning, shear mechanisms	Hinge level considered; detailed boundary conditions not explicitly specified.	LV1 and LV2 not directly comparable; LV2 is mechanism-specific and more reliable
(Chellini et al. 2014)	Santa Maria del Mar, Barcelona, Spain	Façade upper part, façade towers, transversal nave	Upper façade overturning, tower overturning, transversal nave mechanism	Ground-level and elevated mechanisms treated with different demand equations	Some mechanisms emerged only from multilevel analyses; limited masonry mechanical characterization yields to qualitative results

Across the reviewed paper, LV2 and linear kinematic analysis emerge as a useful tool that lies between rapid screening and full numerical modelling, but they

have some limitations that are worth paying attention to. Their main strength is that they are highly practical; they isolate the possible local mechanisms, provide mechanism-specified safety indicators, and assist in ranking the vulnerable and critical macro-elements for further investigations. This is evident in studies where linear kinematic analysis successfully highlighted critical macro-elements, such as façades, apses, belfries, and nave walls, often in good agreement with observed damage and crack patterns or with the results of vulnerability assessments obtained from simplified surveys (Laterza et al. 2017; Briceño et al. 2021; Contrafatto et al. 2022; Korkmaz et al. 2023).

One of the major limitations is that the LV2 is highly dependent on a priori selection of collapse mechanisms. In several papers, the mechanisms were derived from prior LV1 assessment or observed damage and crack patterns. As a result, LV2 does not capture the full damage scenario of the church, especially when multiple interacting mechanisms govern the seismic response of the church. This was explicitly observed in the paper, where only selected mechanisms were checked by kinematic analysis, while pushover analysis showed a broader damage pattern (Briceño et al. 2021; Diana et al. 2023).

Another limitation concerns the strong sensitivity of linear kinematic analysis results to boundary conditions assumed for the macro-element under investigation. The reviewed papers show that predicted collapse mechanisms and safety factors can significantly change depending on support conditions, hinge location, wall interlocking, and the presence of any tie-rods. In the single-nave study by Contrafatto et al. (2022), the governing mechanism shifted from façade overturning to local bending when RC beams and wall interlocking were introduced. Therefore, the mechanism selection must account for masonry quality, ties, and adjacent structural parts (Betti et al. 2021).

The third limitation concerns the simplified constitutive assumptions behind the linear kinematic analysis, which assumes masonry as rigid blocks with no tensile strength and finite compressive strength. These assumptions often make the method conservative. This is useful for screening, but it becomes critical when masonry texture, fractional redistribution, and crack propagation play a significant role. Betti et al. (2018) explicitly showed that the no-tension rigid-block assumptions make LV2 conservative, and Valente and Milani (2019) showed that neglecting interlocking for the façade mechanism led to low mechanism activation multipliers, unless some useful interlocking was introduced.

Moreover, the reliability of LV2 is directly affected by the lack of information on connections and construction details. Several studies mentioned that some mechanisms could not be assessed, or were only approximately assessed, because the information on the junctions, connections, or support conditions was incomplete. In Diana et al. (2023), some macro-elements were excluded from the analysis because of the lack of information on junction details. In Chellini et al. (2014), it was mentioned that the obtained results were considered qualitative because of the incomplete characterization of masonry mechanical properties, and more reliable outcomes could be obtained by a proper characterization of masonry mechanical properties.

Another important remark from the reviewed studies is that linear kinematic analysis is often effective at identifying vulnerable mechanisms. In some cases, LV2 correctly identified the critical macro-elements but remained over-conservative compared to the actual observed damage or refined numerical models. It was shown that linear kinematic analysis is valuable for preliminary identification of vulnerable macro-elements, but they cannot reproduce the response with the same reliability as numerical models (Formisano et al. 2022).

Overall, the reviewed papers showed that LV2 and linear kinematic analysis are valuable tools in identifying probable collapse mechanisms and guiding deeper investigations. However, their outcomes strongly depend on the mechanism selection, boundary conditions, and the relative complete knowledge of construction details.

2.2.2.2 Nonlinear kinematic analysis

Nonlinear kinematic analysis is the evolution of the linear kinematic analysis approach used for seismic assessment of local mechanisms governing the response of macro-elements. While linear kinematic analysis is used to determine the multiplier that activates the mechanism, non-linear kinematic analysis continues the mechanism through increasing displacement and evaluates the capacity beyond the onset of the mechanism. In this way, the method provides a more complete description of the seismic response of local mechanisms, since it considers both the onset of the mechanism and its evolution up to a significant displacement or collapse.

This method evaluates the evolution of the mechanism till collapse through a pushover curve, which relates to the load factor and the horizontal displacement of the center of gravity point. The curve is obtained by applying the theorem of virtual

work on the varied kinematic configurations of the mechanism under investigation. The same assumptions as the linear kinematic analysis are also adopted in this method: masonry is assumes to have no tensile strength, infinite compressive strength, and no sliding between the blocks. Along this incremental kinematic mechanism, the contribution of different factors, such as frictional resistance and presence of tie-rods, can be taken into account (Lagomarsino 2015; Casapulla and Argiento 2016; Casapulla et al. 2021b)

Table 5: Overview of nonlinear kinematic analysis analysis applications to URM churches in the literature

References	Case study	Macro-element studied	Collapse mechanism	Boundary conditions / interaction with adjacent elements	Limitation/remarks
(Casapulla et al. 2025)	14 real churches from Ischia Island expanded to 500 simulated façades via Monte Carlo	Church façades	Simple out-of-plane rocking	Three cases: free rocking, interlocking with sidewalls, and advanced restraint with sidewall interlocking plus tie-rods.	the onset of mechanism depends mainly on façade/sidewall slenderness under restraint, while life-safety and severe damage states depend mainly on façade thickness.
(Ceroni et al. 2025)	178 Central Italy churches expanded to 800 simulated façades	Church façades of single-nave churches	Simple out-of-plane rocking	Two cases: interlocking with sidewalls, and advanced restraint with sidewall interlocking + tie-rods.	the onset of the mechanism is sensitive to interlocking-related parameters, while tie-rods mainly reduce life-safety and severe damage states vulnerability and seismic input strongly affects life-safety and severe damage states fragility.
(Casapulla et al. 2021b)	San Michele Arcangelo church, Lisciano (Italy)	Main façade	out-of-plane rocking and overturning	Sidewall friction considered; free and restrained cases compared	Rigid-block, predefined mechanism, simplified masonry/interlocking; friction raises activation capacity but matters less at large displacement.
(Valente and Milani 2019)	San Paolo church, Porporana; San Pietro Apostolo church, Bondeno	Façade, tympanum, side chapels, nave walls, triumphal arch, apse, bell-tower belfry	Façade overturning, tympanum overturning, side-chapel overturning, nave-wall overturning, triumphal-arch	NLKA was perform with and without considerring interlocking	NLKA outcome depends strongly on assumed interlocking, while real connection quality remains only approximately represented.

			mechanism, apse overturning, belfry mechanism		
(Jorquera et al. 2017)	San Francisco church, Santiago, Chile	Main façade gable, rear presbytery wall, north and south transept walls; transverse arcade system also checked by NLKA	Gable overturning, transept-wall simple overturning, in-plane transverse-arcade mechanisms	Transept walls modeled without effective interlocking restraint; rocking checked as two-sided, one-sided, and one-sided with roof overburden at the top.	results were highly sensitive to rocking idealization and restitution assumptions.
(Endo et al. 2015)	San Marco church, L'Aquila	Façade, nave wall, chapel arches/buttresses, apse, façade in-plane macro-element	Façade overturning, nave-wall overturning, apse overturning, façade in-plane mechanism	façade assumed partially connected to orthogonal walls.	NLKA captured the most critical local mechanisms, and global interaction needed FEM support.
(Criber et al. 2015)	St. Gemma church, Goriano Sicoli	Façade, top façade/tympanum, transept wall, lateral walls, apse, arch-column system	Global façade overturning, top-façade overturning, transept wedge overturning, lateral-wall overturning, apse overturning	Lateral-wall mechanisms checked with/without iron ties; the connections of others were neglected	confidence factor FC = 1.35 reflects limited knowledge; interactions/restraints from adjacent elements are simplified, not modeled in detail, making the results conservative
(Boscato et al. 2014)	S. Pietro di Coppito church, L'Aquila	Façade, top edge of façade, triumphal arch	Façade overturning/rocking, partial collapse of upper façade edge, in-plane deformation of triumphal arch	The façade restraints were neglected; the partial restraint by orthogonal walls was considered	NLKA was sensitive to the assumed period; the standard code period underestimated demand, while the modal period of the façade macro-element gave a more realistic prediction

Building on the limitations and strengths highlighted for linear kinematic analysis, the reviewed paper shows that nonlinear kinematic analysis can be understood as an extension of the same logic as linear kinematic analysis, with the ability to follow the mechanism beyond the onset of the mechanisms up to the collapse. Therefore, its main strength is in providing a more detailed representation and deeper interpretation of the mechanisms already selected. This can explicitly be observed in the façade and transept-wall studies, where nonlinear kinematic analysis was used to move from simple activation checks to displacement-based assessment of local mechanisms (Boscato et al. 2014; Jorquera et al. 2017).

Nonlinear kinematic analysis can also help in distinguishing between the mechanisms that are just activated and mechanisms that are likely to experience severe instability. This is particularly important for URM churches, where many macro-elements can be vulnerable in terms of the activation of mechanisms, but not all of them evolve toward collapse under the same seismic input. In the reviewed paper, there are some studies where life-safety and severe damage limit states, namely LS1 and LS2, were verified separately (Endo et al. 2015; Jorquera et al. 2017; Casapulla et al. 2021b).

Another strength of this method is its ability to account for restraints during the evolution of the mechanism. While LV2 showed sensitivity to wall interlocking, ties, and support conditions, the reviewed nonlinear kinematic analysis studies clarify how these restraints influence the mechanism as the displacement increases. In the studies where the façade overturning was investigated, it was shown that the sidewall friction resistance can significantly increase the activation capacity and stability, whereas its influence is decreased as detachment progresses (Casapulla and Argiento 2016; Casapulla et al. 2021b).

However, many of the limitations discussed for linear kinematic analysis remain present in the nonlinear method. First, nonlinear kinematic analysis depends on a predefined mechanism. It improves the description of the response, but if the assumed mechanisms are poorly selected or not the actual governing ones, the nonlinear refinement cannot resolve that issue. Several papers were based on simple rocking of façades, while broader interactions among multiple mechanisms at the same time was not explored (Criber et al. 2015; Endo et al. 2015).

The second major limitation is that the results remain sensitive to boundary conditions and input assumptions. The assumptions on wall interlocking, roof burden, and tie-rods directly influence the predicted response. For this reason, nonlinear kinematic analysis can be more effective when it is used together with other methods rather than in isolation. In several papers, it was combined with linear limit analysis, fragility analysis, and finite element-based procedures. When the church exhibits strong structural interactions, complex modal participations, or uncertain restraint conditions, refined numerical models are still needed to complement kinematic analysis (Boscato et al. 2014; Jorquera et al. 2017; Valente and Milani 2019).

Overall, the reviewed papers suggest that linear kinematic analysis is effective for rapid identification and ranking the potential local mechanisms, while nonlinear kinematic analysis is valuable when the same mechanisms need to be assessed in

terms of displacement development up to the ultimate condition of the considered mechanisms.

2.2.3 Numerical approaches at the building scale

In the literature, various models are suggested for modeling masonry structures, and these models differ in their degrees of simplification (Cattari et al. 2022a; Monteferrante et al. 2023). This classification of masonry modeling approaches encompasses two fundamental criteria. These criteria include the scale of analysis, distinguishing between material and structural element perspectives, and the type of description of the masonry, categorized as continuum or discontinuum.

At the material scale, the composite nature of masonry material is of paramount importance. This material can be viewed as either heterogeneous or homogeneous, leading to the differentiation of two primary modeling categories (D'Altri et al. 2020):

1. **Discrete Interface Models (DIM):** These models, often referred to as "micro-models," offer a highly detailed approach to model masonry behavior. In this approach, no simplifications are employed. Each constituent of masonry, such as individual blocks and mortar joints, is explicitly modeled separately. These components are subsequently assembled using interface elements, thereby providing a comprehensive representation of masonry based on the distinct properties of each constituent and the interactions at their interfaces.

2. **Continuum Constitutive Law Models (CCLM):** In contrast, the Continuum Constitutive Law Models, typically termed "macro-models," simplify the masonry material by considering it as a homogenous entity governed by continuum constitutive laws. Although these models offer less details in their representation, they can be applied to larger structural segments and even complex geometries. However, it is important to acknowledge that the use of nonlinear constitutive laws remains imperative to ensure an accurate portrayal of structural behavior, which does introduce computational challenges.

Transitioning to the element scale, the underlying concept revolves around identifying sections within the masonry continuum that experienced damage. This information is often derived from observations of post-earthquake damage. In this context, masonry is not perceived as a continuous, indistinct medium but rather as a collection of entities with common mechanical behaviors. Two distinct modeling approaches are typically applied at this scale:

1. **Macro-Block Models (MBM):** These models employ a discrete approach, focusing on a set of masonry bodies interconnected through interfaces. The shape of each body is determined based on observed recurring crack patterns following past seismic events. Each masonry body is generally assumed to be rigid, with nonlinearity concentrated at the interfaces, occasionally capable of transferring frictional forces.

2. **Structural Elements Models (SEM):** Also referred to as "macro-element models," these models involve identifying macroscopic structural elements within the masonry structure. These macro-elements are characterized by a limited set of static and kinematic variables and are used to represent damage, cracking, sliding, and rotations within predefined zones. Structural Element Models, which may include Equivalent Frame models, offer the advantage of a reduced parameter count and computational effort in the modeling and structural analysis phases. Nevertheless, it is crucial to note that these models assume that damage can only occur within the designated zones established by the user, leaving other elements undamaged.

The choice of a suitable modeling approach, as previously explained, depends on the seismic response characteristics displayed by a structure. Seismic responses can be classified into in-plane and out-of-plane mechanisms. Within both of these response categories, various models offering differing levels of accuracy can be employed. While this distinction is not intended to be rigid, in practice, discrete models such as MBM and DIM are often employed to describe local mechanisms, whereas continuous models like SEM and CCLM are better suited for the analysis of a building's global response.

Specifically, when investigating the global response of buildings, the utilization of DIM, although applicable in principle to entire structures, frequently results in an impractical computational burden from an engineering perspective. Conversely, discrete MBM are generally only applicable in exceptional cases where the global response manifests as entirely independent masonry walls that can be analyzed in isolation.

Various studies in the literature adopted numerical modeling to evaluate the seismic performance of URM churches. Brandonisio et al. (2008) proposes a two-steps procedure applied to ten basilica churches. In the first step, each church is analyzed in the linear range with 3D finite element models consisting of shell elements setup in SAP2000, to determine the static and dynamic properties, the distribution of internal forces, and the seismic demand on each macro-element. In the second step, the complex 3D structure is decomposed in its constituting macro-

elements, and each macro-element is analyzed in the non-linear range up to collapse to determine its horizontal capacity. The results of the first step (strength demand) and second step (strength capacity) are then compared to assess the safety level of each macro-element, and therefore of the whole structure.

Starting from the previous study, Valente et al. (2020) performed extensive nonlinear dynamic numerical simulations in Abaqus on a detailed 3D FE of the ten churches above-considered, adopting for masonry a damage plasticity material exhibiting softening in both tension and compression. Different parameters are assessed as output of the NLDA, i.e., damage distribution, energy density dissipated by tensile damage and maximum normalized displacements for the different macro-elements composing the churches. The numerical simulations aim to: assess the damage distribution and identify the most vulnerable elements of the churches; provide a comprehensive numerical estimation of the parameters affecting the seismic response of the churches; assess their seismic vulnerability as a function of the geometrical and typological characteristics of the main macro-elements.

Lagomarsino et al. (2019b) introduced a macro-element-based approach in which the interactions among macro-elements are implicitly considered through a suitable redistribution of forces. This procedure firstly requires the identification of macro-elements, depending on their geometry and constructive details. Then, the best modelling strategy is selected for each macro-element (in the examined proposal, a macro-block model and an equivalent-frame model were adopted to describe the out-of-plane and in-plane response of macro-elements, respectively). Finally, the seismic performance of each macro-element is assessed individually via NLSA, and the overall fragility curve of the church in the longitudinal and transversal directions is generated by combining the results from all the macro-elements. A key requirement for effectively implementing this approach is the use of a 3D finite element model of the church, which is essential for determining how loads are distributed among the various macro-elements. This model provides critical coefficients that adjust the capacity curves of each macro-element. These modifications reflect the intricate interactions between the different parts of the structure and can either enhance or reduce the overall structural capacity, depending on how the macro-elements influence each other.

Degli Abbati et al. (2019) introduced a novel procedure centered on performing multiple pushover analyses using a comprehensive 3D model. This innovative method addresses the interdependent interactions between various structural components by applying specific load patterns to individual microelements within the building. The procedure involves several key steps:

Modal Analysis: The process begins with a modal analysis using a 3D finite element model of the entire structure. This step is essential for identifying the modes that influence the dynamic behavior of each macro-element, along with their corresponding mode shapes.

Defining Load Distributions: Based on the modal shapes identified, the next step is to define load distributions for each macro-element. These distributions are derived from the previously determined mode shapes and are applied to the structure's individual macro-elements.

Pushover Analysis: Once the load distributions are established, pushover analyses are carried out by applying these loads to the entire numerical model. This step assesses the structural response under increasing loads, up to the point of collapse.

Conversion to Capacity Curves: In the final phase, the pushover curves for each macro-element are converted into a simplified capacity curve, representing a single degree of freedom system. This capacity curve forms the basis for seismic performance evaluation.

Malena et al. (2022) proposes a two-step procedure. The first step is based on the detection of the main vibration modes with identification of the structural bi-dimensional macro-elements that are responsible for the overall seismic vulnerability. The second step is based on the non-linear finite element analysis of the previously identified macro-elements, to evaluate the failure pattern caused by the earthquakes. This procedure aims to establish a link between the global behavior of the church and the assessment of the local mechanisms, re-evaluating the value of modal analysis to be associated with non-linear seismic assessment. The first step provides a reasonable estimate of the dynamic actions induced by the earthquake, while the second step carries out the structural assessment in the non-linear field with an acceptable computational effort. This last step mainly requires the selection of a robust non-linear model capable of assessing seismic vulnerability. As a good compromise between accuracy and simplicity, in the study, masonry is described as an anisotropic elasto-plastic medium, whose yield criterion is derived via homogenization (de Felice et al., 2010; Malena et al., 2019) (de Felice et al. 2010; Malena et al. 2019). In contrast to the more sophisticated material models available in the literature, which require several constitutive parameters, the proposed model only requires a few parameters for its definition.

de Felice et al. (2022) proposes an integrated methodology for assessing the seismic safety of churches, from photogrammetric survey to collapse mechanisms analysis. As a first step, a photogrammetric survey is carried out, and a 3D model is obtained through structure from motion software. This model allows to derive geometrical details and block shape and arrangement through a semi-automatic edge detection technique based on orthophotos processing. Then, the resulting geometry is imported in the Distinct Element code UDEC. Finally, the local collapse mechanisms are analyzed, both in terms of failure development and capacity curve, by applying an automatic pushover algorithm.

2.4 Conclusions

Chapter 2 examined the seismic performance and recurrent vulnerabilities of URM churches and the main assessment methods available in the literature, ranging from territorial-scale screening methods to local kinematic approaches and building-scale numerical analyses. This chapter emphasized that the seismic behavior of churches is strongly affected by their configurational complexity, weak structural connections, and the dominance of local OOP mechanisms, making their assessment more challenging than that of ordinary masonry buildings. It also demonstrated that no single method is universally sufficient: empirical and simplified approaches are valuable for preliminary assessment and ranking and for identifying critical mechanisms, whereas more advanced numerical strategies are required to study structural interactions and damage progression in more detail.

The discussion about numerical models further clarified the issue. Refined models provide the possibility of capturing the global dynamic properties, the redistribution of forces, the interaction among macro-elements, and the correlation between IP and OOP responses. However, the review also shows that no modeling strategy is universally the best option. Simplified approaches are attractive due to their efficient computational effort and practical usability, but they may become insufficient when local mechanisms and structural interactions play significant role in the seismic performance of the structures. On the other hand, more refined models are able to provide richer description of the behavior of structures, with greater modeling and computational cost.

A key conclusion of this chapter is that the seismic assessment of URM churches cannot rely on one single modeling strategy. There is a gap between territorial methods, local verifications, and refined numerical approaches, as each of them tend to address only part of the problem; large-scale methods support

prioritization, local methods focus on individual mechanisms, and global numerical approaches capture the structural interactions, but none of them alone can resolve the need for a reliable practitioner-oriented tool for seismic assessment of URM churches whose behavior lies between fully box-like and fully independent macro-elements.

These observations directly motivate the objectives of the following chapters of the thesis. Chapter 4 addresses one of the issues emerging from the literature, namely the trade-off between modeling accuracy and computational cost through a comparative study of FEM, EFM, and DEM approaches. Chapter 5 proposes an integrated practitioner-oriented approach for seismic assessment of URM churches, aiming at linking global numerical modeling and local mechanism approaches. Finally, Chapter 6 moves the thesis from assessment to intervention design by proposing a retrofit decision-support framework for vulnerable secondary elements.

Chapter 3

The case study of Bussana Vecchia ruined church

3.1 Introduction

Following the review of the available methods for the seismic assessment of URM churches in Chapter 2, this chapter introduces the case-study adopted throughout the thesis: the Church of Nostra Signora delle Grazie e Sant'Egidio in Bussana Vecchia, Italy. The selection of this case study is also motivated by its conservation condition. As a partially ruined monument, it represents a category of historical structures for which reconstruction is not intended. Instead, safety must be ensured to protect users and tourists through the stabilization of the current (as-is) damaged configuration (Degli Abbati et al. 2024). Similar conservation strategies were also observed for the remaining and surviving structures after 1968 Sicily earthquake in the Italian village of Poggioreale (Carocci et al. 2023), and after World War II in the French village Oradour-sur- Glane (Helbling 2019).

Like many URM churches, this case-study exhibits several features that make the assessment of its seismic behavior particularly challenging, including a tall bell tower, elongated longitudinal walls, tall columns, and the lack of the nave's vault, leading to the potential activation of local mechanisms. These characteristics make it appropriate for the objectives of this thesis, which are the comparison of modeling strategies and the development of an integrated practitioner-oriented seismic assessment framework.

This chapter presents the historical development, structural features, and background that are necessary to reach the objectives of the thesis.

3.2 Historical Background

The Church of NS Signora delle Grazie e Sant'Egidio was built outside the city walls between the 13th and 14th centuries. Then, it underwent a series of restoration efforts, completed in 1404, which did not alter the church's original load-bearing structure. Due to the increase in population, the church was reconstructed on the original site to allow for its expansion. A new structure was built in 1505 with three naves separated by stone columns. Between 1605 and 1615, the bell tower was demolished and rebuilt at least twice, and a sacristy was added on the southern side of the main structure.

In 1650, a structural modification to the previous load-bearing system took place: the columns dividing the church into three naves were removed, and the church was transformed into a single hall with side chapels. This layout remains to the present day. This modification included the installation of tie rods and bolts to connect the new structural system to the existing walls. The last known modification that altered the structural behavior occurred around 1690 and involved the construction of a northern sacristy attached to the existing church (Calvini 1941, 1987).

3.3 The 1887 Earthquake and Observed Damage

In February 1887, a powerful earthquake struck the Ligurian coast, causing widespread destruction and loss of life (Ferrari 1991). The seismic event occurred in multiple tremors, with the strongest shaking recorded at 06:22 and 08:51 local time. These shocks caused severe damage along the coastline, particularly between Sanremo and Alassio. The earthquake's epicenter was likely offshore, near Imperia, with an estimated moment magnitude between 6.4 and 7.0. One of the hardest-hit locations was Bussana Vecchia, which recorded 53 casualties. The village was abandoned after the earthquake due to extensive damage and was later rebuilt in 1894, becoming known as Bussana Nuova (the new part of Bussana).

Figure 2: Seismic hazard in Liguria (MPS04, http://zonesismiche.mi.ingv.it/). The star indicates the location of the Bussana village.

This devastating event left a lasting mark on the Church of NS Signora delle Grazie e Sant'Egidio, which had undergone various architectural changes and experienced damage from earlier events before the 1887 earthquake. Although the church's vault experienced damage in previous seismic events, it cracked along its entire length, split into two sections, and collapsed due to the 1887 earthquake. Currently, the church is in a state of ruin, with the absence of the vault and lack of protective elements accelerating the degradation of structural and non-structural elements.

3.4 Structural Features of the Church

The Church of N.S. delle Grazie e S. Egidio has a single nave and three altars on each side. These altars are positioned in the space created by the two-layered longitudinal walls. The longitudinal walls are constructed from split stones, while

the vaults and chapels are made of brick. The distinction of materials shows that the external and internal structures were built in two different historical periods.

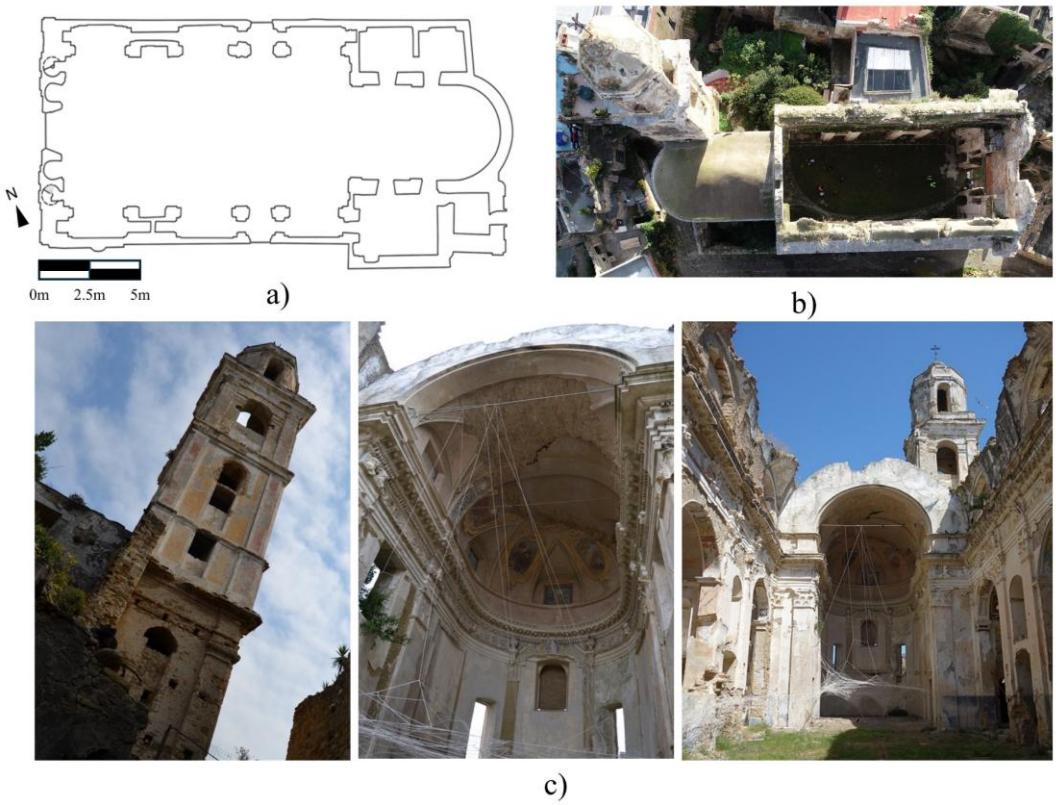

Figure 3: Current plan, aerial, and sectional views of the Church of Nostra delle Grazie e S. Egidio (Italy)

In 1650, when the pillars that divided the church into three naves were demolished to create a single and large hall with three alters on each side, the new structure was connected to the original walls through tie-rods and bolts. Above the roof level, the church has three lunettes on the north and south facades, while below the roofline, where the nave section housing altars extends outside, the altars' roof is covered with irregularly cut slate slabs.

The current layout of the church contains a single nave with a length of 19 meters and a width of 9 meters. The apse is located at the eastern end of the structure, and it extends 9.7 meters in length and 5.5 meters in width. Due to this elongated layout, lack of internal diaphragms, and heavy masonry construction, the church exhibits structural vulnerabilities against seismic events.

3.5 Conclusions

This chapter introduced the Church of Nostra Signora delle Grazie e Sant'Egidio, located in Bussana Vecchia, Italy, as the adopted case-study of the thesis. It presented its historical developments, architectural configuration, and structural characteristics. The church represents a particularly significant benchmark for this research because of its structural complexity and presence of the features that are typical of vulnerable URM churches.

The information discussed in this chapter and the maps of the current state of the church were then used to construct its numerical model and used in the comparative seismic analyses, discussed in Chapter 4, and in the development of the integrated seismic assessment framework in Chapter 5.

Chapter 4

Comparative modeling strategies for churches: EFM vs FEM vs DEM

4.1 Introduction

This chapter discusses one of the central objectives of the thesis: the comparative evaluation of different modeling strategies for the seismic assessment of historical URM churches. Since the behavior of churches, due to their complex configuration and several structural features that prevent them from having a box-like behavior, is more complicated than other types of structures, the selection of an appropriate modeling strategy to evaluate their seismic response is a critical step in the assessment process.

A wide range of numerical approaches is currently available for masonry structures, each based on different mechanical assumptions. Among some of the simplified approaches used for URM churches, beam-based approaches are referred to those where the structure is treated as an assembly of nonlinear members, forming the so-called Equivalent Frame models (EFM). One of the earliest models based on the equivalent beam approach was proposed by Tomazevic (1978), the so-called POR (storey-mechanism) method, in which the seismic damage is exclusively due to the shear failure of fix-fix piers, modeling spandrels and floors as rigid. More recent and advanced EFM idealize URM systems as an assembly of piers and spandrels connected through rigid nodes (Magenes and Della Fontana 1989; Roca 2006; Chen et al. 2008; Lagomarsino et al. 2013; Sangirardi et al. 2019). In EFM, plasticity is lumped into pier and spandrel nodes and usually described by defining zero-length hinges (Cattari et al. 2022a). EFM advantages are a low computational cost, automatic a priori discretization (Dolce 1991), and a limited number of required inputs, which can be identified through basic in-site tests, making this a preferred approach by practitioners and more suitable for preliminary design and ordinary assessment purposes (Lagomarsino et al. 2013; Cattari et al. 2021). Despite recent developments (Vanin et al. 2020a, b), the use of EFM is

though limited to the simulation of IP responses stemming from box-behavior, only considering the stiffness contribution of OOP-loaded elements (Kallioras et al. 2017) – this naturally poses a challenge when simulating the OOP-dominated seismic response of URM churches. The presence of irregular openings in URM churches can also make the EFM a priori idealization of piers, spandrels, and rigid nodes more impractical, leading to epistemic modeling errors resulting in unrealistic and unconservative predictions (Parisi and Augenti 2013; Berti et al. 2017; Quagliarini et al. 2017; Cattari et al. 2022b; Morandini et al. 2022).

To overcome these issues, continuum macro-models based on the Finite Element Method (FEM) have been used to assess the seismic behavior of URM churches, treating URM as a homogeneous continuous deformable body, without distinction between blocks and mortar (Gambarotta and Lagomarsino 1997; Lourenço et al. 1998; Lourenço 2002). This requires appropriate constitutive laws, homogenization frameworks, and appropriate calibration exercises (Lourenco et al. 2007; Milani and Valente 2015), at the cost of a higher computation burden but capturing both IP and OOP modes. FEM is, though inherently limited in simulating discontinuities, separation and local failure mechanisms, such as rocking, sliding, and block overturning, which are relevant to URM churches with low-quality connections and materials (Pulatsu et al. 2016).

Discontinuum models, originally developed for solving soil mechanics problems (Goodman et al. 1968; Cundall 1987) and idealizing URM as an assembly of mechanically interacting discrete, provide a powerful yet similarly costly alternative to FEM that naturally handles large displacements/rotations, detachment and re-contact, collisions. Malomo and Pulatsu (2024) refer to three main discontinuum models whose employment is predominant in current URM research: the Distinct Element Method (DEM) (Cundall 1971; Kassotakis et al. 2020; Pulatsu et al. 2023), the Applied Element Method (AEM) (Meguro and Tagel-Din 2001; Malomo et al. 2019; Khattak et al. 2023), and the Non-Smooth Contact Dynamics (NSCD) (Jean 1999; Beatini et al. 2017; Schiavoni et al. 2023). In DEM, selected for this work, URM discretization is typically based on the actual geometry and size of the units, which are expanded to account implicitly for the unit-mortar mechanics through zero-thickness nonlinear interfaces (meso-scale modelling, sometimes referred to as simplified micro-modelling). Studies (Sarhosis and Lemos 2018) demonstrated that simulating explicitly and discretizing internally units and mortars at the micro-scale (also called detailed micro-modelling) can lead to increased accuracy. However, recent progress has shown that when fracture-energy-based constitutive laws are adopted, size effect can be significantly reduced, allowing for

reliable predictions even with using larger-than-actual blocks (Pulatsu et al. 2020; Zhang et al. 2024).

Despite the presence in recent literature of various valuable contributions comparing DEM and FEM (Baraldi et al. 2018; Malomo and DeJong 2022) or EFM and DEM/FEM (Cattari et al. 2021; Davis et al. 2024), a quantitative study focusing on URM churches that directly compares the applicability of EFM, FEM, and DEM altogether is presently missing. This chapter aims to fill this knowledge gap through a case-study approach, where the historic URM Church of Nostra Signora delle Grazie e Sant'Egidio in Bussana Vecchia (Italy) is conveniently taken as a reference to perform pushover-based comparative seismic analyses exercises.

4.2 Basis of Adopted Numerical Models

This section describes the development of the continuum model (FEM), discontinuum model (DEM), and equivalent frame model (EFM) of the Church of Nostra Signora delle Grazie e Sant'Egidio. For each numerical approach, the main modeling steps, underlying assumptions, and adopted constitutive laws are summarized.

4.2.1 Continuum models

The church's FEM model was developed in ABAQUS, and its geometry was derived by processing high-resolution laser scans in a simplified manner, retaining only structurally significant components and systems. Furthermore, minor geometric irregularities, such as slight variations in wall thickness, were averaged to simplify the meshing process, decreasing model complexity without impacting analysis results. 4-node 3D tetrahedral elements (C3D4) were used for meshing the structure, similarly to (Milani et al. 2018; Aguilar et al. 2019; Giordano et al. 2019), allowing flexibility to mesh intricate elements, such as vaults, arches, and connections between different members (see Figure 4(a)). Once the numerical FEM of the church was created, a preliminary mesh sensitivity analysis was conducted in the linear elastic range to ensure adequate stress/strain verifications and computational efficiency. The natural period of the structure as derived from modal analysis was selected as a comparative parameter across different mesh sizes, with 300 mm considered satisfactory since the variation in the natural period became negligible – see Figure 4(b).

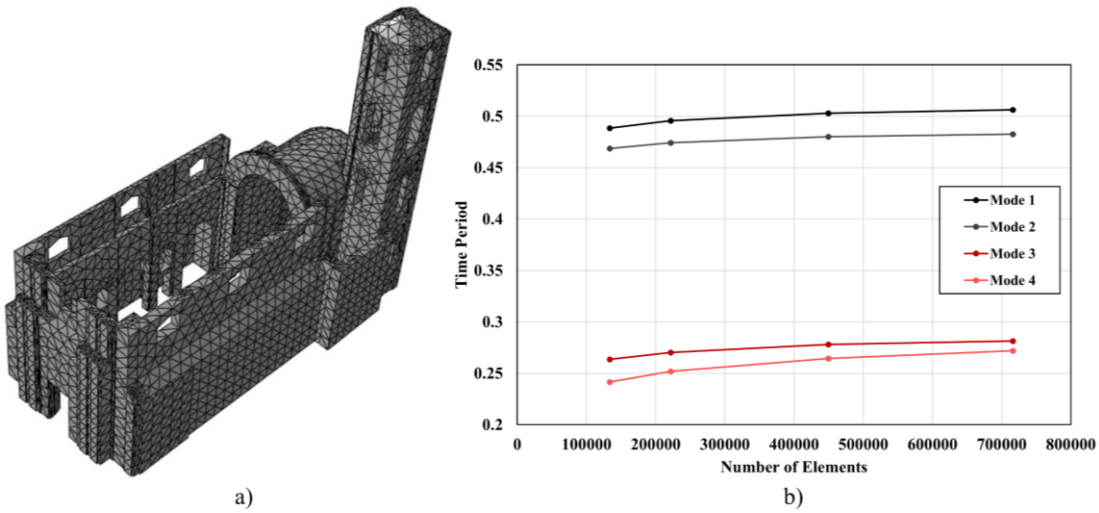

Figure 4: (a) 3D FEM of the church and (b) mesh sensitivity

In the absence of direct experimental investigations on the material of the structure, which were impractical to perform given the heritage status of the church, URM mechanical parameters were selected based on those proposed in the Italian Guidelines for the Assessment and Reduction of Seismic Risk of Cultural Heritage (Directive P.C.M., 2011) and the Italian Technical Standards for Construction (NTC, 2018) – assuming average values (Table 6) for split stone masonry and conservatively adopting the suggested 1.3 corrective factor, as supported by a relatively good residual quality of mortar and absence of pre-existing severe widespread cracking documented onsite. These parameters represent the homogenized macro-scale URM mechanical properties, accounting for the behavior of stones and mortar layers at the structural level.

Table 6. The adopted URM mechanical properties in FEM

f_m (MPa)	E (MPa)	w (KN/m^3)	Poisson Ratio	Density (kg/m^3)
4.16	2262	21	0.2	2140

To simulate the URM nonlinear behavior under seismic loading, the Concrete Damage Plasticity (CDP), fully available in the standard ABAQUS package, was adopted (Figure 5). Originally proposed by Lee and Fenves 1998 for quasi-brittle materials, it has been widely and successfully used for URM (Valente and Milani 2016; Degli Abbati et al. 2019; Ravichandran et al. 2021) because of its ability to capture the plastic deformations and stiffness degradation under tension and compression. CDP is based on the non-associated plasticity (Lee and Fenves 1998),

where the plastic potential function governs the material's inelastic behavior. Masonry typically uses a dilatancy angle (Ψ) of 10° to account for the inelastic volumetric expansion under shear (Milani et al. 2018). Furthermore, it is typically believed that a smoothing parameter (ε) equals 0.1 (van der Pluijm 1993). The model uses a multiple-hardening Drucker-Prager yielding surface, which is determined by the ratio of the second stress invariant (ρ) and the biaxial-to-uniaxial compressive strength ratio (f_b/f_c), which regulates compressive and tensile yielding. To guarantee a representative simulation of masonry failure, typical values of ρ = 2/3 and f_b/f_c = 1.16 are utilized (van der Pluijm 1993). Regarding the boundary conditions, it was simplistically assumed that the base of the church is completely fixed in all directions – the potential impact of this choice is further discussed in the conclusions.

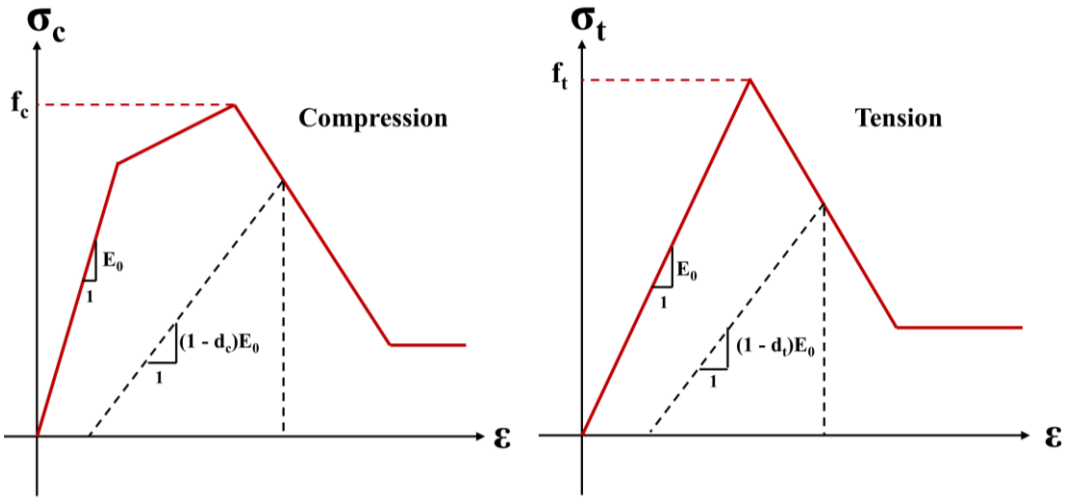

Figure 5: Adopted constitutive law for URM in FEM

4.2.2 Equivalent frame models

The EFM model of the church was developed using 3Muri commercial software distributed by STADATA, which is based on the TreMuri research program developed at the University of Genova by Lagomarsino et al. (2013). This approach has been proven reliable when simulating URM box-like behavior (Morandi et al. 2019; Silva et al. 2021; Degli Abbati et al. 2022)). In accordance with the principles of the EFM modeling approach, the walls are the primary load-bearing elements, while the horizontal diaphragms, in addition to distributing gravitational loads, are considered as connecting and stiffening elements, responsible for distributing seismic forces among different walls. The flexural behavior of floors and the OOP response of the walls are neglected in this model,

allowing it to evaluate the global behavior of the structure governed by the IP behavior of the walls.

The development of the church's EFM started with simplifying the geometry of the church, idealizing walls as equivalent planar frames where deformable elements (parts where nonlinear response is concentrated) are connected through rigid nodes (parts of the wall that do not experience any damage). According to the actual damage caused by past earthquakes, showing that the cracks and failure modes are usually concentrated at some specific parts of the wall, the walls are divided into elements called piers (vertical elements) and spandrels (horizontal elements). These masonry elements, according to NTC 2008, are modeled as nonlinear beam elements, idealized based on the arrangement of openings and structural layouts (Cattari et al. 2021). The software automatically generates the mesh, following the criteria suggested by Lagomarsino et al. (2013) for the mesh geometry definition, creating masonry piers, spandrels, and the rigid nodes connecting them. If necessary, it is also possible to manually modify the mesh when some modification of the mesh geometry must be implemented in the model. Figure 6(a-b) shows the 3D geometrical and EFM of the church, identifying its structural elements. The URM mechanical properties adopted for piers and spandrels (Table 6) match those used in the FEM (§4.2.1): E = 2262 MPa, G = 942 MPa, $\nu = 0.20$, $\rho = 2140$ kg/m³.

Once piers and spandrels were defined, the 3D model of the church was constructed by assembling 2D modelling of the walls and introducing diaphragms. The diaphragms are modelled as 3- and 4-node finite orthotropic membrane elements (Lagomarsino et al. 2013), identified by the Young modulus E_{1eq} along the principal direction (floor spanning orientation), the Young modulus along the perpendicular direction E_{2eq}, the Poisson ratio *v,* and the shear modulus G_{eq}. The values were used for properties of diaphragms are: E_{1eq} and E_{2eq} = 877.87 MPa, G_{eq} = 292.62 MPa (for the apse vault), and E_{1eq} and E_{2eq} = 1399.35 MPa, G_{eq} = 466.45 MPa (for the barrel vaults of the lateral chapels). These values are automatically computed by the software as described in Cattari et al. (2008).

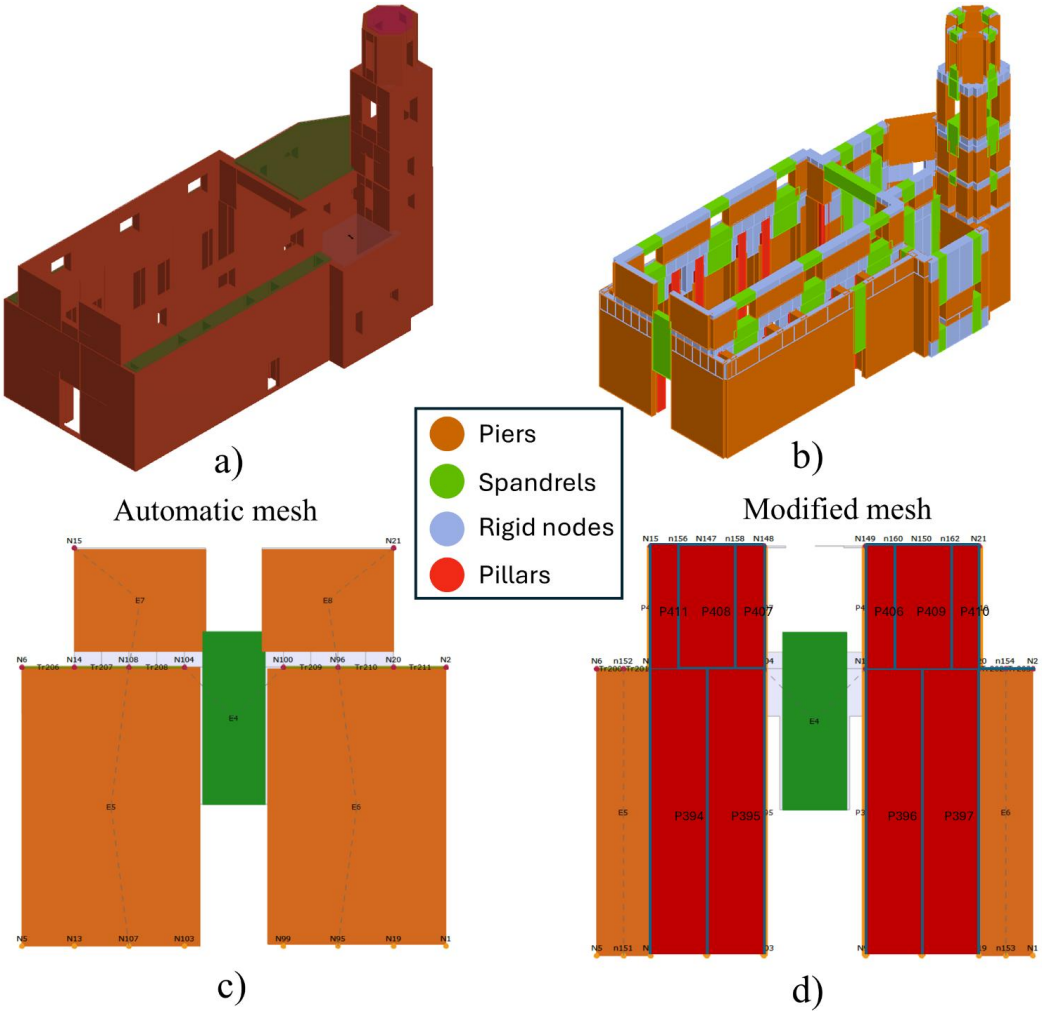

Figure 6: (a) The 3D view of the EFM of the church, (b) The 3D view of the meshed model, (c) and (d) mesh modifications of the façade to include 3D-pier elements (red elements)

In 3Muri, the structural elements are modeled as nonlinear bidimensional beams, following a bilinear elastic-perfectly plastic constitutive law, with limits on maximum (ultimate) displacement and stiffness degradation in the nonlinear range. Failure modes under horizontal forces include flexural-rocking, shear-sliding, and diagonal shear cracking. The maximum strength of the panel is computed according to the simplified criteria proposed in the literature to interpret the failure modes that may occur in the panels, as discussed by Calderini et al. (2009). The strength is calculated as the minimum value between the predictions from the strength domains, which are based on the failure criteria evaluated according to the current axial stress acting on the element. Collapse occurs when the panel reaches its ultimate drift capacity, which is specific to each failure mode. For more details, the interested reader can refer to Calderini et al. (2009).

To consistently compare the result of the EFM with those obtained using the FEM and DEM, an appropriate modeling strategy was employed to account for the OOP response of some elements whose OOP mechanisms cannot be neglected, particularly the longitudinal walls and façade. To this end, some elements with stiffness in both directions, called 3D-piers (red elements in Figure 6(b-d)), were introduced by manually altering the mesh generated by the software. Figure 6(c-d) shows the automatic and modified mesh for the façade of the church in 3Muri software. The failure criteria of these elements consider both IP and OOP response, assumed as independent; recent studies are devoted to understanding the possible interaction (Kesavan and Menon 2022; Krishnachandran and Menon 2023).

4.2.3 Discontinuum models

The DEM of the church was first geometrically created using Rhinoceros 3D (McNeel and Associates 2015) and then developed in 3DEC, distributed by Itasca Consulting Group Inc (2013). The method proposed by Zhang et al. (2024) was used to model the Church of Nostra Signora delle Grazie e Sant'Egidio at the macro-level in order to overcome the significant computational cost typically associated with the DEM meso-modelling of large-scale masonry structures (Galvez et al. 2023). The proposed model, which is a macro-discontinuum model, was designed to minimize computational cost by using the least number of blocks necessary to reproduce the seismic failure mechanisms such as sliding, rocking, and diagonal cracks, while employing the linearized fracture-energy-based Mohr-Coulomb constitutive model proposed by Pulatsu et al. (2020). It employs the EFM-inspired discretization, which divides the frames into piers, spandrels, and nodes, enabling the consideration of IP/OOP failures. It was demonstrated that the proposed macro-model has good agreement with its more sophisticated meso-scale counterparts and can be 150 times faster than them (Zhang et al. 2024).

Following this, the simplified EFM geometry of the church with pier-spandrel discretization used in 3Muri was employed. The 2D discretized frames were extracted from 3Muri and transformed into solids with Rhinoceros, and a simple algorithm developed using the open-access visual programming language of Grasshopper (plugin of Rhinoceros 3D) was used to discretize each element (piers, spandrels, and nodes) into eight rigid blocks. By doing so, the number of blocks reduces significantly, consequently reducing the number of interface contacts. Ultimately, by assembling all the discretized frames, the 3D DEM of the church was created. In order to evaluate the damage and failure of the apse's vault explicitly, not possible with EFM, the latter was modeled and assembled with the

rest of the structure. Moreover, corner elements were introduced at the connections among the IP- and OOP-loaded walls (Malomo and DeJong 2021, 2024). These elements consist of rigid blocks with the height identified in a way that enables the crack to propagate around the corners. This can be achieved by inserting nonlinear interfaces at the same height as the interfaces on both sides of the corners. Figure 7 summarizes the transition from EFM geometry to the final DEM of the church.

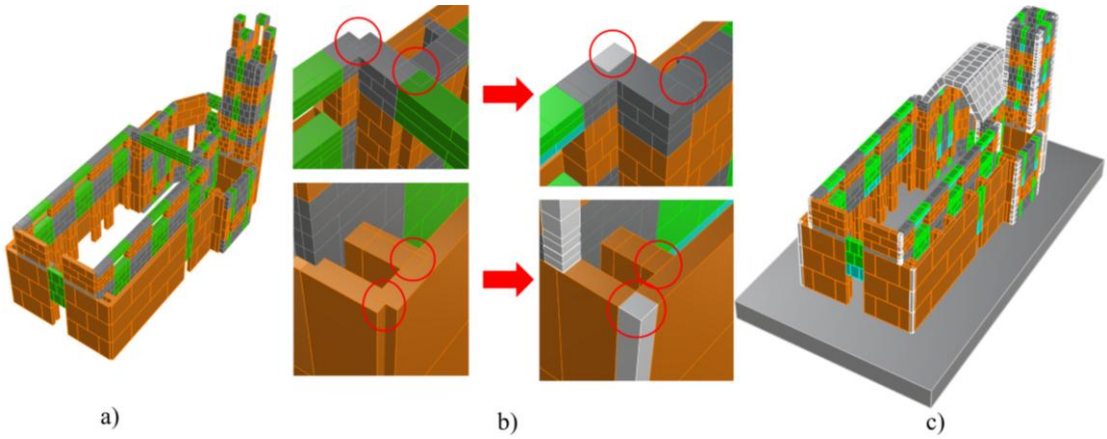

Figure 7: (a) The 3D view of the EFM-equivalent model, (b) Introducing boundary elements and eliminating intersections, and (c) The final DEM model of the church

Although modeling masonry structures with larger-than-actual size of the blocks has some advantages, such as lowering computational costs, it poses some challenges in defining the interfaces' constitutive laws. The size of the blocks can significantly affect the mechanical behavior of the masonry; consequently, it may cause block-size-dependent results. As demonstrated in literature, adopting the widely used simple Mohr-Coulomb with tension cut-off, considering the brittle behavior for the masonry, along the large blocks can overestimate the elastic stiffness and the peak strength of the masonry (Godio et al. 2018; Sarhosis and Lemos 2018).

To mitigate these block-size-dependent effects, specific adjustments were introduced in the definition of interfaces' constitutive laws. First, the normal and shear stiffness values were calibrated relative to the size of the blocks to maintain the deformations realistically and prevent artificially stiff behavior. Additionally, instead of using standard Mohr-Coulomb with tension cut-off, the fracture energy-based contact laws were adopted. Pulatsu et al. (2020) proposed new elastic-softening contact constitutive laws that incorporate fracture energies. In the mentioned study, three different shear and tension softening models (linear, polynomial, and exponential) were introduced and validated against experimental

tests. It was demonstrated that these models are able to capture the post-peak behavior of masonry in both shear and tension, which is a more realistic representation of the masonry behavior than the elastic perfectly plastic constitutive law. Furthermore, due to the consideration of fracture energies in the proposed contact laws, the dependency of the results on the block size is significantly reduced. In the current work, the Mohr-Coulomb with linear softening constitutive law for tension, compression, and shear was adopted in order to simulate the nonlinear behavior of the contacts (Figure 8).

The values of the mechanical properties are the same as the two other models, while the adopted contact law requires the cohesion (c_0), residual cohesion (c_{res}), friction angle (φ_0), and residual friction angle (φ_{res}), reported in Table 7.

Table 7: The properties of the Mohr-Coulomb model used in DEM with linear softening constitutive law

c_0 (MPa)	c_{res} (MPa)	$\varphi_0 = \varphi_{res}$ (deg)	G_c	G^I_f	G^{II}_f
0.1268	0	30	8000	15	125

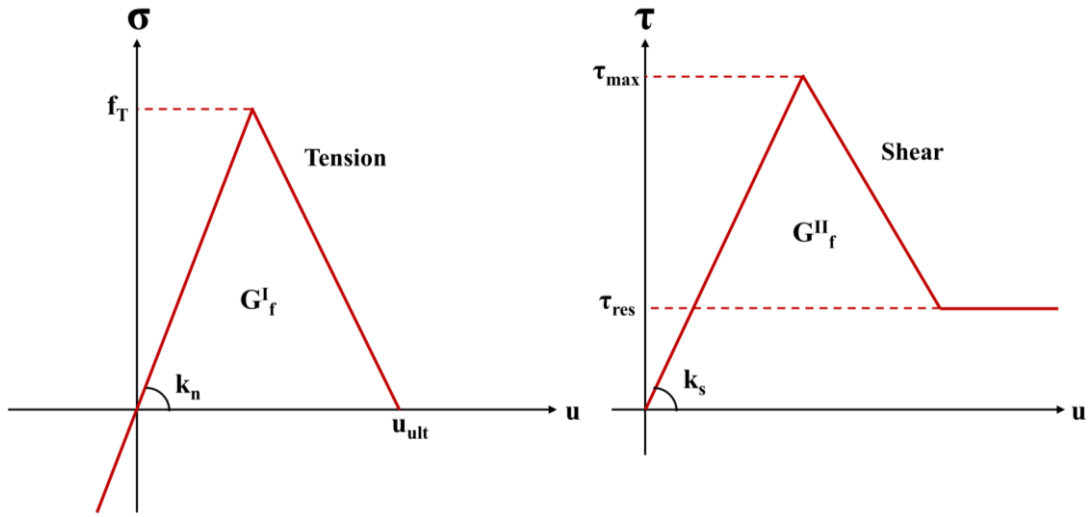

Figure 8: Adopted constitutive law for URM in DEM

4.3 Cross-calibration and Comparison of Modal Response

4.3.1 Parameter cross-calibration and elastic alignment

To ensure the compatibility and consistency of results across the three modeling strategies, a series of preliminary cross-calibrations and sensitivity analyses were

carried out. The main objective was to align the elastic and plastic properties of the models, despite their different natures and modelling principles. Specifically, the sensitivity analysis was conducted on the tensile strength and strain capacity of URM in the FEM; the resulting tensile parameters were then adopted in the EFM and DEM to improve consistency among the constitutive assumptions adopted by the three modeling approaches. For DEM, attention was also given to the equivalent elastic properties of the joints.

Masonry tensile strength is generally too low and even negligible in comparison to its compression strength (Page 1979). However, it can significantly affect the simulated seismic responses (Cattari et al. 2022a). The URM tensile capacity is handled differently by each of the considered modeling techniques, requiring calibration. The EFM model developed in 3Muri neglects the tensile strength of the masonry, while it cannot be neglected within the constitutive laws adopted in the other two models. The tensile strength and stiffening must be defined explicitly within CDP, the adopted constitutive law for FEM, to govern crack initiation and propagation effectively. In ABAQUS, tension stiffening is essential for the stability of the model, and specified using either stress-strain law or a fracture energy-based cracking criterion – a very low tensile stiffening can lead to local early cracking failure and introduce unstable global behavior in the model, leading to convergence issues (Wang and Milani 2023). For FEM, the sensitivity analysis involved creating several models of the church with varying tensile strength and strain parameters and subjecting them to lateral loads to investigate their effects on the global behavior of the structure and the model stability. Finally, the values of 0.024 and 0.05% were adopted for the maximum tensile strength and strain of the masonry, respectively. Figure 9 shows the effects of the decreasing values of tensile parameters on the pushover curves of the FEM model. As expected, reducing the tensile strength leads to a progressive decrease in lateral stiffness and the overall strength of the model. The original value of the tensile strength (black curve) yields the highest base shear, while reduced values are associated with softer behavior. The curve corresponds to 1/10 of the tensile strength (light gray curve), stops at its initial steps, and is unable to experience further displacements, indicating that the model faced convergence issues. This termination indicates that the tensile strength of the masonry was too low, consequently having lower tensile fracture energy, making the model unable to redistribute effectively the stresses after cracking initiated.

Although FEM provides a more detailed representation of geometry and stress redistribution, its nonlinear response is highly dependent on constitutive assumptions, particularly tensile strength and strain parameters in CDP framework.

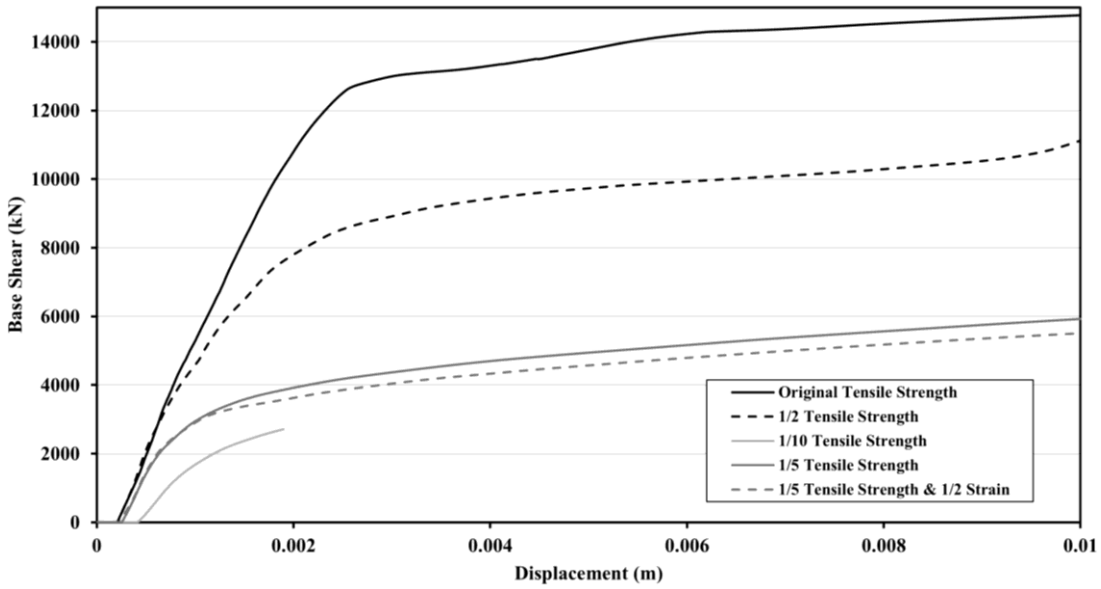

Figure 9: The effects of tensile strength and strain on the FEM pushover curves in the X direction

In DEM, to calibrate the elastic range of the behavior, a sensitivity analysis was performed on the normal and shear stiffness (k_n and k_s), while maintaining the block sizes constant. The main objective was to close the first modal natural periods of DEM with those obtained from FEM and EFM, ensuring that all the models have relatively consistent elastic stiffness. Since the stiffness of the structure in DEM is not defined directly by setting a value for the Young modulus, but exhibits itself through the interaction of the contact interfaces ($k_n=E/d$, $k_s=G/d$, where d is the distance between blocks' centroids), it was crucial to calibrate the stiffness of the joints locally in a way that the model can replicate the global elastic behavior observed in FEM and EFM.

Table 8: The natural periods for the first four modes of the DEM of the church

Modes	Case 1	Case 2	Case 3 (40% reduction)	Case 4 (50% reduction)	Case 5 (45% reduction)
1	0.530	0.384	0.500	0.543	0.517
2	0.443	0.293	0.380	0.415	0.397
3	0.346	0.262	0.341	0.371	0.355
4	0.320	0.252	0.328	0.357	0.341

Table 8 reports the results of the performed sensitivity analysis. This analysis was started by giving the constant value of $1e^9$ for the normal and shear stiffness to all the contact interfaces (Case 1). Then, due to the utilization of larger-than-actual

unit blocks and to reduce its effects on the results, the joint stiffness was calibrated based on the block sizes (Case 2). Case 2 shows the lowest natural periods across all the models, indicating the highest overall stiffness among the examined models. In Cases 3-5, the normal and shear stiffness of the joints were progressively reduced by decreasing the Young modulus by 40%, 50%, and 45%, respectively. Among them, Case 5 demonstrates better agreement with FEM and EFM modal outputs. Table 9 reports the natural periods for modes 1-4 for all three models.

Table 9:The natural periods for the first four modes of EFM, FEM, and DEM and the percentage error of each model computed with respect to the mean period value for each mode.

Modes	EFM	FEM	DEM	Error EFM (%)	Error FEM (%)	Error DEM(%)
1	0.529	0.503	0.517	2.5	-2.5	0.19
2	0.473	0.480	0.397	5.1	6.7	-11.8
3	0.459	0.278	0.355	26	-23.6	-2.4
4	0.436	0.265	0.341	25.6	-23.6	-1.7

In addition to comparing natural periods across all the models, to ensure that the models are compatible with each other to have more reliable comparisons, the mode shapes of the first-four modes of EFM, FEM, and DEM were compared as well. Figure 10 shows the mode shapes of modes 1-4 for the EFM, FEM, and DEM.

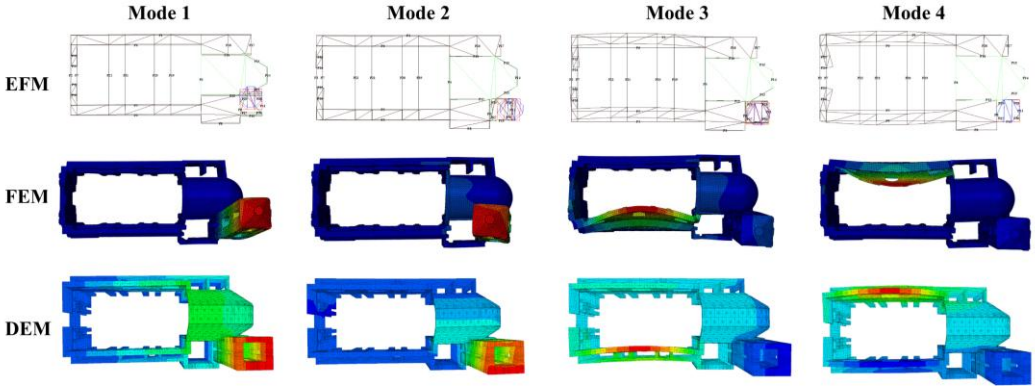

Figure 10: Comparison of the first four mode shapes obtained from EFM, FEM, and DEM of the church

As Figure 10 depicts, the three modeling strategies capture similar structural deformations and identify comparable mode shapes. The first and second modes of the church are associated with the response of the bell tower in Y and X directions, respectively, indicating that this element is probably the most vulnerable component and has a significant dynamic contribution. Mode 3 and Mode 4 involve

the OOP response of the longitudinal walls. All three modeling strategies (EFM, FEM, and DEM) successfully identified these dominant responses, confirming their alignment and consistency despite the differences in their underlying assumptions and level of discretization.

4.3.2 Modal comparison: MAC index

The mode shapes obtained from the modal analysis on the three churches modeled based on EFM, FEM, and DEM were compared using the MAC index. The MAC is a statistical indicator that quantifies the similarity between two different mode shapes and is calculated as the normalized scalar product of two sets of vectors φ_A and φ_B (Allemang 1980, 2003). In Equation 10, the numerator represents the squared product of the two mode shapes and the denominator normalizes this product by the magnitudes of the mode shapes.

$$\mathrm{MAC}(\varphi_A, \varphi_B) = \frac{|\varphi_A^T \times \varphi_B|^2}{(\varphi_A^T \varphi_A) \times (\varphi_B^T \varphi_B)} \tag{10}$$

The MAC index results in a value between 0 (no correlation) and 1 (perfect correlation), and the resulting scalars are arranged in the MAC matrix (Pastor et al. 2012). To calculate MAC, it is necessary to consider analogous nodes on the three models. The selected nodes were primarily on the vulnerable macro-elements of the church, which were identified from the mode shapes. Totally, 44 nodes were selected from the longitudinal walls, façade, apse, and bell tower of the church (20 nodes on the first level, 20 nodes on the second level, and 4 nodes on the third level). These nodes were consistently matched across all the EFM, FEM, and DEM to ensure fair comparisons. Table 10 presents the MAC matrices comparing the first four modes of FEM, DEM and EFM.

Table 10: MAC matrices for FEM, DEM, and EFM (The MAC indexes are in percentage)

	FEM vs DEM (%)				FEM vs EFM (%)				DEM vs EFM (%)			
Modes	**1**	**2**	**3**	**4**	**1**	**2**	**3**	**4**	**1**	**2**	**3**	**4**
1	49	42	1	1	32	60	1	0	90	7	14	0
2	41	33	1	0	69	38	1	0	0	72	2	2
3	18	0	89	7	16	7	36	26	11	9	63	15
4	16	12	3	86	12	10	34	20	5	4	22	38

The FEM-DEM matrix demonstrates that the DEM, despite having more simplified geometric and discretization, can capture satisfactorily the OOP response of the longitudinal walls (modes 3 and 4) with strong correlations (85% to 88%). The moderate correlation for modes 1 and 2 (49% and 33%) indicates that the DEM

replicates the response of the bell tower in both main directions relatively well. However, there are some differences resulting from different modeling assumptions. Utilizing more simplified geometry and coarser discretization in DEM can lead to different mass and stiffness distributions compared to FEM, which is a finely meshed and highly detailed model. This shows that although DEM's simplified geometry causes some differences in how the tower and walls contribute to mode shapes, its block-based approach can capture the main responses, especially the OOP mechanisms.

The FEM-EFM matrix shows good correlations in the first two modes (59% - 68%), while the correlations for modes 3 and 4, compared to FEM-DEM, significantly drop to 33% and 36%, respectively. This shows that EFM does not reliably catch the OOP response of the longitudinal walls despite defining in some macro-elements 3D-piers, with stiffness and strength in the two orthogonal directions. In addition to employing simplified geometry, EFM neglects the OOP stiffness of most of the macro-elements, leading to more differences in stiffness distribution throughout the structure, which can affect the mode shapes.

Finally, the DEM-EFM matrix shows that these models are strongly aligned with each other in capturing the response of the bell tower, with high correlations in modes 1 and 2 (89% and 71%). This is reasonable since the geometry of the DEM was directly extracted from the EFM-inspired discretization, dividing the frames into piers, spandrels, and nodes. However, the correlations for modes 3 and 4, the OOP of the walls, are moderate (62% and 37% respectively). This moderate correlation can be because of the fundamental difference between these two modeling strategies in how the mass and stiffness distributions affect the mode shapes and modal displacements, especially for the modes where the OOP mechanisms of the components are dominant. For these modes, the displacement of the walls and façade in DEM results from both the OOP response of the walls themselves and the IP response of the buttresses connecting the exterior and interior walls. In contrast, in the EFM, the OOP stiffness of the walls is neglected, and the OOP displacement of the walls is just a result of the IP response of the buttresses.

It should be noted that the relatively low diagonal MAC values and the presence of significant off-diagonal values are mainly associated with the difference in modal characteristics of the modeling strategies. For modes 1 and 2, DEM and EFM capture the response of the bell tower along the principle axes of X and Y, while FEM exhibits the response of the tower along the diagonal direction between the two axes. Therefore, each FEM MAC value partially correlates with corresponding values of DEM and EFM, resulting in comparable diagonal and off-diagonal values.

The similar effect is observed for modes 3 and 4, which are associated with the OOP response of the longitudinal walls. FEM and DEM captured the response of the lateral walls independently, while in EFM, walls vibrate together, resulting in the distributed modal correlations for modes 3 and 4 between FEM/DEM and EFM.

In summary, the comparison of the MAC matrices demonstrates how the level of refinement and the underlying assumptions of the models can have some effects on capturing the key structural behaviors. Among the mentioned strategies, the FEM provides the most detailed geometric and continuum representation of the church, at least in the initial elastic field. The DEM, despite its more simplified geometry and discretization, has a relatively good agreement with FEM, especially in the modes that OOP mechanisms are dominant. The EFM, as the most simplified strategy, performs well in capturing dominant IP responses but underestimates OOP responses.

4.4 Comparative Seismic Analysis

This section presents a comparative seismic analysis of the Church of Nostra Signora delle Grazie e Sant'Egidio based on the modeling strategies described in the previous sections. The aim is to evaluate the consistency and differences among these modeling strategies in terms of dynamic properties, global capacity, and failure mechanisms. The primary metrics used in this comparative analysis are pushover curves to assess the global lateral capacity of the church and failure mechanisms to identify the local damage mechanisms. The results can assist in choosing a suitable modeling strategy for complex religious URM structures by providing insights into the trade-offs between accuracy and computational costs.

4.4.1 Global capacity comparison: Pushover curves

International codes consider global seismic assessment procedures for structures based on linear and non-linear, static and dynamic analyses, which mainly differ in the way that forces are distributed. Linear analysis assumes that the forces are distributed proportionally to the initial stiffness of the elements, whereas non-linear analysis accounts for stiffness degradation and load redistribution due to damage progress and crack propagation, providing a more realistic structural response near collapse (Magenes 2006). Among non-linear approaches, dynamic analyses are the most sophisticated; however, these analyses are computationally intensive, necessitate the selection of spectrum-compatible accelerograms, and require high expertise to interpret the results. Therefore, the non-linear static (pushover) analyses are preferred due to their reduced computational effort and

easiness in interpreting the results (Mouyiannou et al. 2014; Lagomarsino and Cattari 2015a; Pantò and Caliò 2021). For these reasons, the pushover analysis was adopted in this study to assess the seismic behavior of the church.

For the comparative assessment, the pushover analyses were performed in both the longitudinal (X) and transversal (Y) directions of the church. To ensure consistency across all the three modeling strategies, the same mass-proportional lateral loads were applied in each direction, with considering different control nodes: i) one at the right side of the apse, close to the bell tower, representing the global behavior of the church, ii) one at the back of the apse vault for the +X direction, iii) one at the top of the façade for the -X direction, iv) one at the top of the northern longitudinal wall for the +Y direction, and v) one at the top of the southern longitudinal wall for the -Y direction.

Preliminary pushover analyses revealed that the most vulnerable component of the church is its bell tower, which governs the global response. Its early failure, especially in the X direction, prevented the observation of the progress of damage in the other macro-elements of the church, thereby limiting the assessment of its global seismic behavior. Therefore, in order to investigate the damage evolution throughout the entire structure and exclude the bell tower from the analyses, the elastic material properties of URM were assigned to it. The base shear-displacement curves obtained from the EFM, FEM, and DEM models in both X and Y directions are shown in Figure 11.

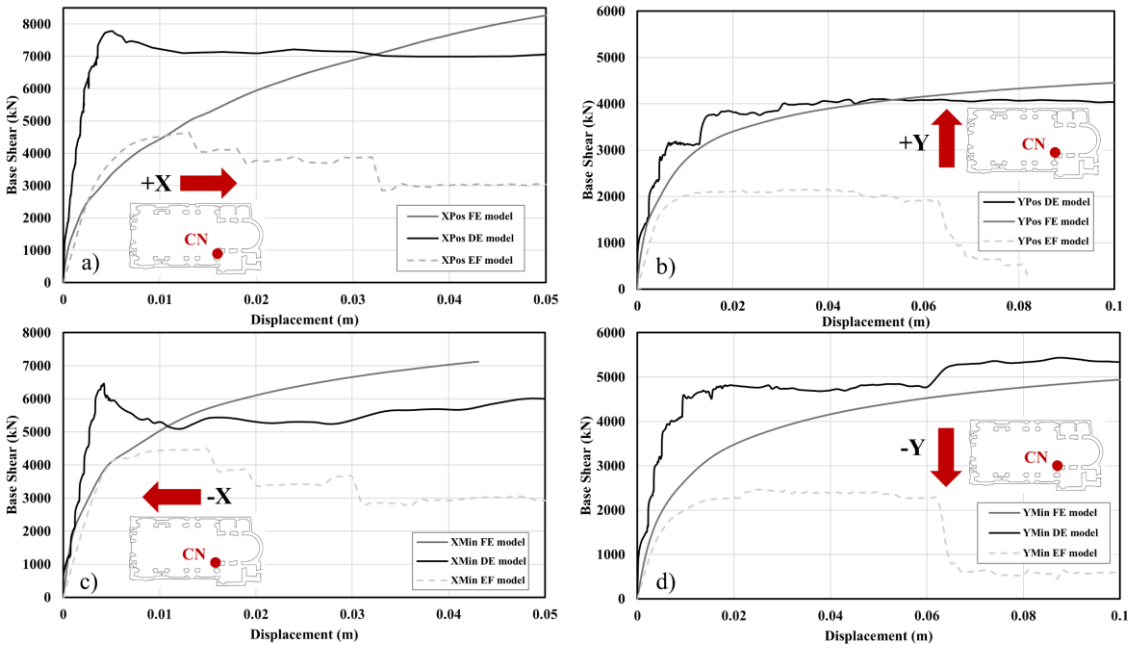

Figure 11: The base shear-displacement (pushover) curves of EFM, FEM, and DEM in the a & c) X direction and b & d) Y direction.

The modeling strategies differ in discretization, failure representation, adopted constitutive laws, and redistribution, leading to distinct pushover curves: FEM shows a gradual and smooth behavior with gradual stiffness degradation; DEM exhibits fluctuations due to the separation and collision of the blocks; EFM would likely show conservative with the overall lower capacities, as it cannot fully capture the 3D interactions and load redistributions that govern the real structure behavior.

From the comparison of the pushover curves, the church has greater vulnerability in the Y direction across all the modeling strategies. In both the positive and negative Y direction, the maximum base shear is lower than that in the X direction. This could mainly be due to the structural configuration; the response of the structure in the Y direction primarily consists of the OOP response of the longitudinal walls, which are more susceptible to instability due to their slenderness and lack of a vault. In contrast, the structure in the X direction benefits from the walls acting IP and supporting the façade and apse, resulting in higher stiffness and strength.

In addition, the EFM is able to capture the initial stiffness of the church reasonably well, showing that the behavior of the church is relatively close to the one obtained by FEM and DEM in the elastic range. However, it underestimates the maximum strength of the structure, remaining on the safe side for assessment

purposes. In order to have a deeper understanding of the behavior of the church and the performance of all the three numerical modeling procedures, the pushover curves were also assessed with considering the control nodes on the critical macro-elements in each direction.

A) The longitudinal direction (+X and -X)

In the longitudinal direction (Figure 12), the pushover curves were assessed by considering the control nodes on the back of the apse vault and the top of the façade for the +X and -X directions, respectively. In this direction, the two longitudinal walls are subjected to IP loading, whereas the façade (west) and apse (east) are subjected to OOP actions. In the +X direction (pushes towards the apse), FEM and DEM exhibit relatively similar initial stiffness and reach almost the same peak base shear of approximately 6000-6500 kN, while EFM shows a lower peak base shear (approximately 4500 kN), although it reproduces the initial stiffness relatively similar to the refined models. In the -X direction (pushes towards the façade), the peak strengths are lower (5500-6500 kN). This difference is likely because the critical macro-element in this direction, which is the façade subject to the OOP loadings, has fewer transversal restraints (being connected only to the longitudinal walls) than the apse, whose behavior governs the response in the +X. Therefore, the façade is more vulnerable when subjected to OOP actions, while under the reversed loading (+X), the stiffer and well-connected apse provides a greater resistance, delaying the activation of its overturning mechanism.

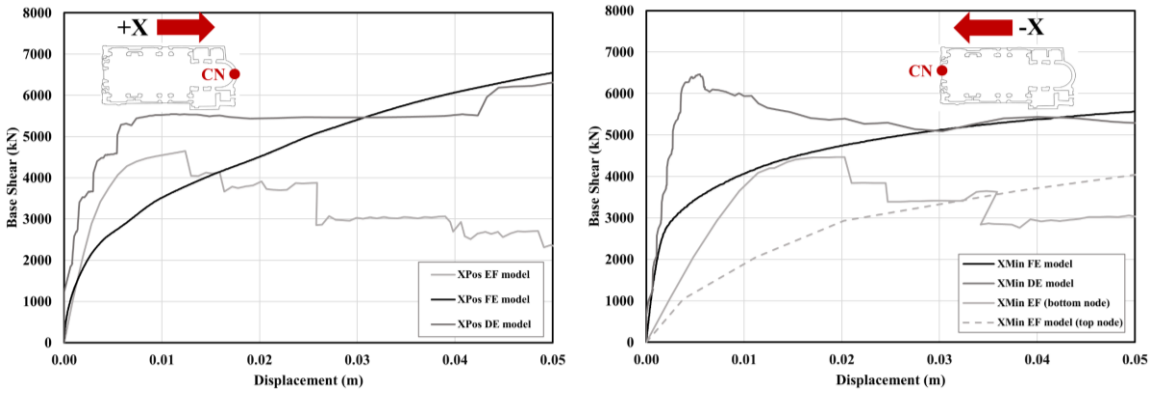

Figure 12: The pushover curves in the longitudinal direction considering control nodes on the critical macro-elements

Therefore, since the OOP mechanism of the façade is more critical in the longitudinal direction, two control nodes were considered for the façade in the EFM model: one at the bottom of the top pillar element of the façade and one at its top.

Regarding the bottom node, EFM shows softer behavior and again underestimates the lateral strength, with the peak base shears of approximately 4500 kN— roughly 70-80% of the values predicted by the other two approaches. The curve obtained from the top control node indicates that the upper pillar element exhibits much lower initial stiffness and an earlier onset of damage, highlighting the activation of the local OOP mechanism in the early stages. This difference is primarily attributed to the inherent limitation of the EFM approach in capturing the full OOP stiffness contribution. These results show that the manual addition of the pillars at the macro-element, whose OOP response may be critical, although underestimating the stiffness and strength provided by the actual 3D geometry, improves the representation of the OOP behavior and can be useful to identify the early activation of local mechanisms for subsequent retrofitting design purposes.

B) The transversal direction (+Y and -Y)

In the transversal direction (Figure 13), the pushover curves were assessed by considering the control nodes on the top of the northern and southern longitudinal walls for the +Y and -Y directions, respectively. In this direction, the two longitudinal walls of the nave are loaded OOP, while the perpendicular walls (including the façade, triumphal arch, and apse return walls) act as buttresses, being subjected to IP loadings. In the +Y direction, both FEM and DEM show high initial stiffness and reach the peak strength of approximately 4000 – 4300 kN. In the -Y direction, DEM shows a slightly stiffer behavior than the one obtained by FEM, and both curves reach the peak strength of approximately 5000-5200 kN. The difference is likely due to the different geometry and connections on the north and south sides of the church (presence of the northern sacristy walls and the tower on the southern side).

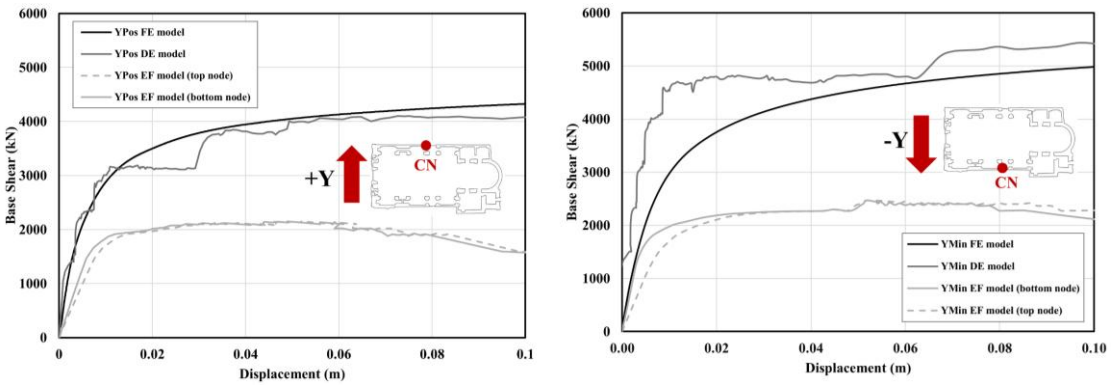

Figure 13: The pushover curves in the transversal direction considering control nodes on the critical macro-elements

For the EFM in both the transversal directions, two additional control nodes were considered on the 3D-pier elements located at the top of the nave walls, one at the top and one at the bottom of the elements, in order to evaluate how this model captures the OOP response of these macro-elements. The comparison shows that the EFM reproduces a softer behavior than the one obtained by the refined models and underestimates the lateral capacity, with the peak base shear of approximately 2500 kN (50% of the values predicted by the other two approaches). In addition, in contrast to the behavior of the façade in -X direction, the pushover curves obtained from the top and bottom control nodes are very close to each other, although the curve obtained from the top node shows a slightly softer behavior, confirming that the OOP response of the façade is more critical than that of the longitudinal walls.

This confirms the limitation of the EFM approach in capturing the OOP response of the elongated nave walls. As observed in both the longitudinal and transversal directions, the pier-spandrel idealization, even when supplemented by 3D-pier elements, cannot reproduce the real 3D responses captured by the continuum and discontinuum models.

Overall, whenever OOP mechanisms, whether of the façade (longitudinal direction) or of the longitudinal walls (transversal direction), play a significant role, which is quite common in structures with irregular configurations, FEM and DEM yield the higher lateral capacity and initial stiffness. EFM produces lower capacities (40-60% lower than the ones predicted by FEM and DEM), leading to a safe-side assessment of the seismic capacity.

4.4.2 Failure mechanisms and damage patterns

Since the damage presentations differ in the three modeling approaches, comparing them according to either the equal displacements or base shear would not be a fair comparison. According to the Eurocode 8 (EN 1998-3 2006), three limit states can be defined for URM structures based on the severity of damage: Damage Limitation (DL), Severe Damage (SD), and Near Collapse (NC). Following this, three performance levels were defined for the three approaches to compare damage at the comparable physical conditions of the structure. The DL performance level corresponds to the onset of localized damage, where the structure is essentially elastic, and damage is concentrated in limited regions. SD represents an intermediate condition, characterized by the propagation of cracks and stiffness reduction, indicating how damage spreads in the structure and which failure mechanisms begin to govern the response of the structure. Finally, NC corresponds to the formation of collapse mechanisms and final failure modes in one or more

macro-elements. Because FEM, DEM, and EFM express damage through different variables and indicators, applying a single universal threshold cannot be meaningful. Therefore, model-specific criteria were adopted to ensure that DL, SD, and NC correspond to comparable conditions of the structure across all three approaches. Table 11 reports the criteria adopted to identify performance levels for each modeling approach.

Table 11: Adopted criteria for defining performance levels in FEM, DEM, and EFM

	FEM	DEM	EFM
Damage Limitation (DL)	A change in the initial stiffness	First interface sliding/separation	First plastic hinge (change in the initial stiffness)
Severe Damage (SD)	80% of the NC base shear	Peak of the pushover curve	Peak of the pushover curve (development of failure mechanisms)
Near Collapse (NC)	Last step of the curve	80% of the peak shear/ Activation of the mechanism	First significant drop in the base shear

Because FEM and DEM provide a richer and more explicit representation of damage and failure mechanisms, the comparison of damage was first carried out between these two approaches. This allows identifying the critical macro-elements and failure mechanisms in each direction in the highest level of detail. As these critical macro-elements were recognized, the EFM results were assessed to examine whether it can reproduce the same failure mechanisms. This sequential comparison ensures that EFM, as a simpler methodology that produces more conservative results, is evaluated against two refined approaches and its capabilities are assessed in a meaningful way.

All three modeling approaches indicate that the structural response is mainly governed by flexural and rocking OOP mechanisms of the slender longitudinal walls in the Y direction, whose stability is further compromised due to the lack of a vault and limited restraints. In this direction, the lack of effective transverse connections and constraints, and the presence of elongated, slender walls significantly reduce box-like behavior, leading to lower lateral resistance. On the other hand, the OOP overturning mechanisms of the apse and façade, together with the IP shear mechanisms of the longitudinal walls, govern the behavior in the X direction. In this configuration, longitudinal walls act predominantly IP and, through their interactions with the apse and façade, which provide transversal constraint, develop a partial box-like behavior of the structure. These IP

mechanisms enhance the load distribution among orthogonal elements and increase the lateral stiffness compared to the Y direction, where the response is mainly dominated by OOP mechanisms. A more detailed examination of the failure mechanisms and damage evolution is presented in the following subsections.

A) The longitudinal direction (+X and -X)

Figure 14 illustrates the pushover curves in the longitudinal direction for both FEM and DEM, with the DL, SD, and NC performance levels marked according to the criteria defined in Table 11.

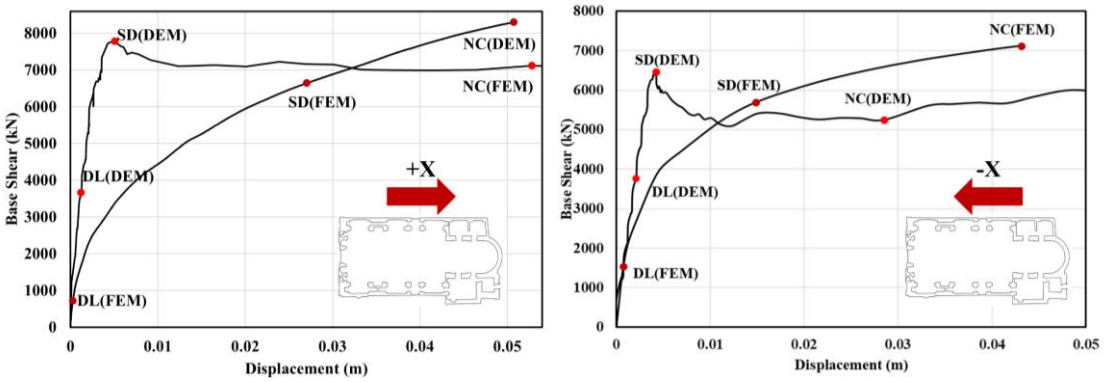

Figure 14: Performance levels on the longitudinal pushover curves of FEM and DEM

Based on the performance levels identified in Figure 14, the corresponding damage patterns were compared to determine the governing mechanisms in the longitudinal direction.

Table 12: Damage and failure mechanisms at DL, SD, and NC performance levels in +X direction

PL	Macro-element	DEM	FEM	Damage/Mechanism
DL	Apse	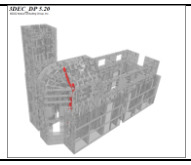	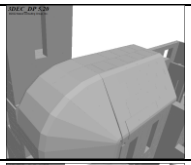	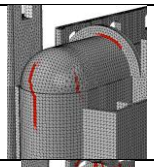	Initiation of the OOP flexural-torsional response of the apse
SD	Apse	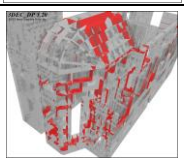	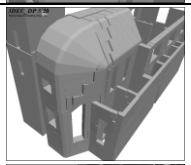	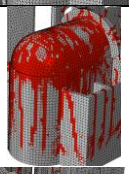	Progression of the OOP flexural-torsional mechanism of the apse vault
	Façade	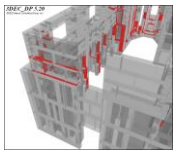	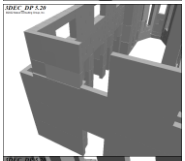		OOP mechanism of the façade
	Northern Longitudinal wall	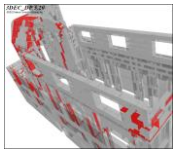	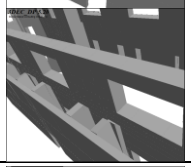	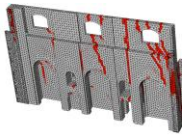	IP shear mechanism of the northern longitudinal wall
NC	Apse	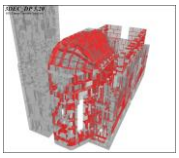	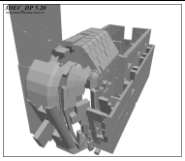	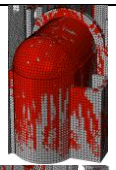	Full OOP mechanism of the apse
	Façade	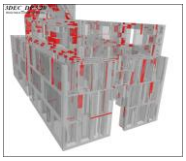	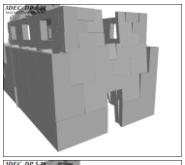	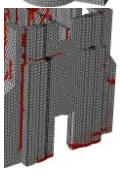	Full OOP mechanism of the façade
	Longitudinal walls	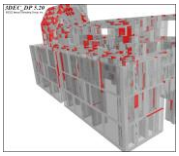 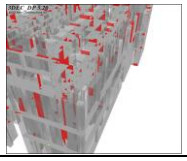	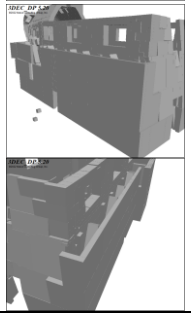	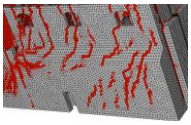 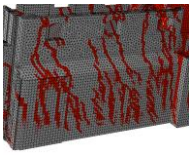	Full IP shear mechanism of both the longitudinal walls

Table 13: Damage and failure mechanisms at DL, SD, and NC performance levels in -X direction

PL	Macro-element	DEM	FEM	Damage/Mechanism
DL	Longitudinal walls	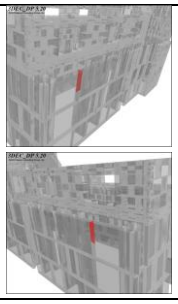	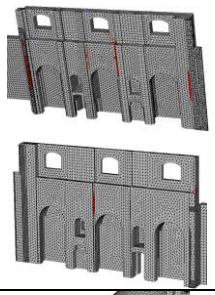	Initiation of the IP shear mechanism of both the longitudinal walls
SD	Apse	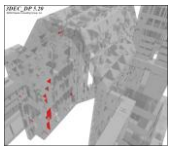	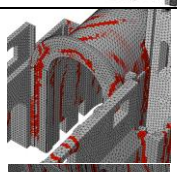	Flexural response of the apse vault OOP response of the apse walls
	Longitudinal walls	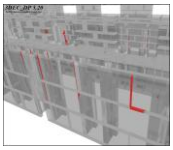	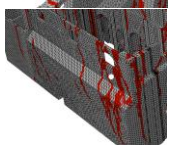	IP shear response of the façade, with the damage concentration close to the façade
NC	Apse	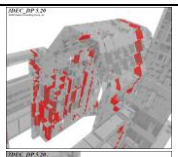	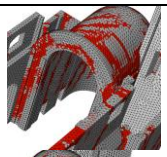	Full OOP response of the apse
	Façade	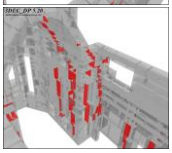	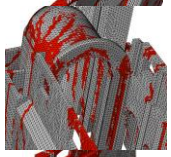	Full OOP mechanism of the façade
	Longitudinal walls	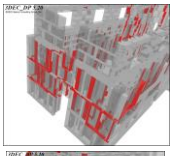	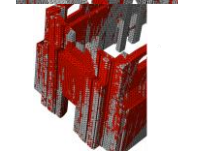	Full IP shear mechanism of both the longitudinal walls

In the +X direction, both models exhibit that the damage initiates from the apse. At DL, the first cracks appear as vertical cracking on the right side of the apse back wall, indicating the initiation of an OOP flexural-torsional response, in which the torsional component is mainly due to the asymmetric restraint introduced by the tower. As the structure progresses to the SD performance level, the OOP response of the apse becomes more pronounced and is accompanied by the onset of the OOP response of the façade and IP shear response of the northern longitudinal wall, both of which are influenced by the same torsional behavior. At NC, both models anticipated a full OOP mechanism of the apse and façade with a fully developed IP shear mechanism of the longitudinal walls as the final collapse mechanisms.

In the -X direction, the damage is first observed in the longitudinal walls. At DL, the initial vertical cracks indicate the onset of an IP shear response of these macro-elements. At SD, the damage of the longitudinal walls was intensified and accompanied by the activation of the OOP flexural response of the apse, expressed through the vertical cracks in the apse walls. Finally, the collapse mechanism predicted by both models at NC is a full OOP mechanism of the apse and façade, together with an IP shear mechanism of the longitudinal walls.

The damage patterns reported for the longitudinal direction clearly indicate that the behavior of the church in ±X direction is mainly governed by the combination of the OOP response of the apse and façade and the IP shear deformation of the longitudinal walls. FEM and DEM consistently reproduced the same sequence of damage progression and final collapse mechanisms.

B) The transversal direction (+Y and -Y)

Figure 15 illustrates the pushover curves in the transversal direction for both FEM and DEM, with the DL, SD, and NC performance levels marked according to the criteria defined in Table 11.

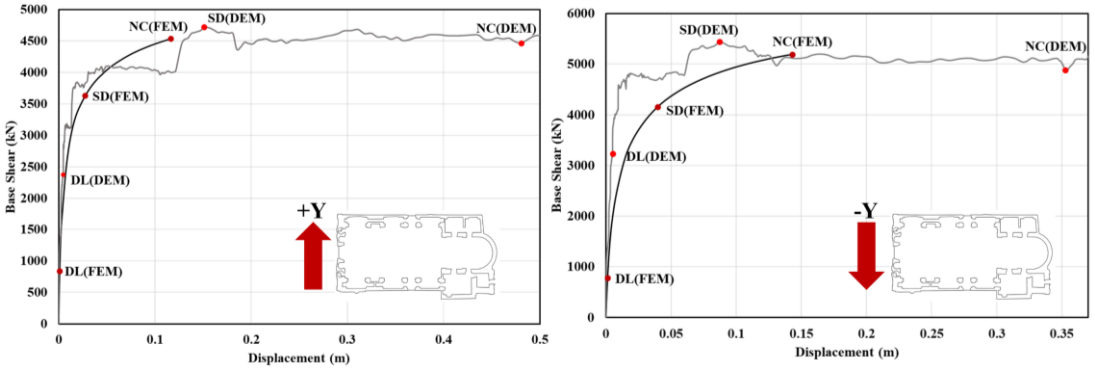

Figure 15: Performance levels on the transversal pushover curves of FEM and DEM

Based on the performance levels identified in Figure 15, the corresponding damage patterns were compared to determine the governing mechanisms in the transversal directions. Table 14 and Table 15 report damage patterns and mechanisms at all the performance levels in the transversal direction.

Table 14: Damage and failure mechanisms at DL, SD, and NC performance levels in +Y direction

PL	Macro-element	DEM	FEM	Damage/Mechanism
DL	Apse	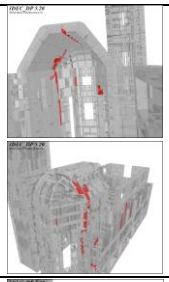	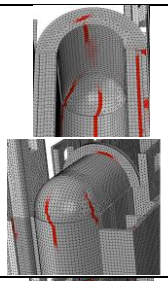	Flexural and shear response of the apse vault
SD	Apse	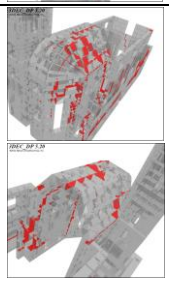	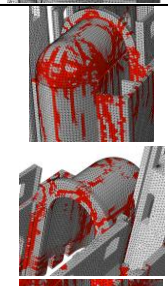	Progression of the flexural mechanism of the apse vault Increased torsional deformation of the apse
	Sacristy	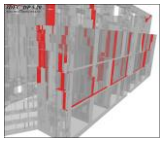	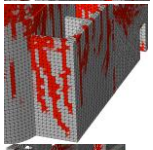	OOP rocking
	Façade	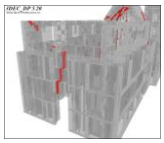	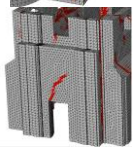	IP shear response of the façade
	Northern Longitudinal wall	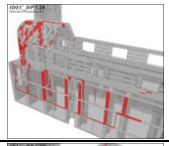	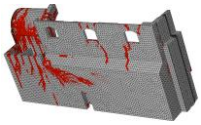	OOP response of the longitudinal wall
NC	Apse	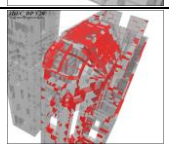	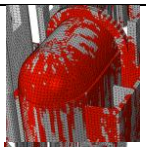	Full flexural and torsional mechanism of the apse
	Façade	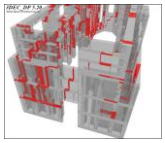	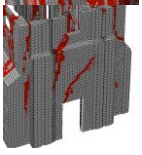	Full IP shear mechanism of the façade
	Longitudinal walls	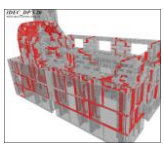	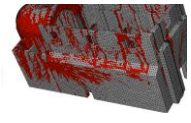	Full OOP mechanism of both the longitudinal walls

Table 15: Damage and failure mechanisms at DL, SD, and NC performance levels in -Y direction

PL	Macro-element	DEM	FEM	Damage/Mechanism
DL	Northern Longitudinal wall	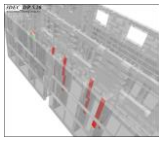	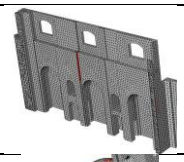	Initiation of OOP mechanism of the longitudinal wall
SD	Apse	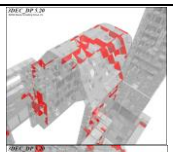	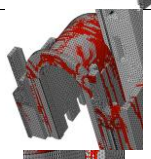	Flexural and shear mechanisms of the apse vault
	Sacristy	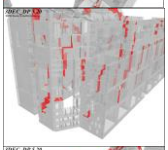	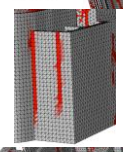	OOP rocking
	Façade	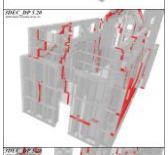	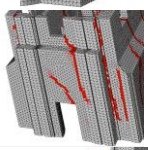	IP shear response of the façade
	Longitudinal walls	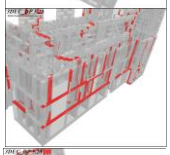	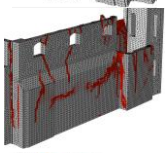	OOP response of the longitudinal walls
		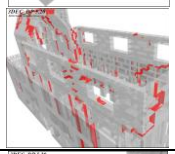		
NC	Apse	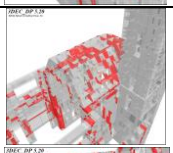	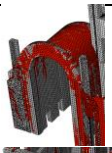	Full flexural and shear mechanisms of the apse
	Façade	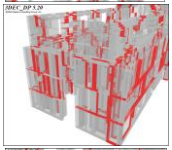	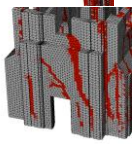	Full IP shear mechanism of the façade
	Longitudinal walls	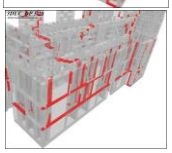	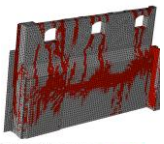	Full OOP mechanisms of both the longitudinal walls
		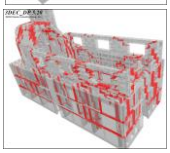	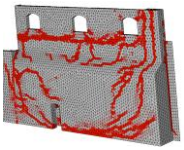	

In the +Y direction, both models show that damage initiates from the apse. At DL, the first cracks consist of a longitudinal crack along the intrados of the vault, indicating the initiation of a flexural response, and vertical cracking concentrated at the back of the apse caused by the pushing forces transmitted by the tower. As the performance level progresses to SD, this mechanism becomes more pronounced and is accompanied by the onset of OOP rocking response of the longitudinal wall and IP shear cracking in the façade. At NC, FEM and DEM converge to the same mechanisms: a full OOP mechanism of the longitudinal walls along with the flexural-shear response of the apse and IP shear mechanism of the façade.

In the -Y direction, damage at DL is characterized by the initiation of OOP displacement of the northern longitudinal wall, forming the vertical cracks captured in both models. At SD, damage progresses with the development of longitudinal and transversal cracks in the apse vault, indicating a flexural-shear mechanism, together with the IP shear cracking in the façade, exhibiting the onset of the IP rocking of this macro-element. At NC, both models again predict the same collapse scenarios: a full flexural-shear mechanism of the apse, a full IP shear mechanism of the façade, and a complete OOP rocking mechanism of both the longitudinal walls.

The damage patterns reported in Table 14 and Table 15 show that, in the transversal direction, the response of the church is mainly governed by the OOP rocking of the nave longitudinal walls, interacting with flexural-shear deformation of the apse and shear damage in the façade, with FEM and DEM predicting the same sequence of damage progression and final collapse mechanisms.

C) Comparison with the EFM mechanisms

Following the identification of main failure mechanisms through the detailed comparison of FEM and DEM, the performance levels of DL, SD, and NC were also identified for the EFM according to the criteria defined in Table 11, which are shown in Figure 16.

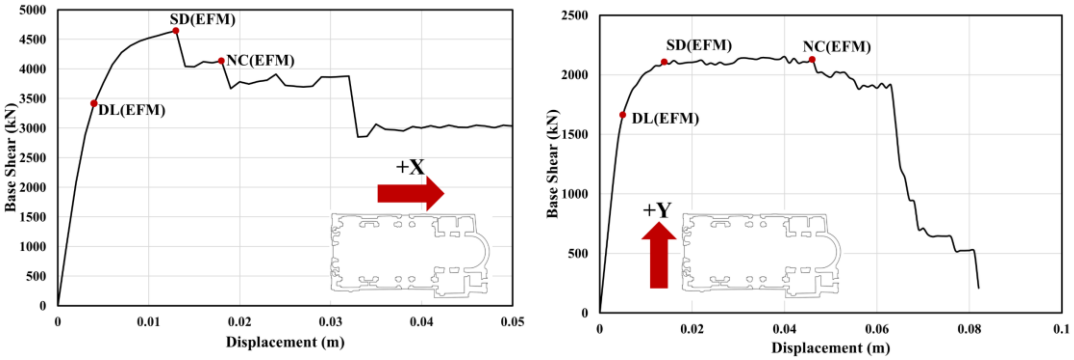

Figure 16: Performance levels on the +X and +Y directions of EFM

The comparison was carried out in terms of the activation, evolution, and final mechanisms at the DL, SD, and NC for the +X and +Y directions, with considering FEM and DEM as reference models to evaluate whether EFM is capable of predicting similar mechanisms. Given that the 3D-piers were only defined for the macro-elements of façade and longitudinal walls, it is possible to evaluate the potential OOP mechanisms of these macro-elements. The color legend for the damage in EFM, which was shown in Table 16 and Table 17, is as follows: yellow and red are for flexural OOP and IP mechanisms, respectively; light and dark blue are for OOP and IP failures, respectively; and orange is for the combination of IP and OOP mechanisms.

For the longitudinal direction (Table 16), EFM predicts, at the DL performance level, the onset of IP flexural responses of the longitudinal walls with the initiation of an OOP mechanism of the façade. At SD, these mechanisms became more pronounced and were accompanied by the IP shear and flexural response of the apse and sacristy walls. Finally, at NC, while FEM and DEM predicted the OOP response of the apse and EFM cannot capture it, EFM predicted a full OOP mechanism of the façade with a fully developed IP flexural mechanism of the longitudinal walls, which is aligned with the responses obtained from the other two approaches.

Table 16: Damage and failure mechanisms at DL, SD, and NC performance levels of EFM in the +X direction

PL	Macro-element	EFM	Damage/Mechanism
DL	Longitudinal walls		Initiation of the IP flexural mechanism of both the external longitudinal walls
	Façade	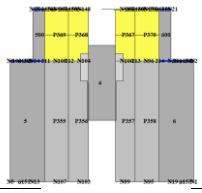	Initiation of the OOP mechanism of the facade
SD	Apse walls	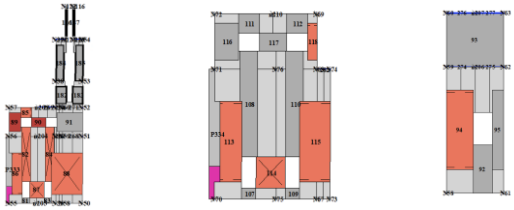	IP flexural and shear mechanisms of the apse walls
	Longitudinal walls	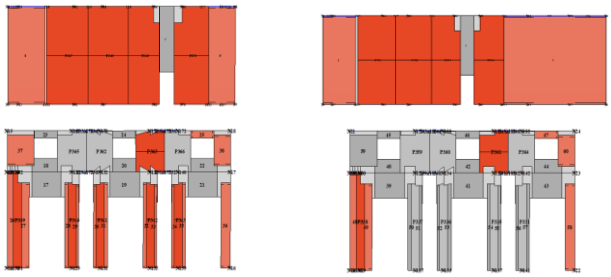	IP flexural mechanism of the exterior and interior longitudinal walls
	Facade	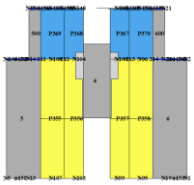	OOP mechanism of the façade
NC	Façade	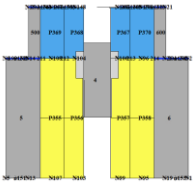	Full OOP mechanism of the façade
	Longitudinal walls	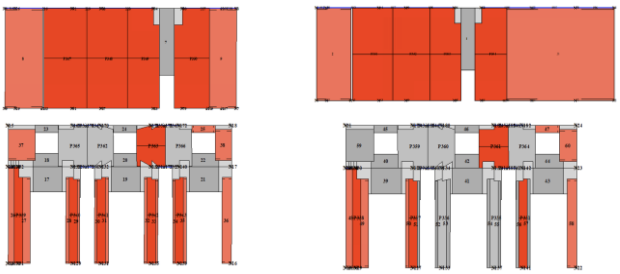	Full IP shear mechanism of both the longitudinal walls

In the transversal direction (Table 17), EFM, at the performance level of DL, shows the onset of the IP flexural response of the façade and apse triumphal arch, and the OOP response of the southern longitudinal wall. At SD, the OOP response of the both longitudinal walls was activated and the IP mechanism of the façade was pronounced, which is aligned with the mechanisms predicted by FEM and DEM at this performance level. Finally, at NC, EFM predicted identical damage mechanisms with the other two approaches: a full OOP mechanism of the longitudinal walls together with the a full IP flexural mechanism of the façade.

Table 17: Damage and failure mechanisms at DL, SD, and NC performance levels of EFM in the +Y direction

PL	Macro-element	EFM	Damage/Mechanism
DL	Longitudinal walls	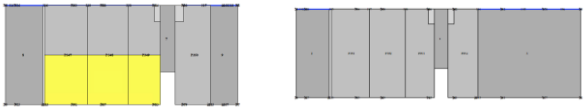	Initiation of the OOP flexural mechanism of both the southern wall
	Façade	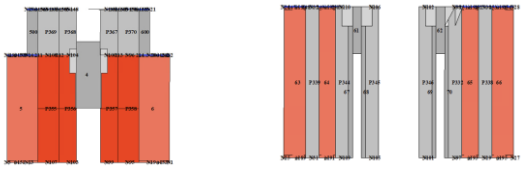	Initiation of the IP mechanism of the facade
SD	Longitudinal walls	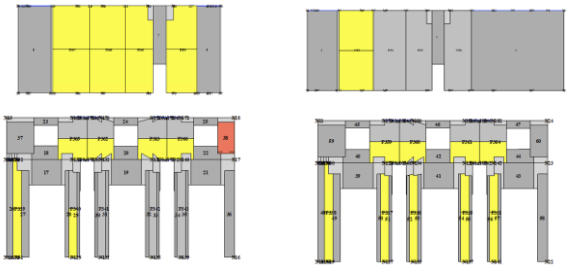	OOP flexural mechanism of the exterior and interior of the both longitudinal walls
	Facade	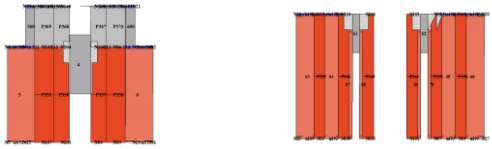	IP mechanism of the façade
NC	Façade	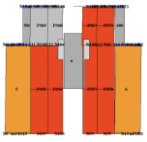	Full IP mechanism of the façade
	Longitudinal walls	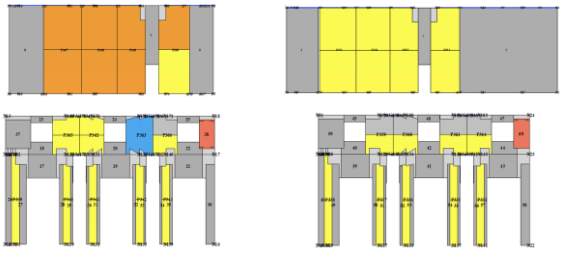	Full OOP mechanism of both the longitudinal walls

Overall, the comparison demonstrates that, by adopting 3D-pier elements, the EFM is able to capture OOP responses of macro-elements whose behavior is governed by local OOP mechanisms, such as longitudinal walls, when the church is subjected to horizontal loads in the Y direction. Moreover, it is also capable of capturing the torsion behavior that FEM and DEM predicted in the transversal direction, by exhibiting 3D-pier elements of the longitudinal wall and façade that experienced the combination of IP and OOP mechanisms (Orange elements). In addition to OOP mechanisms, the results showed that EFM can also capture IP mechanisms of elements that were proved to be vulnerable in the longitudinal direction by two other approaches. However, the main difference arises in the representation of the damage mechanism governing the response of the apse vault, which is one of the vulnerable macro-elements in FEM and DEM, since it is not feasible to explicitly model it in EFM and evaluate its damage patterns. As a result, EFM predicted the IP and OOP mechanisms of critical macro-elements, particularly at the SD and NC performance levels with a good agreement with mechanisms observed in FEM and DEM.

4.5 Conclusions

This study presents a comparative seismic assessment of the ruined URM Church of Nostra Signora delle Grazie e Sant'Egidio using three different modeling approaches: a continuum finite element model (FEM), an equivalent frame model (EFM), and a discontinuum discrete element model (DEM). The FEM was developed using detailed maps derived from laser scanning campaigns, making it the most refined model of the church; then, geometrical simplifications were introduced to develop the EFM and DEM to reduce the computational effort while maintaining the main characteristics and load-bearing system of the structure.

The modal analyses demonstrate the satisfactory consistency among three modeling approaches in identifying the main mode shapes and dynamic properties. The first two modes are associated with the response of the bell tower, while higher modes are associated with the OOP response of the nave longitudinal walls. The MAC matrices showed that DEM is closer to FEM than EFM, especially for the modes that the OOP mechanism of the walls governs the behavior. This indicates that macro-block DEM, despite its simplified discretization and larger-than-unit blocks, has a strong ability to reproduce the dynamic behavior of the church, while EFM is less reliable when OOP responses govern the seismic behavior.

The pushover curves exhibit a relatively constant trend, despite of their distinct characteristics in terms of damage representations, leading to different non-linear responses. The FEM considers the structure as a continuum deformable body and represents more detailed load redistribution, resulting in a smooth nonlinear response. The DEM was able to capture local damages, such as sliding, separation, and rocking of blocks, leading to fluctuating but more physically meaningful responses. The EFM, the most simplified approach, efficiently reproduced the global behavior of the structure; however, its inability to capture full OOP mechanisms, despite of defining 3D-piers in critical macro-elements, resulted in anticipating lower stiffness and maximum strength compared to the other two approaches.

The comparative analyses revealed that all three modeling approaches identified consistent structural mechanisms. The structural response is highly direction-dependent, with the Y direction as the most vulnerable direction. In this direction, the response is dominantly governed by flexural and rocking OOP of the slender longitudinal walls, whose stability was significantly reduced due to the absence of a vault. Conversely, in the X direction, the response is the combination of the OOP response of the apse and façade with the IP shear mechanism of the longitudinal walls, contributing to the development of a partial box-like behavior and enhancing load distribution among the orthogonal elements. Despite the differences in discretization and constitutive assumptions, all modeling strategies identified these dominant mechanisms and confirmed the Y direction as the most vulnerable.

The comparison of damage mechanisms confirmed that FEM and DEM reproduce the same damage pattern and evolution with good consistency at three performance levels of Damage Limitation, Severe Damage, and Near Collapse. The EFM, when complemented with 3D-pier elements in nave longitudinal walls and façade, was able to capture the activation of OOP mechanisms of the relevant macro-elements. However, its simplified idealization prevents it from explicitly modeling some critical macro-elements, especially those involving curved shapes such as apse vaults. Therefore, EFM can support safe-side seismic assessment and identify main critical damage mechanisms, while FEM and DEM can be better options for detailed assessments.

Overall, this study shows that the choice of the modeling strategy for the seismic assessment of URM churches should be dependent on the objectives of the assessment. For preliminary, rapid, and computationally efficient analyses, which are usually more favorable to engineers and practitioners, EFM is a practical option.

For more reliable and detailed predictions of stiffness and local damage evolution in churches whose behavior is governed by OOP mechanisms, which may be necessary for retrofitting designs, FEM and DEM are suitable options.

Chapter 5

A practitioner-oriented seismic assessment framework for churches (modal pushover + nonlinear kinematics)

5.1 Introduction

The comparative assessment represented in Chapter 4 highlights the complexity of the seismic assessment of URM churches through a single modeling strategy. Although each modeling strategy provides valuable insights into the behavior of structures, the choice of an appropriate strategy strongly depends on the expected response of the structure under investigation. This becomes more critical when the OOP local mechanisms and interaction among macro-elements play significant roles in the mechanisms governing the seismic response.

Due to their complicated behavior and the domination of OOP mechanisms, global numerical models often fail to capture the independent local mechanisms, while simplified kinematic limit analysis, although widely common because of its efficiency, neglects the interaction between adjacent elements. Another challenge is the lack of a standard framework and tool to perform seismic analysis and verification for this type of structure. Existing guidelines and codes, such as the Italian Directive for seismic risk assessment of cultural heritage (Decree of the Italian Prime Minister 2011), Italian Technical code for Construction (NTC 2008), and Eurocode 8 (EN 1998-1 2006; EN 1998-3 2006), offer a general framework but leave a large room for engineering judgements when applied to URM churches. This gap highlights the need for assessment procedures that can be applicable for practitioners and engineers, explicitly accounting for dynamic interactions among the elements and local mechanisms.

The present chapter proposes a practitioner-oriented approach for the seismic assessment of URM churches that combines pushover-based approaches with nonlinear kinematic analysis (NLKA). The novelty of this approach is the integration of the global response obtained from pushover analyses with the local mechanisms captured by NLKA, thereby overcoming the limitations of each of these methods when they are used in isolation. In this way, the proposed approach explicitly considers the interaction between macro-elements while being able to capture the post-peak behavior of local collapse mechanisms. The procedure can provide practitioners and experts with a reliable and practical tool to assess and verify the seismic behavior of monumental heritage URM churches.

The proposed approach in this work has two phases: First, a modal pushover analysis (MPA) is performed on a global finite element (FE) model to capture the interaction among the macro-elements and derive capacity curves. Then, NLKA is performed to complement the global behavior by presenting the post-peak behavior of local mechanisms. The structure of the rest of the chapter is as follows: Section 5.2 reviews the main challenges associated with the seismic assessment of URM churches and provides an overview of the current available methodologies proposed by guidelines and codes. Section 5.3 describes the proposed procedure and its required steps in detail. Then, the procedure was applied to a case study, which is the Church of Nostra Signora delle Grazie e Sant'Egidio, located in Imperia, Italy, and was hit by an earthquake in 1887 (Sections 5.4). Finally, Section 5.5 summarizes the conclusions and implications for practice.

5.2 Review of Available Methodologies and Challenges

5.2.1 Open issues on modelling and analysis methods

Due to the importance and complex behavior of URM churches, performing seismic assessment for them is associated with some issues and challenges. First of which is choosing the best modeling strategy that balances the computational effort with the accuracy of the solutions. Utilizing simplified approaches in order to reduce the computational cost can adversely affect the accuracy of solutions, since they are not fully able to capture OOP mechanisms and properly consider the interaction among the macro-elements (Lagomarsino et al. 2019b; Nale et al. 2021). Therefore, seismic assessment of URM churches requires more refined and detailed models like finite element (FE) (Elyamani et al. 2017; Betti et al. 2018; Ciocci et al. 2018) or discrete element (DE) modeling approaches (Mendes et al. 2020; de Felice et al. 2022b; Davis et al. 2024).

The FE models are widely used for analyzing monumental URM structures because of their ability to simulate complex configurations, such as vaults and arches that are common in URM churches. They treat masonry material as a homogeneous continuous deformable body, without any distinction between bricks and mortar (Gambarotta and Lagomarsino 1997; Lourenço et al. 1998). The FE models require appropriate constitutive laws that have to be calibrated through experimental tests or homogenization processes (Milani and Valente 2015; Bartoli et al. 2016). On the other hand, DE models treat masonry structures as an assembly of blocks, either rigid or deformable, interacting through contact surfaces. In the case of rigid blocks, all the deformations and failures will be concentrated at joints, while deformable blocks provide internal stress and strain developing within the blocks (Cundall 1971; Malomo and Pulatsu 2024). The two key features that distinguish DE models from FE ones are their ability to handle finite block displacements and rotations, leading to the capture of the entire detachment, and their automatic recognition of new contacts as the calculation progresses (Cundall and Hart 1993; Lemos 2007).

Another important challenge concerns the procedure for the analysis and verification of URM churches. International codes consider linear and non-linear, static and dynamic procedures. Linear analyses assume that the forces are distributed proportionally to the initial stiffness of the elements and remain constant throughout the loading process. Although these analyses are computationally efficient and straightforward to implement, they often provide overly simplistic assessments and fail to capture the stiffness degradation due to damage progress and crack propagation (Magenes 2006; Sandoli et al. 2021).

Therefore, non-linear procedures are essential for obtaining a reliable assessment of the seismic behavior of such structures. The most advanced procedures are the non-linear dynamic analyses (NLDA) performed by applying a set of seismic inputs (acceleration time-histories) at the base of the structure (Vecchio et al. 2025). However, these are associated with significantly high computational cost and necessitate the selection of spectrum-compatible accelerograms, which can significantly affect the results due to record-to-record variability (Jalayer et al. 2021). For these reasons, the non-linear static analyses (NLSA) —commonly known as pushover analysis — are suggested by codes and are more preferred and widespread among practitioners and engineers for seismic assessment of existing structures (Lagomarsino and Cattari 2015a; Degli Abbati et al. 2025). NLSA are usually based on the application of lateral load patterns (e.g., proportional to mass and elevation) and monitoring the displacement of a control

node as the base shear of the structure increases. In addition, pushover analysis is the standard tool for seismic performance-based assessment (PBA) of existing structures, which checks whether the structure is able to fulfill the selected Performance Levels (PLs) for a specific earthquake hazard level.

Beyond the choice of analysis procedure, another significant challenge for seismic assessment of URM churches lies in the selection of the assessment approach. Typically, there are two different approaches: (i) decompose the asset into distinct macro-elements and perform separate verifications; (ii) develop a global model of the church and verify it by deriving a capacity curve that represents the overall global behavior. The first option, the so-called macro-element approach, was originally proposed by Doglioni et al. (1994) based on the post-earthquake damage assessment of URM churches. Instead of assessing the church as one unit, this method focuses on examining the seismic performance of its constituent parts separately. Although this method can simplify the analysis and assessment procedure, it disregards the dynamic interaction between different macro-elements. It has to be noted that the interactions strongly depend on the quality of the connections, which is difficult to evaluate and mechanically describe. Even when connections are poor, some degree of interaction among them may occur when the seismic actions push one macro-element towards another and vice versa (Lagomarsino et al. 2019b). Another limitation of this method is that its results depend on how the structure is divided into elements, require well-calibrated strength criteria for each type, and often fail to capture the OOP mechanisms (da Silva and Milani 2022). The second alternative can overcome these limitations by explicitly considering the interactions between macro-elements and being able to capture the potential OOP failures.

Several approaches have been proposed in the literature for seismic assessment of URM churches, combining global modeling with macro-element approaches in different ways. Brandonisio et al. (2008) developed a two-step procedure: first, linear 3D finite element models were used to evaluate the dynamic properties and seismic demand on each macro-element; then, the structure was decomposed, and each macro-element was analyzed in a non-linear range up to collapse to determine its capacity, and its safety level was evaluated by comparing the demand with capacity. Valente et al. (2020) extended this work by performing non-linear dynamic simulations on the same churches, adopting a damage-plasticity model for the masonry to quantify damage distribution and seismic vulnerability of each macro-element.

Lagomarsino et al. (2019) proposed a macro-element-based approach in which the interactions between macro-elements are implicitly considered through redistribution of forces, using both macro-block and equivalent frame models to describe IP and OOP responses, respectively. The method relies on a 3D FE model to determine the load distribution and provide critical coefficients that adjust the capacity curves of each macro-element. Similarly, Degli Abbati et al. (2019) used 3D FE models to perform multiple pushover analyses by defining the load patterns based on some selected mode shapes, interesting different macro-elements to evaluate their capacity. Malena et al. (2022) established a link between global behavior of the church and the assessment of local mechanisms by combining modal analysis to identify critical macro-elements with non-linear FE analysis of these elements, using an anisotropic elastic-perfectly plastic model for the masonry to balance the accuracy and computational efficiency. Finally, de Felice et al. (2022a) developed a 3D DE model using photogrammetric surveys and performed automatic pushover analysis to simulate the local collapse of macro-elements and derive their capacity curve.

Building on these previous contributions, the present paper proposes an integrated assessment framework that combines modal pushover analysis (MPA) with nonlinear kinematic analysis (NLKA) for URM churches. Unlike approaches that either rely on a global model of the structure or on just macro-element verifications, the proposed approach establishes a link between the FE model behavior and local mechanisms.

5.2.2 Overview of procedures for the seismic assessment available in the literature and codes

International codes such as Eurocode 8 (EC8) (EN 1998-1; EN 1998-3) and Italian Technical Code for Construction (NTC 2008) suggest using nonlinear procedures for seismic assessment of monumental structures, such as churches. Both documents acknowledge that linear procedures are not sufficiently able to capture the behavior of such structures, and consequently propose nonlinear static analysis (pushover analysis) as a standard tool to obtain the capacity curve and perform seismic verification.

Regarding the modeling strategy, the codes distinguish between utilizing 2D and 3D models. It is emphasized that 2D planar models are acceptable for analysis of the model only if they are regular in plan and elevation. Otherwise, using a spatial 3D model is mandatory. Churches, due to the presence of architectural features such

as tall and slender towers (often attached asymmetrically), large openings along the height, and large vaults that introduce concentrations of mass and stiffness, do not match the requirements for regular buildings. Therefore, developing 3D modeling is essential for a reliable seismic assessment.

A critical issue in pushover analysis is defining the load patterns and choosing control nodes. EC8 expresses that at least two load patterns have to be applied for performing a pushover analysis: (i) uniform pattern (proportional to mass) and (ii) modal pattern (proportional to the first dominant mode). For irregular and complex structures whose higher modes can have significant contributions to their dynamic behavior, EC8 recommends accounting for their influence. Italian guideline allows the use of different load patterns, including multimodal and adaptive ones (Chopra and Goel 2002; Antoniou and Pinho 2004; Galasco et al. 2006; Malena et al. 2025), and emphasize that, in the case of irregular structures, the first-mode load pattern may not be sufficient. This provides engineers greater flexibility to specify appropriate load patterns and account for the impact of higher modes when dealing with structures of complicated behavior, such as historical churches.

The choice of control nodes is equally important as defining load patterns for performing a pushover analysis. The codes propose to consider the control node at the center of mass of the last floor. For regular structures with rigid diaphragms, this assumption can be trusted because their first mode is often dominant and has the greatest displacement at the top level. However, the results of the analysis strongly depend on the position of the control node for cases with flexible floors, such as timber roofs and vaults. Since churches consist of different macro-elements, which can behave separately during earthquakes, with different strengths and stiffness, considering just one control node at its top level (e.g., top of the bell tower) cannot provide a reliable estimate of its behavior. Therefore, it has been suggested that the control node should be selected at the top of the macro-element that is expected to collapse first (Lagomarsino and Cattari 2015b).

In addition to global assessment of structures, both codes emphasize the need to verify possible local mechanisms, which often govern the seismic behavior of URM churches. EC8 distinguishes the verification process depending on the ductile or brittle behavior of the material. In the case of URM, since it does not exhibit ductile behavior (i.e., brittle mechanism), it shall be verified with demands calculated by means of equilibrium. The NTC 2018 goes further and explicitly mentions using the linear and nonlinear kinematic analysis to check the potential local mechanisms in the assessment of structures (Circolare 2019). The kinematic limit analysis evaluates the equilibrium of a rigid block without considering the

material nonlinearities. This method relies on the geometry of the block or macro-element, its self-weight, and the seismic demand at the elevation where the block is located.

In the code-based assessment framework, the global assessment and local verification are performed separately in a way that the global behavior of a church is assessed by developing a 3D model and then is divided into macro-elements, and the OOP mechanisms are checked. The seismic behavior of churches has been evaluated in this manner by several authors (Betti et al. 2021; Briceño et al. 2021; Formisano et al. 2022; Diana et al. 2023; Gunes 2023; Lo Monaco et al. 2023). The limitation of separating global and local checks is that the intersections between the macro-elements are neglected in the local mechanism verifications. Additionally, the prescribed load patterns (i.e., the uniform and first-mode patterns) are not sufficient for irregular structures such as churches, where higher modes and local OOP often govern the seismic response. Finally, the codes' recommendation to adopt one control node ignores the independent behavior of various macro-elements, including towers, apses, façades, etc. These gaps highlight the need for integrated approaches that explicitly link the global and local verifications for URM churches, such as the one proposed in this chapter.

5.3 Adopted Procedure for the Seismic Assessment of Churches and Its Field of Applicability

5.3.1 Decision Tree (When to Use What)

As mentioned in the previous sections, the seismic assessment of URM churches requires the choice of an appropriate analysis strategy that provides engineers and practitioners with a reliable estimation of possible failure mechanisms. The choice of such a strategy is highly influenced by features of the structure that dictate how failures develop, such as the quality of masonry and, more importantly, the effectiveness of connections among macro-elements (D'Ayala and Speranza 2003; Ferreira et al. 2015). Since historical URM churches often exhibit heterogeneous behavior – due to the nature of masonry – (D'Altri et al. 2020), ranging from independent macro-elements to acting as a unit, the choice of an analysis strategy is not unique and straightforward. In this context, a decision process is proposed to guide the selection of a suitable assessment and verification method of URM churches. This process consists of several consequential steps that identify whether the seismic behavior of churches should be assessed through a global model, local verifications, or a combination of both approaches.

1. **Initial screening:** In contrast to new constructions that were designed according to current seismic codes, each URM monumental structure has its own history, and often its behavior cannot be generalized into a standard scheme. Their static and dynamic behavior is influenced by construction techniques, transformations over time, and the quality of materials and connections. Therefore, each monumental structure needs specific modeling, analysis, and experimental tests (Betti and Vignoli 2008; Bartoli et al. 2013).

This first step corresponds to the knowledge phase, which is a fundamental step in choosing a reliable strategy to assess the seismic behavior of URM churches. It requires deep knowledge of the geometry of the structural system, construction details, and mechanical properties of materials. This knowledge can be reached through experimental tests, visual inspection, and on-site surveys. The standards EC8 and NTC 2008 introduce a correction factor (CF) in order to account for uncertainties in knowledge of structural properties. Its value depends on the knowledge level (KL), ranging from 1 to 3, depending on the completeness and reliability of the obtained information. Higher knowledge level (KL3) allows the use of a less conservative factor, while in lower knowledge level (KL1), the reduction needs to be applied by a higher CF (Clementi et al. 2016).

In addition to tests and inspections on the structure itself, knowledge can also be enriched by the observations from past earthquakes. Damage surveys after earthquakes revealed that the OOP mechanisms of different macro-elements, such as façades, longitudinal walls, apses, etc., are of recurrent collapses, mainly due to the lack of sufficient connections (da Porto et al. 2012; Lagomarsino 2012; De Matteis et al. 2019b; Canuti et al. 2021; Ferracuti et al. 2022). To systemize these observations, the Italian Directive for seismic risk assessment of cultural heritage (Decree of the Italian Prime Minister 2011) identifies 28 mechanisms describing the most common collapse mechanisms for churches and introduces a vulnerability index method (Lagomarsino and Podestà 2004a). This index-based procedure, while simple, is applicable to large-scale territorial assessment, enabling rapid and preliminary evaluation of seismic vulnerability of structures and specifying the mechanisms with the highest vulnerability index as the critical ones.

The outcome of this initial screening guides the selection of the most appropriate assessment strategy based on the current situation of the structure and is fundamental for the next steps of the decision process.

2. Weak coupling between macro-elements: When the connections between the orthogonal walls and roof system are poor, the church cannot behave as one

unit, and the walls are not able to provide sufficient restraints for their adjacent parts (D'Ayala and Speranza 2003). In such cases, the structure should be divided into different macro-elements, each analyzed separately to evaluate its capacity and potential collapse mechanism. This lack of proper connections is particularly critical for the structural and non-structural elements located at various levels of the structure (e.g., gables, decorative statues, and chimneys) since they are subjected to the elevation-based amplified seismic input (Menon and Magenes 2011; Degli Abbati et al. 2018; Lagomarsino et al. 2023). In such cases, non-linear kinematic analysis (NLKA) is an effective and computationally efficient method for assessing seismic safety.

NLKA requires only the geometry, self-weight, and FRS at the height of the mechanism to evaluate its displacement capacity and verify the stability of the element against earthquakes. This approach does not require many inputs and the development of detailed models and is efficient for the elements whose connections to other parts of the structure are limited. Several applications demonstrated the ability of NLKA in predicting the activation and ultimate displacement of typical collapse mechanisms in URM churches (D'Amato and Sulla 2021; Contrafatto et al. 2022; Casapulla et al. 2023; Diana et al. 2023; Ghaffarpasand et al. 2024).

3. Macro-elements with interactions: A different condition arises when there are structural connections, restraints, or partial continuity among adjacent parts that are sufficient to prevent macro-elements from acting separately. In these cases, although the structure may not exhibit a fully box-like behavior, the response of macro-elements cannot be assessed independently, since the activation of kinematics in one macro-element is influenced by the presence of neighboring parts.

In this step of the decision tree, one possible condition is that the church exhibits a predominantly global behavior. This typically happens when strengthening interventions, such as stiff diaphragms, tie-rods, or similar interventions, are implemented, thereby enhancing the connection between main macro-elements. In these cases, the seismic behavior of the structure can be assessed by performing global assessment procedures, based on the development of a 3D numerical model of the structure under investigation and the execution of pushover analyses by applying lateral load patterns proportional to the masses.

In contrast, when the response is governed by local mechanisms, as usually occurs in churches with flexible diaphragm and poor structural connections, it cannot be assessed either based on the assumption of fully independent macro-

elements or based on global approaches. Therefore, pure NLKA may not be sufficient, since it does not consider the interactions and force redistribution provided by the actual configuration of the structure. At the same time, global approaches may not be useful in capturing and interpreting local mechanisms efficiently. For this reason, this chapter proposes a framework that adopts a strategy that combines NLKA with pushover analyses. In this framework, a global model of the church is used to perform a modal analysis to identify the modes involving the dynamic response of various macro-elements, participation factors, and their mode shapes. Then, a series of MPA is performed for the selected macro-elements. For each macro-element, the load pattern is derived directly from its most relevant mode shape. Indeed, although the combination of modal load patterns is sometimes proposed in technical codes, it has no theoretical basis, since modal combination should be applied to structural effects, such as displacements and generalized forces, rather than to input actions. Finally, by combining the capacity curves derived from NLKA and MPA, this study tries to capture post-peak behavior up to the ultimate condition, which is often governed by local mechanisms. Therefore, the goal of this chapter is to provide a framework in which engineers can verify local OOP mechanisms while taking into account the interactions among the macro-elements.

5.3.2 Proposed procedure

The proposed procedure in this chapter was built on the approach originally proposed by Degli Abbati et al. (2019) for the seismic assessment of interacting structural units through modal analyses and nonlinear static analyses on a global numerical model. In that procedure, the modal shapes are processed to derive analytical load patterns that are fitted to the response of each macro-element, and then the pushover curves are transformed into SDOF capacity curves for the seismic verification.

Starting from that procedure, the present methodology has two main differences. First, it can be recognized as a more practitioner-oriented version, since it does not require deriving analytical load patterns fitting the modal shapes in plan and elevation for each macro-element. Second, it aims to overcome one of the limitations of pure FE-based procedures when it comes to seismic assessment of churches, which is their inability to capture the post-peak and softening behavior of local mechanisms. For this reason, the capacity curve derived from MPA is complemented by the one derived from NLKA on local mechanisms, which is used to capture the evolution of the mechanism up to collapse.

The field of application is churches whose responses are neither box-like nor governed by completely independent macro-elements. More specifically, this procedure refers to the structural condition identified as point 3 of the described decision tree, where the structural connections are sufficient enough to affect the response of the structure and prevent macro-elements from acting separately and independently. The procedure has eight steps as follows:

1. Construction of a FE model of the entire church, with the aim of explicitly capturing the mutual interactions among macro-elements; the model must represent the global geometry, mass distribution, and the connections among the main macro-elements, so that the dynamic interactions can be taken into account.

2. Execution of a modal analysis in order to identify the mode shapes affecting main macro-elements, compute participation factors, and obtain required dynamic properties.

3. Execution of a series of MPA for each macro-element; in this step, the mode shapes involving the macro-elements whose seismic behavior is intended to be assessed and verified are selected, distinct control nodes are selected for each macro-element, and the load patterns, applied as lumped forces at nodes, are calculated using the following equation (Chopra and Goel 2001, 2002):

$$f_{i,d} = \Gamma_d m_i \phi_{i,d} \tag{11}$$

In Equation 11, $f_{i,d}$ is the nodal force applied at the node *i* for the mode *d*, Γ_d is the modal participation of the mode *d*, m_i is the mass of the node *i*, and $\phi_{i,d}$ is the displacement of the node *i* for the mode *d*. These forces represent the inertial resistance caused by the structure's mass when it deforms according to the mode *d*. When a mode activates the response of one specific macro-element, the corresponding modal load pattern can be adopted to assess the response of that element. Conversely, when one mode involves the response of more than one macro-element, the load pattern is defined by maintaining the forces acting on the macro-element under investigation and setting the forces on other elements to zero.

4. Execution of a local NLKA for each relevant mechanism, with the aim of capturing the softening response of the macro-element and its behavior up to large displacements. If a rectangular rigid block of thickness *2b* and height *2h* is considered, simply supported at the base and subjected only to its own mass *M*, the horizontal inertial seismic action is assumed as: i) proportional to the gravity load

P=Mg through a seismic multiplier α; ii) and applied at a point usually assumed as the gravity center. The value of the multiplier that activates the OOP mechanism (α_0) can be calculated according to Equation 2, where λ is defined as the block slenderness. α_0 is obtained by applying the basic principle of static equilibrium in the initial configuration of the block. Then, by imposing the static equilibrium under an incremental kinematic analysis, that is increasing the rigid block rotation up to the condition of static equilibrium loss, it is possible to obtain the whole capacity curve.

$$\alpha_0 = \frac{b}{h} = \frac{1}{\lambda} \tag{12}$$

5. Transformation of the obtained macro-element's curve from MPA into an equivalent single-degree-of-freedom (SDOF) system (Fajfar 1999); the purpose of this step is to express the MPA-derived capacity curve in the same format as the one obtained from NLKA, allowing the two capacity curves to be merged and subsequently used for the seismic verification. In principle, both curves must be transformed into equivalent SDOF curves; however, since the NLKA is already formulated for a single block governed by one degree of freedom, the SDOF transformation is only required for the MPA curve. The equivalent SDOF curve is obtained by calculating the modal participation factor, Γ, and effective mass, m^*, using Equation 13.

$$\Gamma = \frac{\sum m_i \phi_i}{\sum m_i \phi_i^2} \quad , \quad m^* = \sum m_i \phi_i \tag{13}$$

Where Γ accounts for the contribution of the selected mode to the global dynamic response and m^* represents the portion of the structural mass participated in that mode. The equivalent SDOF capacity curve is then obtained by dividing the displacement d by Γ, and the base shear V by the product of Γm^*.

6. Derivation of the final capacity curve of the macro-element by combining the SDOF version of the MPA and NLKA capacity curves; the final curve consists of the pushover branch up to its interaction with the kinematic curve and, beyond that point, the branch provided by NLKA. If the pushover curve reaches plateau before having an intersection with NLKA curve, the plateau branch is extended until an intersection is attained.

7. Definition of the seismic demand at the position of the macro-element; it can be the ground response spectrum (GRS), or the floor response spectrum (FRS) for structural elements placed at upper levels, where seismic input is amplified by the dynamic properties of the structure. For a given seismic demand, if the response of the macro-element is governed by its global behavior, GRS is used for the seismic verification. Conversely, if the response is governed by the local mechanism of a portion of the macro-element, FRS can be adopted to account for the amplified seismic input at the block's level. Following the formulations proposed by Degli Abbati et al. (2018), two characteristic points of the floor response spectrum in $T=T_0$ and $T=T_k$ can be calculated using the following equations (Burdisso and Singh 1987; Singh and Burdisso 1987; Singh 1988):

$$\mathrm{PFA_{Z,k}} = \mathrm{S_a(T_k)\eta(\xi_k)|\Gamma_k \times \phi_k|}\sqrt{1+4\xi_k^2} \tag{14}$$

$$\mathrm{S_{aZ,k}(T_k)} = \mathrm{AMP_k PFA_{Z,k}} = \mathrm{f_s f_k PFA_{Z,k}} \tag{15}$$

Where $\mathrm{S_{aZ,k}(T_k)}$ depends on the dynamic properties of the main structure, such as the natural periods ($\mathrm{T_k}$), modal participation coefficients ($\mathrm{\Gamma_k}$), modal shapes ($\mathrm{\phi_k}$ (x, y ,z)), and the viscous damping ($\mathrm{\xi_k}$) of the structure. $\mathrm{AMP_k}$ is the amplification factor that depends on the viscous damping of the main structure ($\mathrm{\xi_k}$) and secondary element (ξ), and can be calculated using Equation 16.

$$f_s = \eta(\xi) = \sqrt{\frac{0.1}{0.05+\xi}} \quad . \quad f_k = \xi_k^{(-0.06)} \tag{16}$$

Once these two points are defined, the FRS due to the k^{th} mode can be derived through analytical expressions in Equation 17 and is passed through the above-mentioned values in $T=T_0$ and $T=T_k$.

$$\mathrm{S_{aZ,k}(T_k,\xi)} = \begin{cases} \dfrac{AMP_k PFA_{z,k}}{1+[AMP_k-1]\left(1-\dfrac{T}{T_k}\right)^{1.6}} & T \le T_k \\ \dfrac{AMP_k PFA_{z,k}}{1+[AMP_k-1]\left(\dfrac{T}{T_k}-1\right)^{1.2}} & T > T_k \end{cases} \tag{17}$$

8. Demand/Capacity comparison and seismic verification;

5.4 Application to the Case Study: the Church of Nostra Signora delle Grazie e Sant'Egidio in Bussana

5.4.1 The numerical model of the church

The numerical model adopted in this chapter is the same FE model of the Church of Nostra Signora delle Grazie e Sant'Egidio used for the comparative study in Chapter 4. The model was developed in ABAQUS from the maps derived from laser scanning campaigns, with simplifications aimed to retain the key structural elements while reducing unnecessary complexities. URM was modeled as a homogeneous continuum material through the CDP constitutive law, and the mechanical parameters were adopted according to the Italian Guidelines for the Assessment and Reduction of Seismic Risk of Cultural Heritage (Directive P.C.M., 2011) and the Italian Technical Standards for Construction (NTC, 2018), as discussed in subsection 4.2.1.

In the present chapter, this model was used as the global model to perform the modal analysis and the subsequent pushover analyses, forming the first step of the proposed assessment framework.

5.4.2 Modal analysis and load pattern definition

Once the 3D FE model is completed, the procedure requires performing a modal analysis in order to identify the dynamic responses governing the behavior of the church and to recognize the ones involving the main macro-elements. Besides providing natural periods and participation factors, this step is critical to highlight the structural portions that are engaged the most in each mode.

The examination of the mode shapes was then performed in terms of both the global dynamic properties and the response of individual macro-elements. In this way, the modes predominantly influencing façade, longitudinal walls, bell tower, and apse could be recognized, together with the modes simultaneously activating the response of more than one macro-element. This distinction is essential for the subsequent steps of the procedure and to decide how the loads should be applied to activate the response of the macro-element under investigation. Table 18 reports the first ten modes and their corresponding involved macro-elements.

Table 18: First ten vibration modes and their periods, modal participations, and involved macro-elements

Mode	T	Γ_x	Γ_y	Involved macro-elements
1	0.450	-512.86	370.54	Bell tower
2	0.438	-287.62	-567.05	Bell tower
3	0.227	-15.37	870.93	Longitudinal wall
4	0.202	68.567	625.24	Longitudinal wall
5	0.161	-9.4162	129.58	All the macro-elements
6	0.141	170.52	145.72	Bell tower
7	0.125	-1065.3	-62.227	All the macro-elements
8	0.122	34.27	629.69	All the macro-elements
9	0.117	410.74	-73.822	Longitudinal wall – façade
10	0.105	520.58	1.2385	All the macro-elements

Based on the mode shapes and modal participations, the assessment in this study was focused on the OOP response of the longitudinal wall in the Y direction and the OOP response of the façade in the X direction. Specifically, mode 3 was selected for the longitudinal wall and mode 7 for the façade, since, according to the modal participations and mechanical interpretation of the mode shapes, these modes were found to be the best representation of the considered mechanisms. Figure 17 shows the considered mechanisms and their corresponding mode shapes.

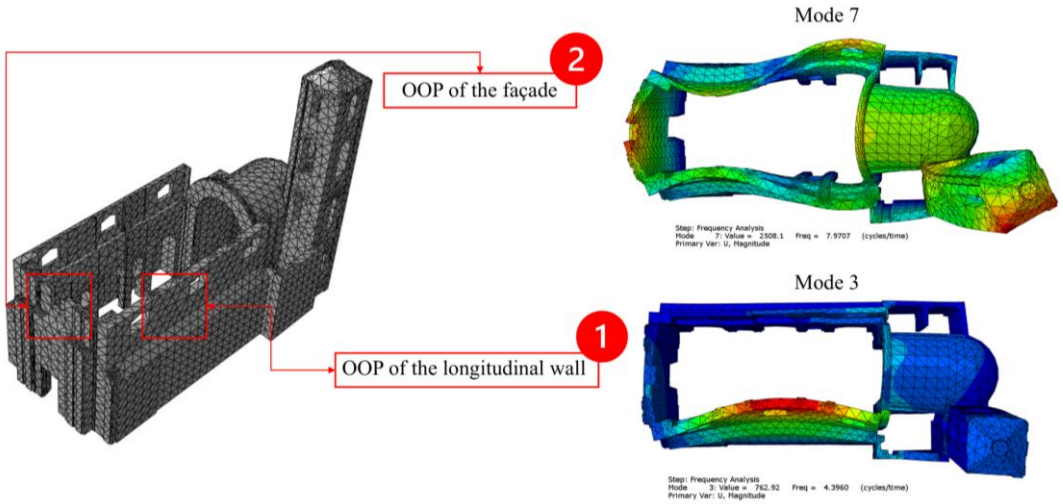

Figure 17: The considered mechanisms and their corresponding mode shapes

Once the relevant mechanisms and their corresponding mode shapes had been selected, the load patterns were defined from the modal shapes according to Equation 11. For the OOP response of the longitudinal wall, mode 3 was adopted, in which the only involved macro-element is the wall under consideration. Therefore, the obtained nodal forces from the mode shape were applied to the whole

church, since it is equivalent to activating that longitudinal wall response. Conversely, mode 7, which was selected for the OOP mechanism of the façade, involves other structural macro-elements in addition to the façade. Therefore, the nodal forces were applied to the façade and its adjacent parts, and the contribution of other macro-elements were set to zero. In this way, the pushover analysis is consistent with the modal information obtained from the global model, while allowing the response of only the specific macro-element under investigation.

5.4.3 Results of the modal pushover analysis

The MPAs were carried out on the global FE model of the church by adopting the load patterns derived from modal shapes, namely mode 3 and mode 7 for the OOP response of the longitudinal wall in the Y direction and façade in the X direction, respectively. The results of the capacity curves and deformed configurations are discussed in this subsection.

For the longitudinal wall, the pushover analysis activated the response of the wall consistent with the mechanism identified by the mode shape of mode 3. Since this MPA predominantly involved the longitudinal wall and marginally affected other macro-elements, the pushover curve can be interpreted as the behavior of the longitudinal wall up to the last point of the analysis, providing a clear description of the initial stiffness and strength of the mechanism. The pushover curve was then transformed into an equivalent SDOF capacity curve according to Equation 13 and the explained process in step 5 of the proposed procedure (§5.3.2). Figure 18 shows the results of the MPA in terms of the deformed configuration, corresponding damage pattern, pushover curve of the longitudinal wall experiencing the OOP mechanism, considering the control node at the top of the wall.

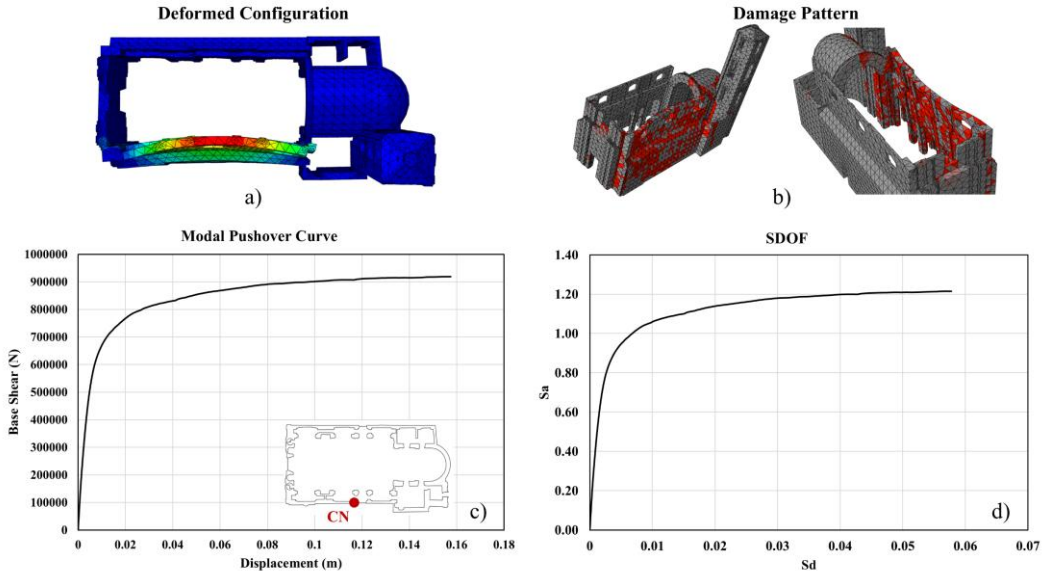

Figure 18: The results of the MPA based on mode 3 in terms of the a) deformed shape of the configuration, b) damage pattern, c) modal pushover curve, and d) transformed SDOF capacity curve

For the façade macro-element, since mode 7 involved almost all the macro-elements, the MPA was performed by restricting the load pattern to the façade contribution. In this way, the analysis highlighted the OOP response of the façade as the prevailing mechanism, while taking into account the dynamic interactions and boundary conditions embedded in the global configuration of the church. The pushover curve was derived by considering a control node at the top of the façade, providing its initial stiffness and maximum strength. It was then transformed into an equivalent SDOF capacity curve according to Equation 13 and the explained process in step 5 of the proposed procedure (§5.3.2). Figure 19 shows the results of the MPA in terms of the deformed configuration, corresponding damage pattern, pushover curve of the façade experiencing the OOP mechanism and its equivalent SDOF curve.

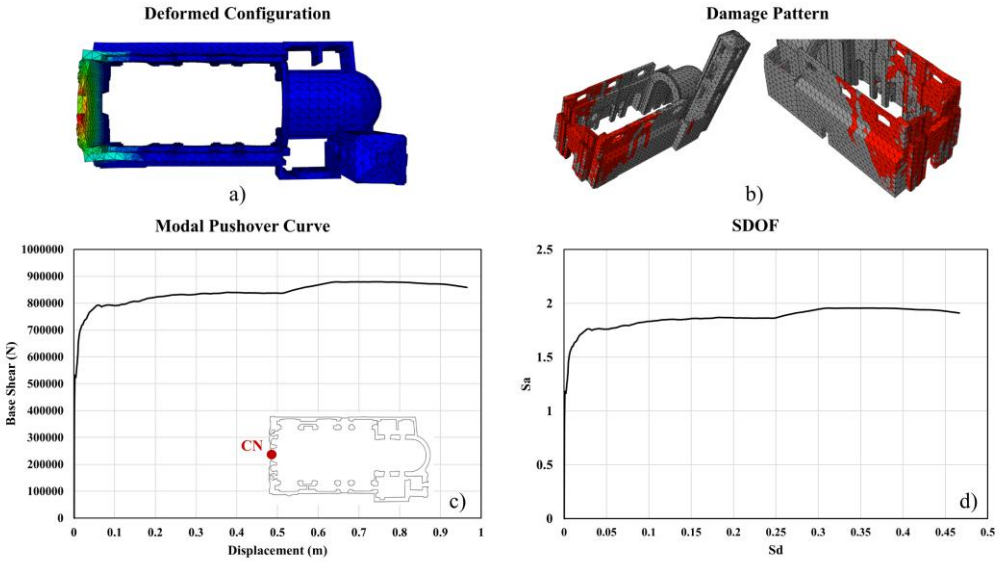

Figure 19: The results of the MPA based on mode 7 in terms of the a) deformed shape of the configuration, b) damage pattern, c) modal pushover curve, and d) transformed SDOF capacity curve

Overall, the pushover and equivalent SDOF curves proved to be useful for capturing the initial nonlinear response of a mechanism while preserving interactions through the global model. However, the results also confirm that performing only a FE-based pushover analysis is not sufficient to describe the evolution of the mechanism up to the ultimate condition and to capture the post-peak softening of the behavior. Therefore, the capacity curve is complemented with the capacity curve obtained by the NLKA in the following subsection in order to provide the post-peak softening and ultimate displacement of the mechanism.

5.4.4 Integration with nonlinear kinematic analysis

For the OOP mechanism of both the longitudinal wall and façade, the MPA-based capacity curves were integrated with the NLKA-based capacity curves. This made it possible to define the final capacity curves for the two macro-elements.

For the longitudinal wall, the NLKA was executed, according to step 4 in §5.3.2, for a block located at the top of the wall, where the most displacement is expected. The analysis was performed under the assumption that the OOP mechanism of the considered block is activated before the global collapse of the wall. Table 19 reports the geometric properties of the block and the results of the NLKA analysis.

Table 19: The geometrical properties of the block located at the top of the wall and the results of the NLKA

b (m)	h (m)	L (m)	α	S_a (m/s^2)	S_d (m)
0.68	3.73	4.014	0.182	1.788	0.34

Figure 20 shows the block under consideration and its NLKA-based capacity curve.

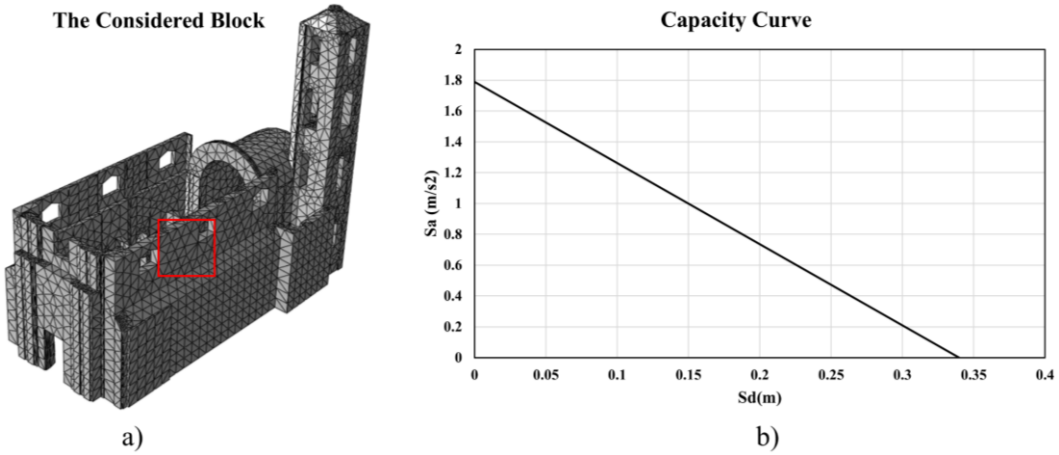

Figure 20: The a) considered block for the NLKA and b) NLKA-based capacity curve

For the façade, the NLKA was performed by considering the OOP overturning mechanism of the front wall, consistent with the response identified by the MPA. For this case, the same assumption of the occurrence of the OOP mechanism of a block located at the top of the façade before its global collapse was made as well. Table 20 reports the geometric properties of the block and the results of the NLKA analysis.

Table 20: The geometrical properties and the NLKA results of the block located at the top of the facade

b (m)	h (m)	L (m)	α	S_a	S_d
0.445	3.12	4.15	0.16	1.569	0.22

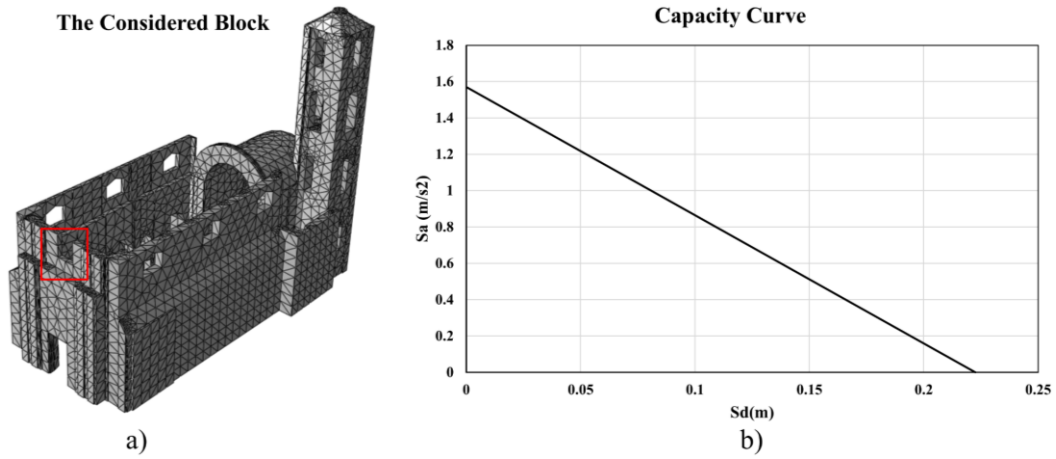

Figure 21: The a) considered block for the NLKA and b) NLKA-based capacity curve

The final capacity curves for both mechanisms were defined by integrating the two curves obtained from the MPA and NLKA. The MPA-based capacity curve represents the initial phase of the final curve, while the curve obtained from NLKA was used to represent the softening evolution up to the ultimate condition. Therefore, two curves were merged by adopting the pushover branch up to its intersection with the NLKA curve; beyond that point, the branch obtained by the NLKA governs the behavior. In the case of the block located on the top of the longitudinal wall, the MPA capacity curve reached a plateau before its intersection with the NLKA curve; therefore, it was extended until the intersection was attained. Figure 22 shows the final capacity curve for the considered blocks experiencing the OOP overturning mechanism.

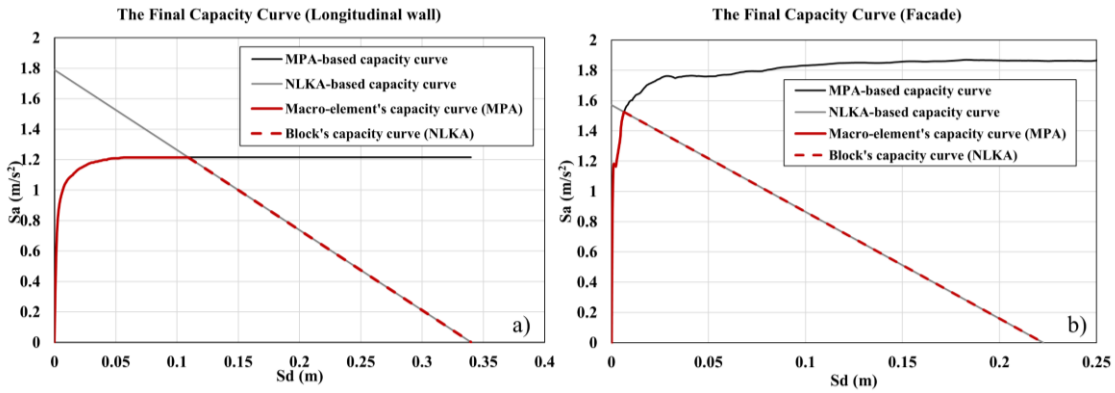

Figure 22: The final capacity curve consists of global behavior obtained by MPA and local behavior obtained by NLKA for the blocks located at the top of the a) longitudinal wall and b) façade

Figure 22 shows that the global behavior of the macro-elements and the local behavior of the upper blocks do not play the same role in the two cases. For the

longitudinal wall, the local mechanism begins at the same strength level as the global macro-element. This means that the peak resistance is mainly governed by the whole longitudinal wall as a part of the church, while the local mechanism controls the strength reduction and the ultimate condition of the collapse. The situation for the façade is different. The MPA-based global curve shows that the façade macro-element can resist a higher spectral acceleration, while the onset of the local mechanism is at a lower level of acceleration and then softens, meaning that the overturning of the upper block becomes critical before the full global capacity can be exploited. Therefore, the local mechanism for the façade controls both the maximum strength of the macro-element and its collapse mechanism.

5.5.5 Results of the seismic assessment

For the final seismic verification, the final capacity curves obtained for the two mechanisms were compared with the seismic demand expressed in a spectral format. The demand was defined consistently with the location of the considered mechanisms in the church.

For the longitudinal wall, the FRS was computed at the level where the block is placed, according to step 7 in §5.3.2, by combining the modes that have a significant contribution on the OOP overturning response. In this study, similar to Degli Abbati et al. (2018), the SRSS combination rule was used, and the peak of the FRS for each mode was calculated using Equation 15. To identify the modes that most significantly influence the FRS, as Table 21 reports, the modal displacement at the position of the base of the block ϕ, the participation factor Γ, the corresponding spectral acceleration $Sa(T_k)$, and the quantity of $((\phi\ \Gamma)\ Sa)^2$ were calculated. The results show that modes 3, 4, and 8 have the most contribution to the FRS for the upper block of the longitudinal wall experiencing the OOP overturning mechanism, with mode 3 being the dominate one.

Table 21: Modal properties and their relative contribution to the FRS for the upper block of the longitudinal wall

Modes	ϕ	Γ	ϕ*Γ	Sa(T_k)	((ϕ Γ) Sa)^2	Contribution(%)
1	0.00002	370.540	0.006	4.074	0.001	0.001
2	-0.00005	-567.050	0.026	4.183	0.012	0.025
3	0.00172	870.930	1.497	4.403	43.439	93.089
4	-0.00038	625.240	-0.240	4.403	1.119	2.397
5	-0.00103	129.580	-0.134	4.403	0.346	0.741
6	-0.00012	145.720	-0.018	4.403	0.006	0.014
7	0.00044	-62.227	-0.027	4.171	0.013	0.028
8	0.00045	629.690	0.285	4.117	1.381	2.960
9	0.00069	-73.822	-0.051	4.031	0.042	0.091
10	0.00014	1.239	0.000	3.835	0.000	0.000
11	0.00064	-166.230	-0.106	3.776	0.159	0.341
12	-0.00034	-308.180	0.105	3.599	0.143	0.307
13	-0.00031	51.527	-0.016	3.547	0.003	0.007
				SRSS	**46.664**	

The same procedure was adopted for the OOP mechanism of the façade. The modal properties at the elevation where the block is placed were then used to identify the relative modal contribution to the final FRS acting on the façade. The results of the relative modal contribution on the FRS were reported in Table 22. The results show that modes 7, 9, 10, and 11 have the most contribution to the FRS for the upper block of the façade.

Table 22: Modal properties and relative contribution to the FRS for the upper block of the facade

Modes	ϕ	Γ	ϕ*Γ	Sa(T_k)	((ϕ Γ) Sa)^2	Contribution(%)
1	0.00000	-512.860	-0.001	4.074	0.000	0.000
2	0.00000	-287.620	0.000	4.183	0.000	0.000
3	-0.00034	-15.370	0.005	4.403	0.001	0.001
4	0.00052	68.567	0.035	4.403	0.024	0.054
5	0.00008	-9.416	-0.001	4.403	0.000	0.000
6	0.00000	170.520	0.000	4.403	0.000	0.000
7	-0.00123	-1065.300	1.308	4.171	29.766	65.977
8	-0.00025	34.270	-0.009	4.117	0.001	0.003
9	-0.00085	410.740	-0.349	4.031	1.985	4.399
10	0.00161	520.580	0.836	3.835	10.283	22.794
11	0.00132	349.900	0.462	3.776	3.041	6.741
12	-0.00019	22.132	-0.004	3.599	0.000	0.001
13	-0.00046	73.144	-0.034	3.547	0.014	0.032
				SRSS	45.116	

The FRS for both the OOP mechanisms was computed by combining the critical modes using the SRSS rule. As shown in Figure 23, for the longitudinal wall, the FRS is primary governed by mode 3, while modes 4 and 8 provide secondary contributions. For the façade, it is dominated by mode 7, while modes 9, 10, and 11 marginally affected the final spectrum. The final FRS shows a significant amplification with respect to the base spectrum, with its peak around $T=0.22s$ and $T=0.15s$ for the longitudinal wall and façade, respectively. This confirms that the seismic demand at the level of the blocks is significantly influenced by the properties of the main structure. Figure 23 shows the considered nodes to calculate the FRS, which is at the base of the blocks experiencing the OOP mechanism, the critical modes' contribution, and the final FRS for both the mechanisms.

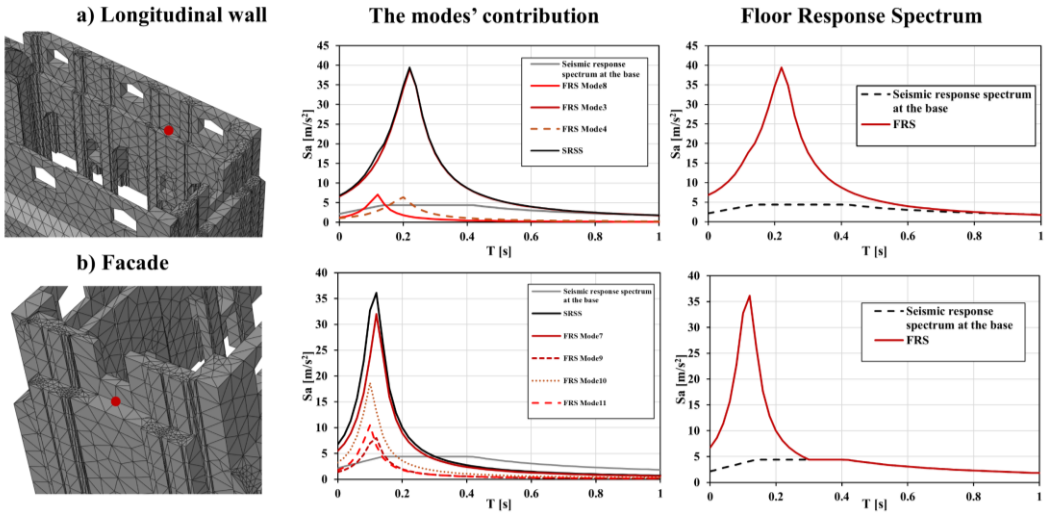

Figure 23: The considered point of the macro-element for calculating FRS, the modes' contribution, and the final FRS for a) the longitudinal wall and b) the façade

The capacity curve was then compared with the demand spectrum using the Capacity Spectrum Method (CSM) in ADRS format to identify the intersection between the overdamped seismic demand and mechanism capacity as the performance point. The displacement corresponding to the performance point, d_{PP}, was assumed as the seismic demand and compared with the near-collapse threshold (DL4). According to Lagomarsino (2015), the near collapse threshold is equal to $0.4d_0$ for a rocking system, where d_0 is the displacement at which the capacity curve becomes zero. Therefore, the mechanism was considered verified when $d_{PP} < 0.4d_0$.

Figure 24 highlights two different verification conditions for the examined mechanisms. For the longitudinal wall (Figure 24 (a & c)), the performance point is located on the plateau of the capacity curve and is clearly lower than the near-collapse threshold. This indicates that the OOP rocking mechanism was activated,

but it did not enter the near-collapse displacement range, meaning that this verification is satisfied. For the façade (Figure 24 (b & d)), the performance point is located on the descending branch of the capacity curve, meaning that the block detached from the facade, and is much closer to the near-collapse threshold. Although the verification is satisfied, the lower distance between the two points indicates that this mechanism is a more critical response. Overall, the results show that the OOP mechanism of the longitudinal wall is a more favorable response, while the façade is more vulnerable, since its performance point was attained closer to the near-collapse displacement range.

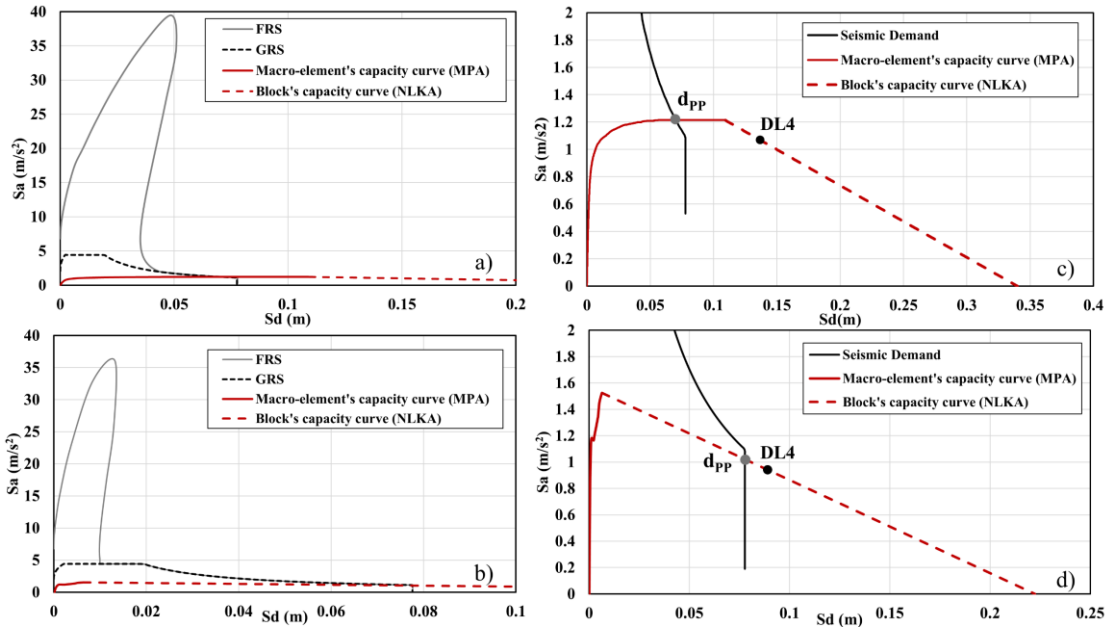

Figure 24: Comparison of the capacity curve and demand spectrum for the a & c) longitudinal wall, and b & d) façade

5.5 Conclusions

The paper proposed a practitioner-oriented procedure for the seismic assessment of unreinforced masonry (URM) churches with integrating the modal pushover analysis (MPA) and nonlinear kinematic analysis (NLKA). This procedure was developed to address a recurrent condition of churches in which the response of the structure cannot be interpreted as either a fully box-like behavior or completely independent macro-elements. In these situations, the seismic behavior is often governed by local out-of-plane (OOP) mechanisms, while the dynamic interactions among macro-elements play a significant role and cannot be neglected.

The procedure was applied to the Church of Nostra Signora delle Grazie e Sant'Egidio located in Bussana Vecchia, a URM church severely damaged by the 1887 earthquake. A global 3D finite element (FE) model of the church was constructed and used to identify the modes governing the response of the main macro-elements and define the corresponding load patterns for pushover analyses. Two relevant OOP mechanisms were considered for the upper blocks of the longitudinal wall and façade. For both cases, the MPA showed to be effective in capturing the initial stiffness and maximum strength of the macro-element. However, a FE-based pushover analysis alone was not sufficient to capture the post-peak behavior of the macro-element, and the point at the end of the pushover analysis is not certainly the ultimate condition of the structure. For this reason, they were complemented by the capacity curves obtained from the NLKA, which was used to represent the behavior of the upper blocks up to the ultimate condition.

The comparison of the two mechanisms highlighted two different scenarios between global and local behaviors. For the longitudinal wall, the global behavior of the macro-element governed the peak strength, while the local mechanism mainly controlled the strength degradation and the ultimate capacity displacement. For the façade, the local overturning mechanism was activated at a lower acceleration level than the one associated with the full global capacity of the macro-element, showing that the local mechanism controlled both the peak strength and the collapse development. These results show that the relationship between the global and local behavior cannot be assumed a priori, but should be considered on a case-by-case basis by using an integrated framework.

The main contribution of the present study is to establish a link between the global behavior obtained from the FE model and the local mechanisms evaluated by the kinematic analysis. This integration preserves the advantages of the FE global modeling in taking into account the interactions between the macro-elements, while overcoming its inability to capture the post-peak behavior and local OOP mechanisms. Its field of application is relevant to the URM churches and heritage structures characterized by flexible diaphragms, partial continuity among the orthogonal structural elements, and complex dynamic interactions among macro-elements. The future developments may include the application of the procedure on a broader class of URM churches, comparison with nonlinear dynamic analyses, and further refinement on its application for professional assessments and retrofit designs.

Chapter 6

Retrofit design and decision-support for vulnerable components: multi-objective optimization for bell gables

6.1 Introduction

The assessment framework discussed in the previous chapter identifies the structural elements and mechanisms that govern the seismic vulnerability of URM churches. Once the most critical vulnerabilities have been identified, the problem shifts from diagnosis to intervention, which requires the selection of optimal retrofitting solutions capable of improving seismic behavior while remaining compatible with the architectural and conservational constraints of churches.

This issue is particularly relevant to secondary elements of churches whose vulnerability can lead to detaching a significant portion of masonry and imposing threats to human safety, even in the case of limited structural damage. Among these, bell gables can be one of the most vulnerable elements due to their slenderness, elevation, and limited restraints, making them susceptible to the OOP overturning mechanism. Therefore, their strengthening can be a relevant representation of the broader field of seismic retrofitting interventions of URM churches.

In these cases, an intervention cannot be designed just by considering the strength increase of the structural element under investigation. Effective and optimal solutions require balancing multiple factors and conflicting objectives, including the improvement of the strength, the structural ductility, and the implementation costs. These aspects are particularly important in the case of

heritage structures, because the designed interventions should be practical, feasible, and compatible with real-project constraints.

To quantify the bell gable's OOP seismic performance according to a displacement-based approach, it is necessary to compare the seismic demand (expressed in terms of FRS) with the structural capacity expressed in terms of capacity curve, obtained through NLKA under specific assumptions (rigid blocks, joints with zero tensile strength, infinite compressive strength and no sliding failures allowed (Heyman 1966)). If the bell gable is not able to fulfill the target performance level, a strengthening intervention is necessary (the most common is the placement of tie rods), and the seismic assessment has to be reappraised in the design configuration to quantify the obtained benefits. It has to be noticed that the results of the assessment in the design configuration are affected by many interacting parameters that govern the block seismic performance, such as ductility, strength, or both. Thus, all the alternatives must be checked to identify the best scenario, i.e., the one that guarantees the highest performance and that is cost-effective. In this chapter, the bell gable was assumed to be placed on the Church of Nostra Signora delle Grazie e Sant'Egidio, so that its seismic behavior and the effectiveness of the retrofitting solutions can be assessed within the structural context of the case-study adopted throughout the thesis.

In this context, to enhance the bell gable's capacity, a vertical tie rod has been employed as a strengthening intervention. The original procedure, proposed by Ghaffarpasand et al. (2023), was applied to the selected case study. The procedure aims to identify the optimal mechanical properties of the vertical tie-rod with the aim of maximizing the capacity and ductility of the bell gable while simultaneously minimizing the overall cost of implementing the retrofitting intervention.

To identify the optimal retrofitting scenarios, the NSGAII-SA algorithm (which stands for Non-Dominated Sorting Genetic Algorithm II & Simulated Annealing) was implemented (Ghaffarpasand et al. 2023), by considering the optimization parameters of tie-rod properties from which the optimal choices are made, including the tie-rod cross-sectional area, pre-stressing load, tie-rod position within the block, and its ultimate strength.

As a result, a series of optimal retrofitting interventions is obtained, each of which consists of different values selected from the possible ranges for the optimization parameters. The algorithm finds a collection of ideal retrofitting options (Pareto front) that have not been dominated by any other retrofitting interventions. The mechanical characteristics of the vertical tie-rod that result in the

maximum capacity parameters and the lowest execution costs are then determined. These results can help the decision-makers to select the most suitable option based also on the available resources.

The aim of this chapter is to develop a decision-support framework for the seismic retrofitting of vulnerable church elements, with a particular application to bell gables. This chapter is organized as follows. First, the seismic vulnerability of bell gables is discussed together with the considered retrofitting solutions for this study. Then, the chapter presents the formulation for the multi-objective optimization problem and the criteria that the solutions are evaluated based on. Finally, a set of optimal solutions is presented for this specific problem, and the prioritization for the selection of the best retrofit option is then discussed based on the available resources and budget.

6.2 Out-of-Plane Seismic Performance

Evaluating the performance of the as-built bell gable and the retrofitted one under each investigated retrofitting scenario will consist of calculating the strength parameters, the ductility parameter, and retrofit costs. While the retrofit costs have been assessed based on market values (as described in detail in §6.4.2), a brief description of the procedure employed to derive the other parameters is as follows.

The strength parameters (namely, α_0 and α_{max}) and the ductility parameter (namely, μ) have been obtained by deriving the capacity curve of a block (representative of a possible bell gable in a church) via linear and nonlinear kinematic analyses. If a rectangular rigid block of thickness *2b* and height *2h* is considered, simply supported at the base and subjected only to its own mass *M*, the horizontal inertial seismic action is assumed as: i) proportional to the gravity load *P=Mg* through a seismic multiplier α; and ii) applied at a control point usually assumed as the gravity center. The value of the multiplier which activates the OOP mechanism (α_0) may be calculated according to Equation 18, where λ is defined as the block slenderness. α_0 is obtained by applying the basic principle of static equilibrium in the initial configuration of the block. Then, by imposing the static equilibrium under an incremental kinematic analysis, that is increasing the rigid block rotation up to the condition of static equilibrium loss, it is possible to obtain the whole capacity curve. Figure 25 (a) illustrates an example of a capacity curve expressed as seismic multiplier α vs. rotation θ, which describes the simple overturning of a block in the as-built configuration (grey line).

$$\alpha_0 = \frac{b}{h} = \frac{1}{\lambda} \tag{18}$$

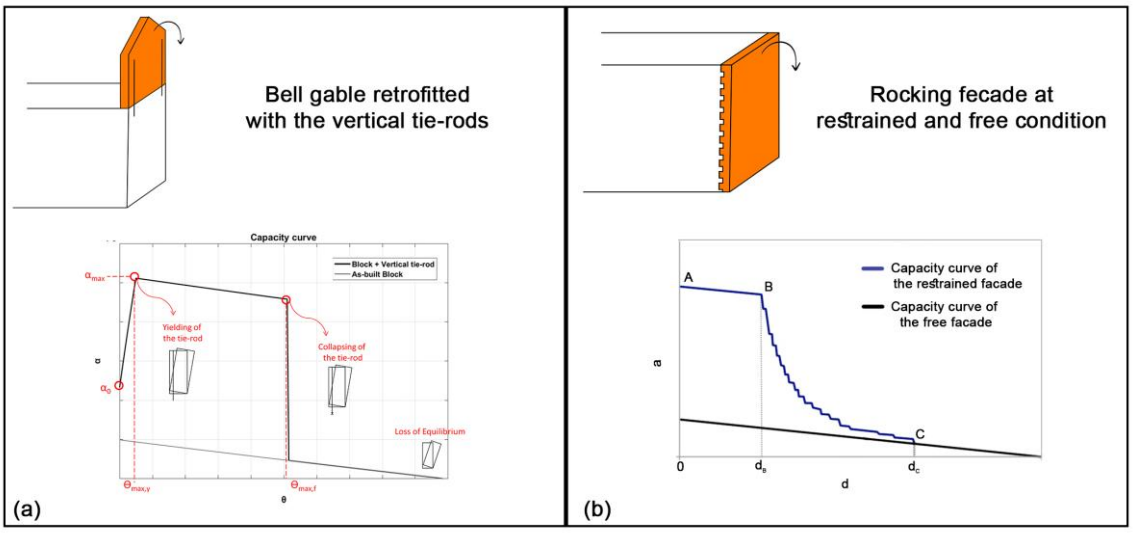

Figure 25: The effect of a) the vertical tie-rods on the capacity curve of the bell gables, b) frictional resistances on the capacity curve of the facade

If the block is retrofitted with a pre-stressed tie-rod, the capacity curve changes as described in Figure 25 (a) (black line): the seismic multiplier which activates the mechanism is higher, then α further increases up to the tie-rod yielding (α_{max}). Then, a decreasing branch starts up to the failure of the tie-rod when the retrofitting intervention is no longer effective, and the capacity curve comes back to the initial one of the as-built block. The length of the decreasing branch in the restored configuration defines the last parameter objective of the optimization problem, which is the ductility parameter μ. It has been calculated according to Equation 19, where $\theta_{max,f}$ and $\theta_{max,y}$ are the rotation of the block corresponding to the tie-rod failure and yielding, respectively.

$$\mu = \frac{\theta_{max,f}}{\theta_{max,y}} \tag{19}$$

Figure 25 (b) illustrates the capacity curves, depicting the relationship between frictional resistances and displacements. In the context of bell gables, due to the lack of adequate connections with other structural components, the impact of frictional resistance on their capacity is relatively minor. Conversely, for larger

macro-elements like facades, frictional resistances can considerably enhance their capacity, as shown in Figure 25 (b) (Casapulla et al. 2021b).

The influence of frictional resistance in macro-blocks is pivotal, particularly regarding the seismic vulnerability of masonry structures. Casapulla et al., (2021) demonstrated in their work to how incorporating frictional resistance into an advanced macro-block model significantly improves predictions of seismic capacity in stone masonry structures. Further expanding on this topic, Funari et al., (2022) introduced a more nuanced method for evaluating the frictional resistance in non-periodic masonry through their study. These contributions emphasize the essential role of the frictional resistance in enhancing the understanding of structural integrity and safety in masonry structures subjected to seismic forces.

Finally, once maximized the strength and ductility parameters while minimizing the retrofit costs, to check if the OOP mechanism is activated or not, the spectral acceleration a_0^* corresponding to the seismic multiplier α_0 was compared for each optimal scenarios with the peak floor acceleration (PFA) at the level where the bell gable was supposed to be placed. Under the rigid block assumption, the mechanism is activated when Equation 20 is established, being e* the fraction of participant mass (equal to 1 for a single block), and PFA is calculated according to Equation 21, as proposed in Degli Abbati et al., (2021).

$$\mathrm{PFA} = \frac{\alpha_0 g}{e^*} \tag{20}$$

$$\mathrm{PFA}_{Z,k} = S_a(T_k)\eta(\xi_k)|\gamma_k \times \psi_k|\sqrt{1 + 4\xi_k^2} \tag{21}$$

In Equation 20, α_0 is the coefficient of the lateral load that activates the kinematic response, $g = 9.81$ is the gravity acceleration, and $PFA_{Z,k}$ represents the k_{th} peak floor acceleration, which is influenced by various factors related to the main structure. These factors include the natural periods (T_k), modal participation coefficients (γ_k), modal shapes (ψ_k *(x y z)*), and the viscous damping (ξ_k) of the structure. Additionally, it is dependent on the ground spectrum $S_a(T_k)$, which is computed considering the natural period T_k of the structure and appropriately adjusted using the damping correction factor $\eta(\xi_k)$.

6.3 Adopted Procedure and Optimization Algorithm

The aim of this chapter is to find the optimal mechanical properties of a vertical tie-rod used as the retrofitting intervention to prevent a bell gable from overturning. These mechanical properties, hereinafter defined as 4Rs, are defined as follows:

- R1 = Transversal area of the tie rod
- R2 = Pre-stressing load
- R3 = Position of the tie rod (d)
- R4 = Ultimate strength of steel

For the purpose of finding optimal solutions, the algorithm of NSGAII-SA was employed. This algorithm is the combination of the NSGA-II (Non-dominated Sorting Genetic Algorithm II) and SA (Simulated Annealing).

Deb et al., (2002) introduced NSGA-II, a highly popular population-based algorithm. During each iteration of this algorithm, a new set of solutions (referred to as the offspring population) is generated through crossover and mutation operations. The individuals within the population are then organized into different fronts through a process called non-dominated sorting, and the individuals within each front are arranged based on their crowding distance values. Because of its efficient non-dominance sorting procedures and its ability to converge towards a diverse set that closely approximates the actual Pareto front, the NSGA-II, is commonly employed in research when seeking optimal solutions in situations where a closed-form expression for the objective function is unavailable (Deb 2001).

The SA (Simulated Annealing) algorithm draws inspiration from the real-world process of annealing solid metals, as outlined by Suppapitnarm et al., (2000). This algorithm operates by considering the probability of accepting a new solution, a probability that varies depending on a parameter known as temperature. Temperature, a virtual element within the algorithm, plays a crucial role in determining the likelihood of accepting a proposed solution. In the context of multi-objective problems, even if a solution does not dominate the current one, it still possesses a certain probability of being accepted. This unique feature enables the algorithm to explore beyond local optima by temporarily moving towards worse solutions in its quest to find the global minimum.

As each iteration progresses, the temperature (denoted as T) decreases, subsequently reducing the probability of acceptance. This reduction in acceptance

probability aids in the convergence process. The non-dominated solutions are preserved and then organized based on their degree of isolation values.

The hybrid NSGAII-SA method, which combines the advantages of the two previous algorithms to produce more accurate findings, was used in this study. This algorithm begins with the creation and evaluation of an initial random population. Unlike the original NSGA-II, it uses an Archive for non-dominated solutions, initialized with NSGA-II's first front. The initial temperature is determined before the main loop and decreases iteratively after finishing each iteration.

New solutions are generated through crossover and mutation operators, forming the offspring population. Dominance status is assessed, and non-dominated solutions are stored in the Archive. Challenges arise when new non-dominated solutions are added to the Archive, including the possibility of some individuals being dominated by or dominating those previously stored in the Archive. To address these challenges, dominance status is identified for all Archive individuals to compute the new global front of non-dominated solutions. Additionally, the Archive's size may exceed a maximum limit, prompting the use of the crowding distance technique to sort and remove individuals, ensuring diversity within the Archive, similar to NSGA-II. This algorithm is described with complete details and used for identifying optimal retrofitting scenarios for an existing curved bridge in Ghaffarpasand et al. (2023). Figure 26 illustrates the flowchart of the algorithm used in this study.

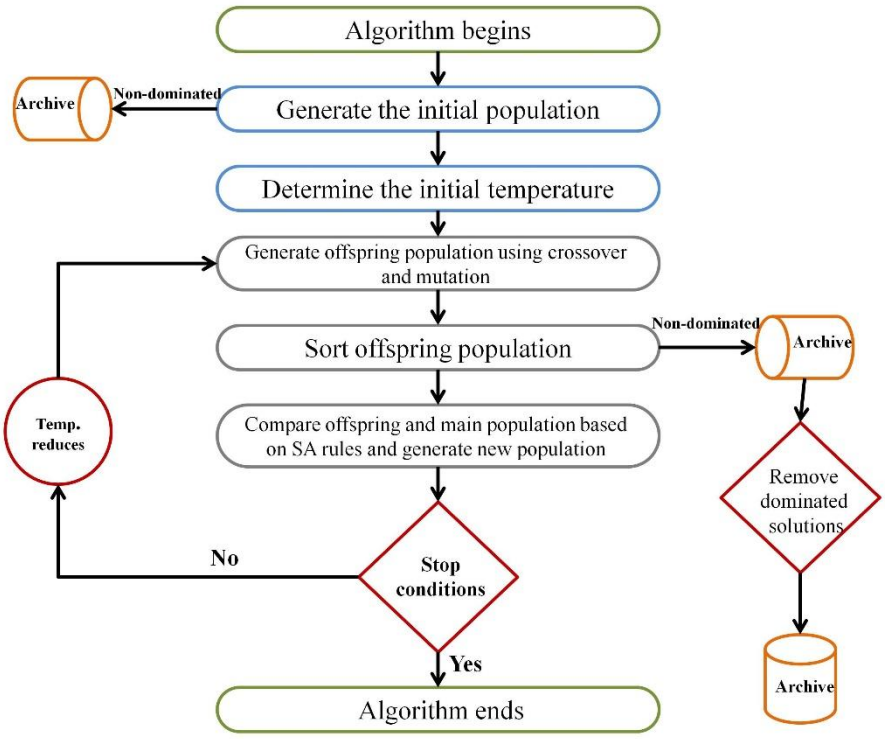

Figure 26: The flowchart of the multi-objective hybrid NSGAII-SA algorithm

For solving an optimization problem, some objectives are needed to be introduced to the algorithm. If there is just one objective, the result of the algorithm will be one optimal solution. In multi-objective optimization problems, instead of a single solution, there exists a set of optimal solutions. In cases where conflicting objectives are present, like in this study where there's a trade-off between maximizing strength and minimizing cost, the algorithm identifies a range of optimal compromises. The ultimate choice among these solutions is left to decision-makers. Therefore, decision-makers can make their selection by considering supplementary information that was not initially incorporated into the optimization model, such as expected post-event resources and engineering judgments.

The optimization objectives in this study are to maximize the strength parameters (α_0 and α_{max}) and the ductility parameter μ in the capacity curve and to minimize the cost of the retrofitting execution.

The mechanical properties mentioned, which the algorithm uses to achieve the optimization objectives, serve as decision variables, and their potential range of values defines the entire design space for the problem. Each retrofitting scenario

will comprise a specific value within the range of variation for each of the aforementioned properties.

The algorithm evaluates each selected retrofitting scenario, implying that it computes all the objectives for that solution and subsequently compares them during the comparison step of the algorithm. Solutions characterized by higher values of α_0, α_{max}, ductility, and lower costs will dominate over worse solutions and are preserved within the Archive. Ultimately, the saved solutions within the Archive represent the optimal solutions and constitute the Pareto front of the problem.

To analyze the results and make well-informed decisions for various scenarios, two distinct geographical areas were considered: one situated in a low seismic activity zone and the other in a high seismic activity zone. Within each of these regions, potential optimal solutions were explored, and discussions were conducted that was related to the specific challenges and conditions associated with the seismicity level of that particular area. This approach allowed for a comprehensive understanding of how the algorithm's results could be effectively applied in real-world scenarios characterized by different seismic risks and conditions.

6.4 Results of the Application to Church Bell Gables

6.4.1 Case study description

The case study considered in this chapter is representative of a brick masonry bell gable, alternatively considered in the as-built configuration and retrofitted with a vertical tie-rod. The bell gable has a thickness and height equal to 60 and 300 cm, respectively. Figure 27 (a) shows a schematic view of the block section, retrofitted with a vertical tie-rod placed at a distance (d) from the block's outer edge. The block is subjected only to its self-weight P (applied in the gravity center G) and to the pre-load F applied at the center of the tie-rod cross-section. Figure 27 (b-c) illustrates an example of an actual bell gable strengthened by means of three vertical external tie-rods.

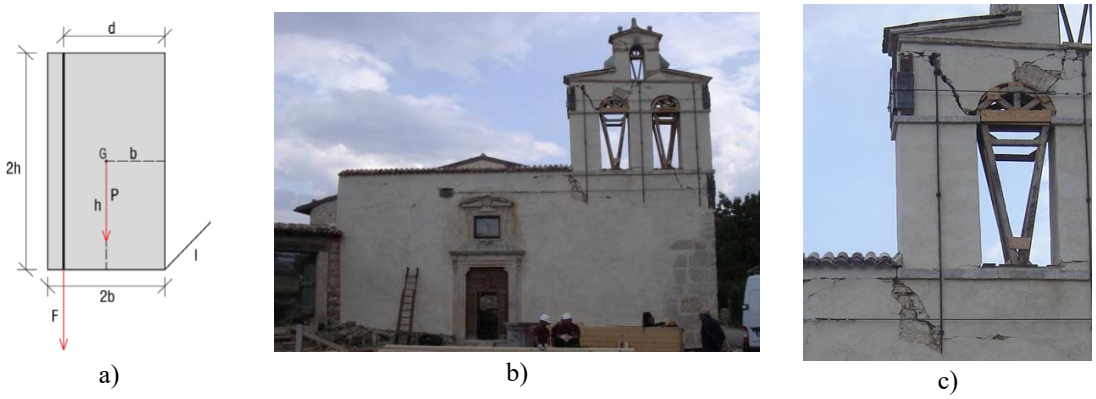

a) b) c)

Figure 27: a) Schematic view of the considered bell gable; b-c) Example of a bell gable retrofitted with vertical tie-rods.

6.4.2 Selection and evaluation of retrofitting scenarios

As mentioned in §6.3, each retrofitting scenario involves the selection of a specific value from the defined range of variations for each of the mentioned 4Rs properties. The ranges of variation of the considered mechanical properties (4Rs) are as follows:

R = {R1, R2, R3, R4}

R1 = {20 mm, 30 mm, 40 mm}

R2 = {0 kN, 10 kN, 15 kN, 20 kN, 25 kN, 30 kN, 35 kN}

R3 = {From 30 cm to 60 cm, with increments of 1 cm}

R4 = {36000 N/cm^2, 43000 N/cm^2, 51000 N/cm^2}

According to the considered ranges for the tie-rod's mechanical properties, there are 1890 feasible scenarios for retrofitting the bell gable. The value of R2 = 0 and R3 = 60 in retrofitting scenarios means that the employed tie-rod was no pre-stressed and it is placed at the outer edge of the bell gable, respectively.

Each retrofit scenario that is chosen by the algorithm is evaluated, meaning that all the objectives are computed for that specific scenario. Firstly, for each scenario, linear and nonlinear kinematic analyses were carried out to compute the horizontal seismic multiplier α_0 and the capacity curve. Then, the strength and ductility parameters were evaluated as described in §6.2. The retrofitting costs were calculated based on market values, as described in more detail below.

The costs of implementing a vertical tie-rod, which is one of the optimization objectives and the last part of the evaluation process of scenarios, consist of the costs for drilling the block (C1), supply and installation of the tie-rod (C2), workers (C3), and the restoration process (C4). The price list that was published in 2023 for the Liguria region was used to compute the mentioned costs (‘Prezzario Regione Liguria - Year 2023)

The cost associated with drilling the block was calculated by the following equation:

$$C1 = H \times D \tag{22}$$

Where, *H* represents the block's height, and *D* corresponds to the cost related to the drilling process per meter, which amounts to 189.75 €.

The cost associated with the supply and installation of standard manufacturing tie-rods, excluding preparatory masonry works (drilling and so on) was calculated through the following formulation:

$$C2 = A_{reb} \times H \times \rho \times S \tag{23}$$

Where A_{reb} is the area of the tie-rod section, ρ is the density of the tie-rod, and *S* is the price of purchasing a tie-rod per kilogram, equal to 24.65 €, according to the Liguria price list.

The calculation of the expenses related to the workforce was conducted using the following formula:

$$C3 = \text{hours} \times W \tag{24}$$

Where *W* is the price of workers per hour, which is equal to 39.10 €.

Finally, the calculation of costs related to the restoration process was conducted through the following equation:

$$C4 = A_{top} \times R \tag{25}$$

In Equation 8, A_{top} is the area of the top surface of the block, and *R* is the cost for external plaster, which is equal to 27.01 €.

The total cost for retrofitting implementation in each scenario is the sum of all the previously mentioned costs.

$$C = C1 + C2 + C3 + C4 \tag{26}$$

Once the calculation of the implementation cost is completed, the evaluation of a scenario concludes, resulting in specific values for all the objectives.

6.4.3 Results of nonlinear kinematic analysis and algorithm performance

Table 23 reports all the optimal retrofitting scenarios among the feasible solutions. None of these should be regarded as a universal solution for the problem at hand. Each of these solutions possesses its own strengths and may excel under different conditions and contexts. The choice of which solution to use depends on many factors, including the specific location of the church, the resources available, the extent of existing damage, the historical experiences with previous hazards, and other relevant factors. These various aspects bring complexity to the decision-making process. Therefore, it is essential for decision-makers to exercise their engineering judgment, considering the intricate interplay of these variables and nuances within the given context. By doing so, they can make informed decisions that align with the unique needs and challenges of the situation at hand, ultimately leading to the most appropriate and effective course of action.

Table 23: The optimal retrofitting solutions for the bell gable

	Retrofitting Scenario	α_0	α_{max}	Ductility	Cost [€]
1)	(20,0,59,51000)	0.1964	1.9988	4.0392	81719
2)	(20,0,54,43000)	0.1964	1.5880	4.7907	81719
3)	(30,0,55,51000)	0.1964	3.7250	4.0392	81833
4)	(30,35000,60,43000)	0.6165	3.5471	5.2840	81977
5)	(40,0,58,51000)	0.1964	6.2653	4.0392	81992
6)	(40,20000,60,43000)	0.4375	5.7247	4.9364	82137
7)	(20,20000,55,43000)	0.4169	1.6183	5.4494	82304
8)	(20,30000,58,36000)	0.5447	1.4682	7.4271	82304
9)	(20,35000,55,36000)	0.5805	1.3985	7.8385	82304
10)	(30,25000,54,51000)	0.4665	3.6526	4.2657	82418
11)	(30,10000,55,36000)	0.3070	2.7814	5.9154	82418
12)	(40,35000,58,36000)	0.6021	4.7759	6.1182	82578
13)	(40,35000,39,36000)	0.4653	3.0013	6.1182	82578

To further orient the decision makers in the selection of the best option, a first step was to identify three ranges of variation for the optimization parameters (Table 24) to highlight those scenarios that tend to minimize the costs without penalizing too much the strength and ductility parameters (green-yellow cells). A second step was selecting only those optimal solutions that avoid the mechanism activation. To do so, it has been necessary to select a specific site and to define the dynamic properties of the Church of Nostra Signora delle Grazie e Sant'Egidio to define the amplified seismic input which is applied at the base of the bell gable.

Table 25 reports the parameters used to calculate the PFA, which was then compared with the acceleration a_0 which activates the OOP response of the bell gable. Two different sites were considered (i.e., Genoa and L'Aquila, characterized by a lower and higher seismic hazard, respectively). The dynamic parameters of the church are representative of an actual case with constructive features typical for these typologies. Table 24 collects all the parameters used to compute the PFA for a return period of 712 years and for Genoa and L'Aquila.

Table 24: The categories of the results and their range of variation

Optimization parameters	Green	Yellow	Red
α_0	0.63-0.47	0.47-0.31	0.31-0.15
α_{max}	7-5	5-3	3-1
Ductility	8-6.75	6.75-5.25	5.25-4
Cost (€)	81500-82000	82000-82500	82500-83000

Table 25: Parameters used to calculate the PFA

Dynamic parameters of the church					Genoa		L'Aquila	
T_k	ξ_k	$\eta(\xi_k)$	γ_k	ϕ_k	$S_a(T_k)$	PFA	$S_a(T_k)$	PFA
0.44 s	0.08	0.88	1.1	1.00	2.21	2.16 m/s2	7.88	8.23 m/s2

Table 26 shows the results of the seismic assessment performed to identify which scenarios avoid the mechanism activation. The parameter ξ_s is calculated as the ratio between capacity and demand. Thus, values higher than 1 mean that the mechanism is not activated. Table 26 shows that the best retrofitting scenario for Genoa is scenario 4. This solution is effective against the mechanism activation and allows, at the same time, to obtain high strength and ductility parameters with low retrofitting costs. Instead, in the case of L'Aquila, no retrofitting scenarios can stop the activation of the OOP response of the bell gable, due to the seismic hazard being higher than that of Genoa. However, among the scenarios associated to the highest ξ parameter (equal to 0.8), scenario 4 is again the one that best balances the higher seismic performance of the bell gable with the lowest retrofitting costs.

Table 26: Evaluation of the local mechanism for each retrofitting scenario

Scenarios	α_0	α_{max}	μ	Cost	a_0	$\xi_{s,Genoa}$	$\xi_{s,L'Aquila}$
1					1.93	0.9	0.3
2					1.93	0.9	0.3
3					1.93	0.9	0.3
4					6.05	2.8	0.8
5					1.93	0.9	0.3
6					4.29	2.0	0.6
7					4.09	1.9	0.5
8					5.34	2.5	0.7
9					5.69	2.6	0.7
10					4.58	2.1	0.6
11					3.01	1.4	0.4
12					5.91	2.7	0.8
13					1.93	2.1	0.6

6.5 Conclusions

The study examines the OOP behavior of a masonry panel, representative of a bell gable subjected to seismic action. The panel is assumed to exhibit a rigid block behavior, with infinite compressive strength, and zero tensile strength. The work applies to the considered case study to select and assess the optimal retrofitting scenarios (*i.e.,* the optimal mechanical properties of a vertical tie-rod) by employing the NSGAII-SA algorithm. Various mechanical properties and configurations (denoted as 4Rs) have been considered to enhance the structural integrity and seismic performance of the bell gable. The 4Rs include the tie-rod diameter, pre-stressing force, positioning distance of the tie-rod, and ultimate strength of steel. This extensive range of properties results in a vast number of possible retrofitting scenarios. Each retrofit scenario was evaluated, considering multiple objectives. Linear and non-linear kinematic analyses were performed in order to assess the seismic OOP response of the bell gable and to define the strength and ductility optimization parameters. In addition to the structural considerations, cost-effectiveness plays a pivotal role in scenario evaluation. The costs associated with drilling the masonry block, supplying, and installing the tie-rod, labor, and restoration were all calculated. The total implementation cost is a critical factor in assessing the feasibility of each scenario. The costs were assessed based on the market values as defined in the latest pricing data for the Liguria region in 2023, ensuring that the estimations are current and accurate. Ultimately, this comprehensive evaluation process results in specific values for all objectives, enabling a detailed comparison of the retrofitting options. The study emphasizes the complexity of retrofitting decisions and the need for a nuanced approach that balances structural integrity, safety, and cost-effectiveness. This research could provide some useful insights and guidance for engineers and stakeholders tasked with retrofitting historic buildings, promoting resilience and sustainability in the face of seismic hazards.

Chapter 7

Conclusions and future work

This thesis addressed the seismic assessment and strengthening of historical and monumental unreinforced masonry (URM) structures, focusing on churches. Churches are among the most vulnerable classes of URM structures due to their complex and irregular configurations, large spatial volumes, flexible diaphragms, and weak connections among macro-elements. These features make churches highly susceptible to Out-Of-Plane (OOP) mechanisms, in contrast to regular structures whose behavior is often governed by In-Plane (IP) responses. Following these, this thesis was structured around four main objectives: (i) the comparison between refined with simplified modeling strategies for URM churches, (ii) the trade-off between the computational cost and the accuracy of the predictions, (iii) the development of a seismic assessment framework that links the global behavior of the structures with their local responses, and (iv) the development of a decision-support framework for the retrofit of vulnerable secondary elements by considering real-project constraints, such as the available budgets. The Church of Nostra Signora delle Grazie and Sant'Egidio, located in Bussana Vecchia, Italy, was adopted as the case-study of this thesis, due to its damaged configuration and a representative of the heritage asset for which reconstruction is not intended; instead, the objective is to ensure its safety in its current situation.

7.1 Main Findings of the Thesis

The first part of the thesis reviewed the vulnerabilities and available seismic assessment methodologies for URM churches in the literature. This review exhibited that the behavior of URM churches cannot often be interpreted through the same assumptions commonly adopted for other types of structures. Churches frequently exhibit partial structural interactions among macro-elements rather than a full box-like behavior, and their seismic response is often governed by local mechanisms involving façades, nave walls, apses, vaults, and secondary elements. This chapter confirmed that the available methods range from territorial and empirical to numerical approaches, but none of them alone can be sufficient for all

purposes. This finding motivated the need for a multilevel strategy that was selected according to the objectives of the assessment.

The first results of the thesis concern the comparison between three modeling strategies applied to the Bussana church: Finite Element Method (FEM), Discrete Element Method (DEM), and Equivalent Frame Model (EFM). All three modeling methods, despite their different assumptions and levels of refinement, predicted similar global behaviors for the church, highlighting that the transversal direction is more vulnerable than the longitudinal one. This is mainly because, in the transversal direction, the response is significantly affected by the OOP mechanism of the longitudinal walls, whose vulnerability is amplified by the absence of the vault and the limited restraints. However, the behavior of the church in the longitudinal direction is the combination of the IP response of the longitudinal walls with the OOP response of the apse and the façade, leading to a partial box-like behavior.

Additionally, the comparative study showed that the three modeling strategies are not equivalent in terms of the level of details of the results and their field of application. FEM and DEM provided the most detailed representation of stiffness distribution, damage evolution, and failure mechanisms. FEM offered a smooth nonlinear behavior, since it treats URM as a continuum deformable body, while DEM, which is an assembly of blocks interacting through their interfaces, showed fluctuations related to the separation and collision of blocks throughout the behavior. In contrast, EFM was computationally efficient and capable of reproducing the elastic behavior of the structure with an acceptable accuracy. It was also capable of capturing the main mechanisms that govern the seismic response in both main directions, especially when complemented with 3D pillars that have both the IP and OOP stiffness. However, it underestimates the lateral capacity of the structure and cannot explicitly capture the mechanisms of the curved macro-elements, such as vaults. Therefore, EFM was proven to be a useful safe-side assessment tool for preliminary analyses and screening the global behavior, while DEM and FEM were shown to be more appropriate approaches for detailed assessments and retrofit design purposes, where detailed damage evolution and local mechanisms are required.

These results directly answer the first two research questions of this thesis. Regarding Q1, the study showed that refined and simplified numerical approaches can provide coherent identification of the global behavior and governing mechanisms while differing significantly in terms of capturing the damage progression, local mechanisms, and stiffness degradation. With respect to Q2, the

thesis demonstrated that simplified strategies, such as EFM, can be useful when the objective is to perform a preliminary assessment or practitioner-oriented safe-side verification, but they need careful interpretation. In addition, the results show that the balance between the computational cost and the accuracy of the model strongly depends on the behavior of the church, the objective of the assessment, and the level of detail needed for decision-making.

The second contribution of the thesis concerns the development of a practitioner-oriented seismic assessment framework discussed in Chapter 5. This procedure is proposed for URM churches whose behavior lies between two extremes: a full global box-like behavior and a set of completely independent macro-elements. The framework combines the Modal Pushover Analysis (MPA), performed on a 3D global FE model, with the Non-linear Kinematic Analysis (NLKA). The idea is that the global model is used to account for the structural interactions, modal properties, and the stiffness and strength of macro-elements when they are a part of a structure, while NLKA is used to complete it by describing the post-peak behavior and the evolution of local mechanisms up to the ultimate condition.

The application of this procedure on the Bussana church highlighted that the relationship between the global and local behavior cannot be assumed a priori. For the longitudinal wall, the global response of the macro-element controlled the maximum resistance, while the local response mainly governed the post-peak branch and the strength degradation up to collapse. For the façade, instead, the local mechanism started at a lower acceleration than the one associated with the global response of the macro-element, thus governing both the peak resistance and the collapse mechanism. This is an important result showing that the global and local responses should not be evaluated separately; instead, for churches with significant structural interactions, they should be integrated into a framework. In this way, the thesis answered Q3 by proposing a procedure that preserves the global modeling advantages while overcoming its limitations in representing local mechanisms.

The last main finding of the thesis concerns Q4 and the transition from assessment to interventions. Chapter 6 proposed a decision-support approach for the retrofit of the vulnerable elements of churches, with a specific application on a bell gable assumed to be placed on the case-study church. The chapter framed the retrofit design into a multi-objective optimization, with accounting for seismic performance and implementation costs simultaneously. The proposed procedure evaluated a large number of retrofitting scenarios for a vertical tie-rod by varying four main properties: tie-rod diameter, its position, prestressing force, and the

ultimate strength of steel. The scenarios were evaluated through linear and nonlinear kinematic analyses to estimate the strength and ductility, and through cost estimation based on the regional market values. The use of NSGAII-SA allows to derive a set of optimal solutions rather than just one solution, leaving it to engineers and practitioners to make decisions about the best option based on the current situation.

7.2 Limitations of the Research and Future Work

Despite of the mentioned contributions of this thesis, there were some limitations throughout the thesis that need to be explicitly acknowledged. The first limitation concerns the study on only one case study. The Church of Nostra Signora delle Grazie and Sant'Egidio is an appropriate case-study for this research due to its complex and damaged configuration, but the conclusions were derived mainly from one church and therefore should not be generalized to all URM churches with different characteristics. Different layouts, vault systems, diaphragm conditions, and material quality can lead to different situations in terms of global and local behaviors. Therefore, it is required to extend the proposed methodologies and frameworks to broader and more diverse typologies of URM churches. This would make it possible to verify the robustness of the obtained conclusions and transform them into more general recommendations for engineering practice.

The second limitation concerns uncertainty in material properties, boundary conditions, and structural details. In the case of heritage structures, performing onsite experimental tests was limited, and some parameters had been selected from codes, literature, or calibration exercises. Future development should include sensitivity analyses and probabilistic approaches for material properties, connections quality, and modeling assumptions. This is especially relevant for heritage and monumental structures, where incomplete knowledge is often unavoidable. Incorporating uncertainties into seismic assessment in a systematic way would strengthen the reliability of the assessment and retrofit decision-making.

The third limitation concerns the framework proposed for the seismic assessment and verification of macro-elements involved by OOP mechanisms. This framework still requires more validation. Although nonlinear static and kinematic analyses are highly valuable and practical, they do not completely replace nonlinear dynamic analyses where record-to-record variability and dynamic interactions become critical. Future developments should include the comparison of the obtained results with the one obtained by nonlinear dynamic analyses and post-

earthquake damage observations. This comparison would clarify the accuracy of the simplified approach of nonlinear static and kinematic analyses and allow its more refinement.

Finally, the proposed NSGAII-SA optimization framework is presently formulated in a deterministic manner and therefore does not account for uncertainties through probabilistic confidence intervals. Future developments should include probabilistic approaches and reliability-based optimization procedures, which could improve the practical applicability of the proposed decision-support framework.

References

Aguilar R, Noel MF, Ramos LF (2019) Automation in Construction Integration of reverse engineering and non-linear numerical analysis for the seismic assessment of historical adobe buildings. Autom Constr 98:1–15. https://doi.org/10.1016/j.autcon.2018.11.010

Allemang RJ (2003) The modal assurance criterion - Twenty years of use and abuse. Sound Vib 37:14–21

Allemang RJ (1980) Investigation of some multiple input/output frequency response funcrion experimental modal analysis techniques. University of Cincinnati

Amitrano L, Longobardi G, Formisano A (2025) A comprehensive multi-level approach for seismic failure analysis of masonry churches in Sorrento (Naples , Italy). Structures 81:110264. https://doi.org/10.1016/j.istruc.2025.110264

Antoniou S, Pinho R (2004) Development and verification of a displacement-based adaptive pushover procedure. J Earthq Eng 8:643–661. https://doi.org/10.1080/13632460409350504

Atamturktur S, Bornn L, Hemez F (2011) Vibration characteristics of vaulted masonry monuments undergoing differential support settlement. Eng Struct 33:2472–2484. https://doi.org/10.1016/j.engstruct.2011.04.020

Aydınalp T, Uzelli T, Sağın EU (2025) Tracing the Origins : Byzantine Lime Mortars from Anaia and St . Jean Churches (Western Türkiye) and Provenances of Natural Stone Aggregates. Geoheritage 17:. https://doi.org/10.1007/s12371-025-01086-5

Baraldi D, Reccia E, Cecchi A (2018) In plane loaded masonry walls: DEM and FEM/DEM models. A critical review. Meccanica 53:1613–1628. https://doi.org/10.1007/s11012-017-0704-3

Bartoli G, Betti M, Giordano S (2013) In situ static and dynamic investigations on the " Torre Grossa" masonry tower. Eng Struct 52:718–733. https://doi.org/10.1016/j.engstruct.2013.01.030

Bartoli G, Betti M, Vignoli A (2016) A numerical study on seismic risk assessment of historic masonry towers: a case study in San Gimignano. Bull Earthq Eng 14:1475–1518. https://doi.org/10.1007/s10518-016-9892-9

Beatini V, Royer-Carfagni G, Tasora A (2017) A regularized non-smooth contact dynamics approach for architectural masonry structures. Comput Struct 187:88–100. https://doi.org/10.1016/j.compstruc.2017.02.002

Berti M, Salvatori L, Orlando M, Spinelli P (2017) Unreinforced masonry walls with irregular opening layouts: reliability of equivalent-frame modelling for seismic vulnerability assessment. Bull Earthq Eng 15:1213–1239. https://doi.org/10.1007/s10518-016-9985-5

Bertolesi E, Adam JM, Rinaudo P, Calderón PA (2019) Research and practice on masonry cross vaults – A review. Eng Struct 180:67–88. https://doi.org/10.1016/j.engstruct.2018.10.085

Betti M, Borghini A, Boschi S, et al (2018) Comparative Seismic Risk Assessment of Basilica-type Churches. J Earthq Eng 22:62–95. https://doi.org/10.1080/13632469.2017.1309602

Betti M, Galano L, Lourenço PB (2021) Territorial seismic risk assessment of a sample of 13 masonry churches in Tuscany (Italy) through simplified indexes. Eng Struct 235:111479. https://doi.org/10.1016/j.engstruct.2020.111479

Betti M, Vignoli A (2008) Assessment of seismic resistance of a basilica-type church under earthquake loading : Modelling and analysis. 39:258–283. https://doi.org/10.1016/j.advengsoft.2007.01.004

Borri A, Castori G, Grazini A (2009) Retrofitting of masonry building with reinforced masonry ring-beam. Constr Build Mater 23:1892–1901. https://doi.org/10.1016/j.conbuildmat.2008.09.012

Borri A, Corradi M, Castori G, et al (2019) Analysis of the collapse mechanisms of medieval churches struck by the 2016 Umbrian earthquake. Int J Archit Herit 13:215–228. https://doi.org/10.1080/15583058.2018.1431731

Boscato G, Pizzolato M, Russo S, et al (2014) Seismic Behavior of a Complex Historical Church in L ' Aquila CHURCH IN L ' AQUILA. 3058:. https://doi.org/10.1080/15583058.2012.736013

Bozyigit B, Ozdemir A, Dalgic KD, et al (2024) Damage to monumental masonry buildings in Hatay and Osmaniye following the 2023 Turkey earthquake sequence : The role of wall geometry , construction quality , and material properties. Earthq Spectra 40:. https://doi.org/10.1177/87552930241247031

Brandonisio G, Lucibello G, Mele E, Luca A De (2013) Damage and performance evaluation of masonry churches in the 2009 L'Aquila earthquake. Eng Fail Anal 34:693–714. https://doi.org/10.1016/j.engfailanal.2013.01.021

Brandonisio G, Mele E, Santaniello R, DE LUCA A (2008) Seismic safety of basilica churches: analysis of ten case studies. In: the 6th International Conference on Structural Analysis of Historic Construction. pp 1261–1269

Briceño C, Noel MF, Chácara C, Aguilar R (2021) Integration of non-destructive testing, numerical simulations, and simplified analytical tools for assessing the structural performance of historical adobe buildings. Constr Build Mater 290:. https://doi.org/10.1016/j.conbuildmat.2021.123224

Burdisso RA, Singh MP (1987) MULTIPLY SUPPORTED SECONDARY SYSTEMS PART I : RESPONSE SPECTRUM ANALYSIS. Earthq Eng Struct Dyn 15:53–72

Calderini C, Cattari S, Lagomarsino S (2009) In-plane strength of unreinforced masonry piers Chiara. Earthq Eng Struct Dyn 243–267. https://doi.org/10.1002/eqe.860

Calvini N (1941) Giornale storico e letterario della Liguria, protocollo II-III (in Italian)

Calvini N (1987) Bussana dall'antico al nuovo paese. Sanremo (in Italian)

Canuti C, Carbonari S, Dall'Asta A, et al (2021) Post-Earthquake Damage and Vulnerability Assessment of Churches in the Marche Region Struck by the 2016 Central Italy Seismic Sequence. Int J Archit Herit 15:1000–1021. https://doi.org/10.1080/15583058.2019.1653403

Carocci CF, Cannizzaro F, Cocina S, et al (2023) Preservation of Abandoned Historic Centres—The Case of Poggioreale antica (Sicily). Land 12:. https://doi.org/https://doi.org/10.3390/land12071376

Casapulla C, Argiento LU (2016) The comparative role of friction in local out-of-plane mechanisms of masonry buildings . Pushover analysis and experimental investigation. Eng Struct J 126:158–173. https://doi.org/http://dx.doi.org/10.1016/j.engstruct.2016.07.036

Casapulla C, Argiento LU, Maione A, Speranza E (2021a) Upgraded formulations for the onset of local mechanisms in multi-storey masonry buildings using limit analysis. Structures 31:380–394. https://doi.org/10.1016/j.istruc.2020.11.083

Casapulla C, Ceroni F, Umberto L (2025) Criteria for identifying vulnerability classes for rocking masonry church façades via fragility curves. Eng Struct 325:119444. https://doi.org/10.1016/j.engstruct.2024.119444

Casapulla C, Maione A, Argiento LU (2021b) Performance-based Seismic Analysis

of Rocking Masonry Façades Using Non-linear Kinematics with Frictional Resistances: A Case Study. Int J Archit Herit 15:1349–1363. https://doi.org/10.1080/15583058.2019.1674944

Casapulla C, Maione A, Ceroni F, et al (2023) Limit analysis and design-oriented approach for out-of-plane loaded masonry walls strengthened by grouted anchors. Eng Struct 285:115991. https://doi.org/10.1016/j.engstruct.2023.115991

Casolo S, Neumair S, Parisi M, Petrini V (2000) Analysis of Seismic Damage Patterns in Old Masonry Church Facades. Earthq Spectra 16:. https://doi.org/https://doi.org/10.1193/1.1586138

Cattari S, Calderoni B, Caliò I, et al (2022a) Nonlinear modeling of the seismic response of masonry structures : critical review and open issues towards engineering practice. Springer

Cattari S, Camilletti D, D'Altri AM, Lagomarsino S (2021) On the use of continuum Finite Element and Equivalent Frame models for the seismic assessment of masonry walls. J Build Eng 43:102519. https://doi.org/10.1016/j.jobe.2021.102519

Cattari S, D'Altri AM, Camilletti D, Lagomarsino S (2022b) Equivalent frame idealization of walls with irregular openings in masonry buildings. Eng Struct 256:114055. https://doi.org/10.1016/j.engstruct.2022.114055

Cattari S, Ottonelli D, Pinna M, et al (2015) Damage and vulnerability analysis of URM churches after the Canterbury earthquake sequence 2010-2011. Proc SECED 2015 Conf Earthq Risk Eng Towar a Resilent World 1–10

Cattari S, Resemini S, Lagomarsino S (2008) Modelling of vaults as equivalent diaphragms in 3D seismic analysis of masonry buildings. In: Proceedings of the Sixth International Conference on Structural Analysis of Historic Construction. Bath, United Kingdom

Ceroni F, Casapulla C, Cescatti E, et al (2022) Damage assessment in single-nave churches and analysis of the most recurring mechanisms after the 2016–2017 central Italy earthquakes. Bull Earthq Eng 20:8031–8059. https://doi.org/10.1007/s10518-022-01507-8

Ceroni F, Umberto L, Casapulla C (2025) A sensitivity study of vulnerability parameters for rocking masonry façades of single-nave churches hit by the 2016 Central Italy seismic sequence. J Build Eng 108:112823. https://doi.org/10.1016/j.jobe.2025.112823

Cescatti E, Salzano P, Casapulla C, et al (2020) Damages to masonry churches after

2016–2017 Central Italy seismic sequence and definition of fragility curves. Springer Netherlands

Chellini G, Nardini L, Pucci B, et al (2014) Evaluation of Seismic Vulnerability of Santa Maria del Mar in Barcelona by an Integrated Approach Based on Terrestrial Laser Scanner and Finite Element Modeling APPROACH BASED ON TERRESTRIAL LASER SCANNER. Int J Archit Herit 3058:. https://doi.org/10.1080/15583058.2012.747115

Chen SY, Moon FL, Yi T (2008) A macroelement for the nonlinear analysis of in-plane unreinforced masonry piers. Eng Struct 30:2242–2252. https://doi.org/10.1016/j.engstruct.2007.12.001

Chopra A, Goel R (2001) A Modal Pushover Analysis Procedure to Estimate Seismic Demands for Buildings: Theory and Preliminary Evaluation

Chopra AK, Goel RK (2002) A modal pushover analysis procedure for estimating seismic demands for buildings. Earthq Eng Struct Dyn 31:561–582. https://doi.org/10.1002/eqe.144

Cianchino G, Masciotta MG, Verazzo C, Brando G (2023) An Overview of the Historical Retrofitting Interventions on Churches in Central Italy. Appl Sci 13:. https://doi.org/10.3390/app13010040

Ciocci MP, Sharma S, Lourenço PB (2018) Engineering simulations of a super-complex cultural heritage building: Ica Cathedral in Peru. Meccanica 53:1931–1958. https://doi.org/10.1007/s11012-017-0720-3

Circolare (2019) Costruzioni esistenti: Supplemento ordinario n. 5 alla GAZZETTA UFFICIALE

Clementi F, Gazzani V, Poiani M, Lenci S (2016) Assessment of seismic behaviour of heritage masonry buildings using numerical modelling. J Build Eng 8:29–47. https://doi.org/10.1016/j.jobe.2016.09.005

Coïsson E, Collini L, Ferrari L, et al (2019) Dynamical Assessment of the Work Conditions of Reinforcement Tie-Rods in Historical Masonry Structures. Int J Archit Herit 13:358–370. https://doi.org/10.1080/15583058.2018.1563231

Contrafatto L, Lo Faro A, Gazzo S, Purrazzo A (2022) Factors Affecting the Seismic Analysis of Historical Masonry Structures: Case of a Single-Nave Church Damaged during the 2009 L'Aquila Earthquake. J Archit Eng 28:1–20. https://doi.org/10.1061/(asce)ae.1943-5568.0000556

Criber E, Brando G, Matteis G De (2015) The effects of L ' Aquila earthquake on the St . Gemma church in Goriano Sicoli : part I — damage survey and

kinematic analysis. Bull Earthq Eng 13:3713–3732. https://doi.org/10.1007/s10518-015-9792-4

Cundall PA (1971) The measurement and analysis of accelerations in rock slopes. University of London (Imperial College of Science and Technology).

Cundall PA (1987) Distinct element models of rock and soil structure. Anal Comput methods Eng rock Mech 129–163

Cundall PA, Hart RD (1993) Numerical modeling of discontinua. Pergamon Press Ltd

D'Altri AM, Sarhosis V, Milani G, et al (2020) Modeling Strategies for the Computational Analysis of Unreinforced Masonry Structures: Review and Classification. Springer Netherlands

D'Amato M, Gigliotti R, Laguardia R (2019) Comparative Seismic Assessment of Ancient Masonry Churches. Front Built Env 5:1–17. https://doi.org/10.3389/fbuil.2019.00056

D'Amato M, Laterza M, Diaz Fuentes D (2018) Simplified Seismic Analyses of Ancient Churches in Matera's Landscape. Int J Archit Herit 14:119–138. https://doi.org/10.1080/15583058.2018.1511000

D'Amato M, Laterza M, Diaz Fuentes D (2020) Simplified Seismic Analyses of Ancient Churches in Matera's Landscape. Int J Archit Herit 14:119–138. https://doi.org/10.1080/15583058.2018.1511000

D'Amato M, Sulla R (2021) Investigations of masonry churches seismic performance with numerical models: application to a case study. Arch Civ Mech Eng 21:1–26. https://doi.org/10.1007/s43452-021-00312-5

D'Ayala D, Speranza E (2003) Definition of Collapse Mechanisms and Seismic Vulnerability of Historic Masonry Buildings. Earthq Spectra 19:479–509. https://doi.org/10.1193/1.1599896

da Porto F, Silva B, Costa C, Modena C (2012) Macro-scale analysis of damage to churches after earthquake in Abruzzo (Italy) on April 6, 2009. J Earthq Eng 16:739–758. https://doi.org/10.1080/13632469.2012.685207

da Silva LCM, Milani G (2022) A FE-Based Macro-Element for the Assessment of Masonry Structures: Linear Static, Vibration, and Non-Linear Cyclic Analyses. Appl Sci 12:. https://doi.org/10.3390/app12031248

Dal Cin A, Russo S (2016) Annex and rigid diaphragm effects on the failure analysis and earthquake damages of historic churches. Eng Fail Anal 59:122–

139. https://doi.org/10.1016/j.engfailanal.2015.09.010

Davis L, Cogliano M, Casotto C, et al (2024) Pragmatic seismic collapse meso-scale analysis of old Dutch masonry churches. Earthq Eng Struct Dyn 53:622–645. https://doi.org/10.1002/eqe.4037

de Felice G, Amorosi A, Malena M (2010) Elasto-plastic analysis of block structures through a homogenization method. Int J Numer Anal Meth Geomech 34:221–247. https://doi.org/https://doi.org/10.1002/nag.799

de Felice G, Choueiri C, Chura RY, Meriggi P (2022a) An integrated approach for the investigation of the seismic behaviour of churches: the case study of St. Maria Maggiore in Tuscania. Procedia Struct Integr 44:2122–2127. https://doi.org/10.1016/j.prostr.2023.01.271

de Felice G, Fugger R, Gobbin F (2022b) Overturning of the façade in single - nave churches under seismic loading. Bull Earthq Eng 20:941–962. https://doi.org/10.1007/s10518-021-01243-5

De Lorenzis L, DeJong M, Ochsendorf J (2007) Failure of masonry arches under impulse base motion. Earthq Eng Struct Dyn 2119–2136. https://doi.org/10.1002/eqe.719

De Matteis G, Brando G, Corlito V, et al (2019a) Seismic vulnerability assessment of churches at regional scale after the 2009 L'Aquila earthquake. Int J Mason Res Innov 4:174–196. https://doi.org/10.1504/IJMRI.2019.096824

De Matteis G, Brando G, Corlito V (2019b) Predictive model for seismic vulnerability assessment of churches based on the 2009 L'Aquila earthquake. Bull Earthq Eng 17:4909–4936. https://doi.org/10.1007/s10518-019-00656-7

De Matteis G, Corlito V, Guadagnuolo M, Tafuro A (2020) Seismic Vulnerability Assessment and Retrofitting Strategies of Italian Masonry Churches of the Alife-Caiazzo Diocese in Caserta. Int J Archit Herit 14:1180–1195. https://doi.org/10.1080/15583058.2019.1594450

De Matteis G, Criber E, Brando G (2016) Damage Probability Matrices for Three-Nave Masonry Churches in Abruzzi After the 2009 L ' Aquila Earthquake. Int J Archit Herit 3058:. https://doi.org/10.1080/15583058.2015.1113340

De Matteis G, Zizi M (2019a) Preliminary Analysis on the Effects of 2016 Central Italy Earthquake on One-Nave Churches. In: In: Aguilar, R., Torrealva, D., Moreira, S., Pando, M.A., Ramos, L.F. (eds) Structural Analysis of Historical Constructions. Springer, Cham, pp 1268–1279

De Matteis G, Zizi M (2019b) Seismic Damage Prediction of Masonry Churches

by a PGA-based Approach. Int J Archit Herit 13:1165–1179. https://doi.org/10.1080/15583058.2019.1597215

Deb K (2001) Multi-Objective Optimization Using Evolutionary Algorithms by Kalyanmoy Deb (z-lib.org).pdf

Deb K, Member A, Pratap A, et al (2002) A Fast and Elitist Multiobjective Genetic Algorithm : 6:182–197

Decree of the Italian Prime Minister (2011) Assessment and Mitigation of Seismic Risk of Cultural Heritage with Reference to the Technical Code for the Design of Construction. Rome

Degli Abbati S, Brunelli A, Rooshenas A, Lagomarsino S (2025) Derivation of fragility curves to assess and compare the effectiveness of retrofitting strategies in URM buildings. Earthq Spectra 1–25. https://doi.org/10.1177/87552930251350158

Degli Abbati S, Cattari S, Lagomarsino S (2018) Theoretically-based and practice-oriented formulations for the floor spectra evaluation. Earthq Struct 15:565–581. https://doi.org/10.12989/eas.2018.15.5.565

Degli Abbati S, Cattari S, Lagomarsino S, Ottonelli D (2021) Seismic Assessment and Strengthening Interventions of Atop Single-Block Rocking Elements in Monumental Buildings: the Case Study of the San Felice sul Panaro Fortress. 1–12. https://doi.org/10.23967/sahc.2021.220

Degli Abbati S, D'Altri AM, Ottonelli D, et al (2019) Seismic assessment of interacting structural units in complex historic masonry constructions by nonlinear static analyses. Comput Struct 213:51–71. https://doi.org/10.1016/j.compstruc.2018.12.001

Degli Abbati S, Morandi P, Cattari S, Spacone E (2022) On the reliability of the equivalent frame models: the case study of the permanently monitored Pizzoli's town hall. Springer Netherlands

Degli Abbati S, Vecchiattini R, Lagomarsino S, Cattari S (2024) A Simplified Procedure for the Out-of-Plane Seismic Assessment of Free-Standing URM Elements: Application to the Abandoned Ancient Village of Bussana (Sanremo, Imperia - Italy). Int J Archit Herit 19:1849–1869. https://doi.org/10.1080/15583058.2024.2375036

Diana L, Reuland Y, Lestuzzi P (2017) SEISMIC VULNERABILITY AS SESSMENT OF " SION CATHEDRAL " (SWITZERLAND): AN INTEGRATED APPROACH TO DETECT AND EVALUATE LOCAL COLLAPSE MECHANISMS IN HERITAGE BUILDINGS. In: Prohitech '17

proceedings (2017): 3rd International Conference on Protection of Historical Constructions. Lisbon, Portugal, pp 1–14

Diana L, Vaiano G, Formisano A, et al (2023) The Seismic Vulnerability Assessment of Heritage Buildings: A Holistic Methodology for Masonry Churches. Int J Archit Herit 00:1–29. https://doi.org/10.1080/15583058.2023.2203097

Dìaz D (2016) Diseño de Herramientas de Evaluación del Riesgo Para la Conservación del Patrimonio Cultural Inmueble. Aplicación en dos Casos de Estudio del Norte Andino Chileno. México: Publicaciones ENCRyM-INAH

Dizhur D, Ingham J, Moon L, et al (2011) PERFORMANCE OF MASONRY BUILDINGS AND CHURCHES IN THE 22 FEBRUARY 2011 CHRISTCHURCH EARTHQUAKE. Bull NEW Zeal Soc Earthq Eng 44:279–296

Doglioni F, Moretti A, Petrini V, Angeletti P (1994) Le Chiese e il Terremoti: Dalla Vulnerabilita` Constatata nel Terremoto del Friuli al Miglioramento Antisismico nel Restauro, Verso una Politica di Prevenzione. Ed Lint

Dolce M (1991) Schematizzazione e modellazione degli edifici in muratura soggetti ad azioni sismiche. L'industria Delle Costr 25:44–57

Elyamani A, Roca P, Caselles O, Clapes J (2017) Seismic safety assessment of historical structures using updated numerical models: The case of Mallorca cathedral in Spain. Eng Fail Anal 74:54–79. https://doi.org/10.1016/j.engfailanal.2016.12.017

EN 1998-1 (2006) Eurocode 8: Design of structures for earthquake resistance — Part 1: General rules, seismic actions and rules for buildings

EN 1998-3 (2006) Eurocode 8: Design of structures for earthquake resistance – Part 3: Assessment and retrofitting of buildings

Endo Y, Pelà L, Roca P, et al (2015) Comparison of seismic analysis methods applied to a historical church struck by 2009 L ' Aquila earthquake. Bull Earthq Eng 3749–3778. https://doi.org/10.1007/s10518-015-9796-0

Fabbrocino F, Vaiano G, Formisano A, D'amato M (2019) Large-scale seismic vulnerability and risk of masonry churches in seismic-prone areas: Two territorial case studies. Front Built Environ 5:. https://doi.org/10.3389/fbuil.2019.00102

Fajfar P (1999) Capacity spectrum method based on inelastic demand spectra. Earthq Eng Struct Dyn 28:979–993. https://doi.org/10.1002/(SICI)1096-

9845(199909)28:9<979::AID-EQE850>3.0.CO;2-1

FathiAzar A, De Angeli S, Cattari S (2024) Towards integrated multi-risk reduction strategies: A catalog of flood and earthquake risk mitigation measures at the building and neighborhood scales. Int J Disaster Risk Reduct 113:104884. https://doi.org/10.1016/j.ijdrr.2024.104884

Fazzi E, Galassi S, Misseri G, Rovero L (2021) Seismic vulnerability assessment of the benedictine basilica typology in central Italy. J Build Eng 43:102897. https://doi.org/10.1016/j.jobe.2021.102897

Ferracuti B, Imperatore S, Zucconi M, Colonna S (2022) Damage to Churches after the 2016 Central Italy Seismic Sequence. Geosciences 12:. https://doi.org/10.3390/geosciences12030122

Ferrari G (1991) The 1887 Ligurian earthquake: a detailed study from contemporary scientific observations. Tectonophysics 193:131–139. https://doi.org/10.1016/0040-1951(91)90194-W

Ferreira TM, Costa AA, Costa A (2015) Analysis of the Out-Of-Plane Seismic Behavior of Unreinforced Masonry: A Literature Review. Int J Archit Herit 9:949–972. https://doi.org/10.1080/15583058.2014.885996

Foraboschi P (2013) Church of San Giuliano di Puglia : Seismic repair and upgrading. Eng Fail Anal 33:281–314. https://doi.org/10.1016/j.engfailanal.2013.05.023

Formisano A, Vaiano G, Davino A, et al (2022) Seismic vulnerability assessment of two territorial case studies of Italian ancient churches: comparison between simplified and refined numerical models. Int J Mason Res Innov 7:172–216. https://doi.org/10.1504/IJMRI.2022.119890

Franchi A, Napoli P, Crespi P, et al (2022) Unloading and Reloading Process for the Earthquake Damage Repair of Ancient Masonry Columns : The Case of the Basilica di Collemaggio Unloading and Reloading Process for the Earthquake Damage Repair of Ancient Masonry Columns : The Case of the Basilica di Collemaggio ABSTRACT. Int J Archit Herit 16:1683–1698. https://doi.org/10.1080/15583058.2021.1904056

Fuentes DD, Baquedano Julià PA, D'Amato M, Laterza M (2021) Preliminary Seismic Damage Assessment of Mexican Churches after September 2017 Earthquakes. Int J Archit Herit 15:505–525. https://doi.org/10.1080/15583058.2019.1628323

Fuentes DD, Laterza M, D'Amato M (2019) Seismic Vulnerability and Risk Assessment of Historic Constructions: The Case of Masonry and Adobe

Churches in Italy and Chile. Aguilar, R, Torrealva, D, Moreira, S, Pando, MA, Ramos, LF Struct Anal Hist Constr RILEM Bookseries 18:1949–1958. https://doi.org/10.1007/978-3-319-99441-3

Funari MF, Pulatsu B, Szabó S, Lourenço PB (2022) A solution for the frictional resistance in macro-block limit analysis of non-periodic masonry. Structures 43:847–859. https://doi.org/10.1016/j.istruc.2022.06.072

G.U.N.47 (2011) Assessment and mitigation of seismic risk of cultural heritage with reference to the technical code for the design of the con- struction, issued by D.M. 14/01/2008, Rome (Italy). In Italian.

Galasco A, Lagomarsino S, Penna A (2006) On the use of pushover analysis for existing masonry buildings. First Eur Conf Earthq Eng Seismol 3–8

Galvez F, Dizhur D, Ingham JM (2023) Adjacent interacting masonry structures: shake table test blind prediction discrete element method simulation. Bull Earthq Eng 1–27. https://doi.org/10.1007/s10518-023-01655-5

Gambarotta L, Lagomarsino S (1997) Damage models for the seismic response of brick masonry shear walls. Part I: The mortar joint model and its applications. Earthq Eng Struct Dyn 26:423–439. https://doi.org/10.1002/(sici)1096-9845(199704)26:4<423::aid-eqe650>3.0.co;2-%23

García N, Meli R (2008) On Structural Bases for Building the Mexican Convent Churches From the Sixteenth Century. Int J Archit Herit 3058:. https://doi.org/10.1080/15583050701842344

Ghaffarpasand B, Abbati SD, Cattari S, Lagomarsino S (2024) OPTIMIZING RETROFITTING SOLUTIONS FOR CHURCH BELL GABLES WITH MULTI-OBJECTIVE ALGORITHMS. In: WCEE 2024 Proceeding. Milan, Italy, pp 1–10

Ghaffarpasand B, Samadian D, Raissi Dehkordi M, et al (2023) Investigation of different resilience-based optimisation strategies for retrofitting curved bridges. Struct Infrastruct Eng 0:1–15. https://doi.org/10.1080/15732479.2023.2165690

Giaretton M, Dizhur D, Porto F, Ingham JM (2014) AN INVENTORY OF UNREINFORCED LOAD-BEARING STONE MASONRY BUILDINGS IN NEW ZEALAND. Bull NEW Zeal Soc Earthq Eng 47:57–74

Giordano E, Clementi F, Nespeca A, Lenci S (2019) Damage assessment by numerical modeling of sant'agostino's sanctuary in offida during the central italy 2016–2017 seismic sequence. Front Built Environ 4:1–17. https://doi.org/10.3389/fbuil.2018.00087

Giresini L (2016) Energy-based method for identifying vulnerable macro-elements in historic masonry churches. Bull Earthq Eng 14:919–942. https://doi.org/10.1007/s10518-015-9854-7

Giuffrè A (1991) Letture sulla meccanica delle murature storiche. Kappa

Godio M, Stefanou I, Sab K (2018) Effects of the dilatancy of joints and of the size of the building blocks on the mechanical behavior of masonry structures. Meccanica 53:1629–1643. https://doi.org/10.1007/s11012-017-0688-z

Goodman R, Taylor R, Brekke T (1968) A MODEL FOR THE MECHANICS OF JOINTED ROCK. SOIL Mech Found Div Proc Am Soc Civ Eng 94:637–659

Gunes B (2023) Seismic Assessment of the Archangeloi (Ba¸smelekler) Church in Kumyaka, Türkiye

Hatır ME, Korkanç M, Başar ME (2019) Evaluating the deterioration effects of building stones using NDT: the Küçükköy Church, Cappadocia Region, central Turkey. Bull Eng Geol Environ 3465–3478. https://doi.org/10.1007/s10064-018-1339-x

Helbling M (2019) Oradour-sur-Glane: French Identity Memorialized. Chang Over Time 9:

Heyman J (1966) The stone skeleton. Int J Solids Struct 2:249–256, IN1–IN4, 257–264, IN5–IN12, 265–279. https://doi.org/10.1016/0020-7683(66)90018-7

Itasca Consulting Group Inc 3DEC. (2013) Three Dimensional Distinct Element Code

Jalayer F, Ebrahimian H, Miano A (2021) Record-to-record variability and code-compatible seismic safety-checking with limited number of records. Springer Netherlands

Jean M (1999) The non-smooth contact dynamics method. Comput Methods Appl Mech Eng 177:235–257. https://doi.org/10.1016/S0045-7825(98)00383-1

Jiménez-Pacheco J, Quezada R, Calderón-Brito J, et al (2022) Characterisation of the built heritage of historic centres oriented to the assessment of its seismic vulnerability: The case of Cuenca, Ecuador. Int J Disaster Risk Reduct 71:. https://doi.org/10.1016/j.ijdrr.2022.102784

Jorquera N, Misseri G, Palazzi N, et al (2017) Structural Characterization and Seismic Performance of San Francisco Church , the Most Ancient Monument in Santiago , Chile Structural Characterization and Seismic Performance of San Francisco Church ,. Int J Archit Herit 11:1061–1085.

https://doi.org/10.1080/15583058.2017.1315620

Kallioras S, Graziotti F, Penna A, Magenes G (2017) NUMERICAL MODELING OF CAVITY-WALL URM BUILDINGS. Eff Bound Elem Confin Lev Behav Reinf Mason Struct walls with Bound Elem

Kappos AJ, Panagopoulos G, Penelis GG (2008) Development of a seismic damage and loss scenario for contemporary and historical buildings in Thessaloniki, Greece. Soil Dyn Earthq Eng 28:836–850. https://doi.org/10.1016/j.soildyn.2007.10.017

Kassotakis N, Sarhosis V, Riveiro B, et al (2020) Three-dimensional discrete element modelling of rubble masonry structures from dense point clouds. Autom Constr 119:103365. https://doi.org/10.1016/J.AUTCON.2020.103365

Kesavan P, Menon A (2022) Investigation of in-plane and out-of-plane interaction in unreinforced masonry piers by block-based micro-modeling. Structures 46:1327–1344. https://doi.org/10.1016/j.istruc.2022.10.105

Khattak N, Derakhshan H, Thambiratnam DP, et al (2023) Modelling the in-plane/out-of-plane interaction of brick and stone masonry structures using Applied Element Method. J Build Eng 76:107175. https://doi.org/10.1016/j.jobe.2023.107175

Korkmaz NG, Korkmaz NM, Sayin B, Uzdil O (2023) A comprehensive proposal for rehabilitation of historic Armenian church belonging to 16th century AD (Diyarbakır, Turkey). Structures 50:118–147. https://doi.org/10.1016/j.istruc.2023.02.021

Krishnachandran S, Menon A (2023) Effect of out-of-plane displacements on the in-plane capacity of lightly precompressed rocking unreinforced masonry piers. Eng Struct 281:115756. https://doi.org/10.1016/j.engstruct.2023.115756

Lagomarsino S (2012) Damage assessment of churches after L'Aquila earthquake (2009). Bull Earthq Eng 10:73–92. https://doi.org/10.1007/s10518-011-9307-x

Lagomarsino S (2015) Seismic assessment of rocking masonry structures. Bull Earthq Eng 13:97–128. https://doi.org/10.1007/s10518-014-9609-x

Lagomarsino S, Cattari S (2015a) PERPETUATE guidelines for seismic performance-based assessment of cultural heritage masonry structures. Bull Earthq Eng 13:13–47. https://doi.org/10.1007/s10518-014-9674-1

Lagomarsino S, Cattari S (2015b) Seismic performance of historical masonry

structures through pushover and nonlinear dynamic analyses. Geotech Geol Earthq Eng 39:265–292. https://doi.org/10.1007/978-3-319-16964-4_11

Lagomarsino S, Cattari S, Angiolilli M, et al (2023) Modelling and Seismic Response Analysis of Existing URM Structures. Part 2: Archetypes of Italian Historical Buildings. J Earthq Eng 27:1849–1874. https://doi.org/10.1080/13632469.2022.2087800

Lagomarsino S, Cattari S, Ottonelli D, Giovinazzi S (2019a) Earthquake damage assessment of masonry churches: proposal for rapid and detailed forms and derivation of empirical vulnerability curves. Springer Netherlands

Lagomarsino S, Ottonelli D, Cattari S (2019b) Numerical Modeling of Masonry and Historical Structures

Lagomarsino S, Penna A, Galasco A, Cattari S (2013) TREMURI program: An equivalent frame model for the nonlinear seismic analysis of masonry buildings. Eng Struct 56:1787–1799. https://doi.org/10.1016/j.engstruct.2013.08.002

Lagomarsino S, Podestà S (2004a) Seismic vulnerability of ancient churches: I. Damage assessment and emergency planning. Earthq Spectra 20:377–394. https://doi.org/10.1193/1.1737735

Lagomarsino S, Podestà S (2004b) Seismic vulnerability of ancient churches: II. Statistical analysis of surveyed data and methods for risk analysis. Earthq Spectra 20:395–412. https://doi.org/10.1193/1.1737736

Laterza M, Amato MD, Díaz D, Chietera M (2017) Seismic analysis methods of ancient masonry churches in Matera. XVII Convegno ANIDIS - L'Ingegneria Sismica Ital

Lee J, Fenves GL (1998) Plastic-Damage Model for Cyclic Loading of Concrete Structures. J Eng Mech 124:892–900

Lemos J V. (2007) Discrete element modeling of masonry structures. Int J Archit Herit 1:190–213. https://doi.org/10.1080/15583050601176868

Lezzerini M, Pagnotta S, Legnaioli S, Palleschi V (2019) Walking in the Streets of Pisa to Discover the Stones Used in the Middle Ages. Geoheritage 11:1631–1641. https://doi.org/10.1007/s12371-019-00372-3

Lo Monaco A, Grillanda N, Onescu I, et al (2023) Seismic assessment of Romanian Orthodox masonry churches in the Banat area through a multi-level analysis framework. Eng Fail Anal 153:107539. https://doi.org/10.1016/j.engfailanal.2023.107539

Lo Monaco A, Ranaldo A, D'Amato M, et al (2026) Multilevel framework for risk assessment of cultural heritage : application to a case study. Procedia Struct Integr 78:544–551. https://doi.org/10.1016/j.prostr.2025.12.070

Longarini N, Crespi P, Zucca M (2022) The influence of the geometrical features on the seismic response of historical churches reinforced by different cross lam roof - solutions. Springer Netherlands

Lourenco PB (2005) Assessment , diagnosis and strengthening of Outeiro Church , Portugal. Constr Build Mater 19:634–645. https://doi.org/10.1016/j.conbuildmat.2005.01.010

Lourenço PB (2002) Computations on historic masonry structures. Prog Struct Eng Mater 4:301–319. https://doi.org/10.1002/pse.120

Lourenco PB, Milani G, Tralli A, Zucchini A (2007) Analysis of masonry structures : review of and recent trends in homogenization techniques 1. Can J Civ Eng 34:1443–1457. https://doi.org/10.1139/L07-097

Lourenço PB, Oliveira D V, Leite JC, et al (2013) Simplified indexes for the seismic assessment of masonry buildings : International database and validation. Eng Fail Anal 34:585–605. https://doi.org/10.1016/j.engfailanal.2013.02.014

Lourenço PB, Rots JG, Blaauwendraad J (1998) Continuum Model for Masonry: Parameter Estimation and Validation. J Struct Eng 124:642–652. https://doi.org/10.1061/(asce)0733-9445(1998)124:6(642)

Lourenço PB, Trujillo A, Mendes N, Ramos LF (2012) Seismic performance of the St. George of the Latins church: Lessons learned from studying masonry ruins. Eng Struct 40:501–518. https://doi.org/10.1016/j.engstruct.2012.03.003

Magenes G (2006) Masonry Building Design in Seismic Areas: recent experiences and prospects from a European standpoint. 1st Eur Conf Earthq Eng Seismol Keynote 9

Magenes G, Della Fontana A (1989) Simplified non-linear Seismic Analysis of Masonry Buildings. In: Proceedings of the fifth international masonry conference

Malena M, Genoese A, Panto' B, et al (2022) Two Steps Procedure for the Finite Elements Seismic Analysis of the Casamari Gothic Church. Buildings 12:1–15. https://doi.org/10.3390/buildings12091451

Malena M, Lorello M, de Felice G (2025) Seismic assessment of masonry churches through combined modal and pushover analysis. Structures 78:109281. https://doi.org/10.1016/j.istruc.2025.109281

Malena M, Portioli F, Gagliardo R, et al (2019) Collapse mechanism analysis of historic masonry structures subjected to lateral loads : A comparison between continuous and discrete models. Comput Struct 220:14–31. https://doi.org/10.1016/j.compstruc.2019.04.005

Malomo D, DeJong MJ (2022) A Macro-Distinct Element Model (M-DEM) for simulating in-plane/out-of-plane interaction and combined failure mechanisms of unreinforced masonry structures. Earthq Eng Struct Dyn 51:793–811. https://doi.org/10.1002/eqe.3591

Malomo D, DeJong MJ (2021) A Macro-Distinct Element Model (M-DEM) for simulating the in-plane cyclic behavior of URM structures. Eng Struct 227:111428. https://doi.org/10.1016/j.engstruct.2020.111428

Malomo D, DeJong MJ (2024) M-DEM simulation of seismic pounding between adjacent masonry structures. Bull Earthq Eng 22:6067–6092. https://doi.org/10.1007/s10518-022-01545-2

Malomo D, Pinho R, Penna A (2019) Simulating the shake-table response of URM cavity-wall structures tested to collapse or near-collapse conditions. Earthq Spectra - Submitt Publ

Malomo D, Pulatsu B (2024) Discontinuum models for the structural and seismic assessment of unreinforced masonry structures: a critical appraisal. Structures 62:. https://doi.org/10.1016/j.istruc.2024.106108

Marotta A, Goded T, Giovinazzi S, et al (2015) AN INVENTORY OF UNREINFORCED MASONRY CHURCHES IN NEW ZEALAND. Bull New Zeal Soc Earthq Eng 48:. https://doi.org/https://doi.org/10.5459/bnzsee.48.3.170-189

Marotta A, Sorrentino L, Liberatore D, Ingham JM (2018) Seismic Risk Assessment of New Zealand Unreinforced Masonry Churches using Statistical Procedures. Int J Archit Herit 12:448–464. https://doi.org/10.1080/15583058.2017.1323242

Marotta A, Sorrentino L, Liberatore D, Ingham JM (2017) Vulnerability Assessment of Unreinforced Masonry Churches Following the 2010–2011 Canterbury Earthquake Sequence. J Earthq Eng 21:912–934. https://doi.org/10.1080/13632469.2016.1206761

Masciotta M, Ramos LF, Lourenc PB (2017) The importance of structural monitoring as a diagnosis and control tool in the restoration process of heritage structures : A case study in Portugal. J Cult Herit 27:36–47. https://doi.org/10.1016/j.culher.2017.04.003

Mayorga ER, Cobo A, Yanes E, Saez A (2018) The Repair of the Structure of Santiago ' s Church (Jerez De La Frontera , Spain) Using Grout- Injection. Int J Archit Herit 3058:. https://doi.org/10.1080/15583058.2018.1515273

McNeel R, Associates (2015) Grasshopper - Extension for Rhinoceros 3D

Meguro K, Tagel-Din H (2001) Applied Element Simulation of RC Structures under Cyclic Loading. J Struct Eng 127:1295–1305. https://doi.org/10.1061/(ASCE)0733-9445(2001)127:11(1295)

Meli R, Sánchez-ramírez R (2007) Criteria and Experiences on Structural Rehabilitation of Stone Masonry Buildings in Mexico City. Int J Archit Herit 3058:2–28. https://doi.org/10.1080/15583050601123118

Mendes N, Zanotti S, Lemos J V. (2020) Seismic Performance of Historical Buildings Based on Discrete Element Method: An Adobe Church. J Earthq Eng 24:1270–1289. https://doi.org/10.1080/13632469.2018.1463879

Menon A, Magenes G (2011) Definition of seismic input for out-of-plane response of masonry walls: I. parametric study. J Earthq Eng 15:165–194. https://doi.org/10.1080/13632460903456981

Meoni A, D'Alessandro A, Cavalagli N, et al (2019) Shaking table tests on a masonry building monitored using smart bricks: Damage detection and localization. Earthq Eng Struct Dyn 48:910–928. https://doi.org/10.1002/eqe.3166

Milani G, Valente M (2015) Failure analysis of seven masonry churches severely damaged during the 2012 Emilia-Romagna (Italy) earthquake: Non-linear dynamic analyses vs conventional static approaches. Eng Fail Anal 54:13–56. https://doi.org/10.1016/j.engfailanal.2015.03.016

Milani G, Valente M, Alessandri C (2018) The narthex of the Church of the Nativity in Bethlehem: A non-linear finite element approach to predict the structural damage. Comput Struct 207:3–18. https://doi.org/10.1016/j.compstruc.2017.03.010

Miltiadou-fezans A, Kalagri A, Anagnostopoulou S (2024) Design and Application of Mortars and Grouts for the Restoration of the Byzantine Church of Panaghia Krena in Chios Island, Greece. Buildings. https://doi.org/https://doi.org/10.3390/buildings14082542

Mishra M, Puneeth R, Ramana G V. (2022) Seismic vulnerability assessment of old churches in the twin cities of Bhubaneswar and Cuttack using the macroelemental approach. Front Built Environ 8:1–15. https://doi.org/10.3389/fbuil.2022.1018922

Monteferrante C, Cattari S, D'Altri AM, et al (2023) An energy-based methodology to estimate the ultimate condition of complex continuous masonry structures. Eng Fail Anal 151:107370. https://doi.org/10.1016/j.engfailanal.2023.107370

Morandi P, Manzini CF, Magenes G (2019) Application of seismic design procedures on three modern URM buildings struck by the 2012 Emilia earthquakes : inconsistencies and improvement proposals in the European codes. Springer Netherlands

Morandini C, Malomo D, Penna A (2022) Equivalent frame discretisation for URM façades with irregular opening layouts. Bull Earthq Eng 20:2589–2618. https://doi.org/10.1007/s10518-022-01315-0

Mosoarca M, Fofiu M, Endo Y (2025) Diagnosis and preliminary structural analysis of a historic masonry church in Craiova , Romania. Eng Fail Anal 181:1–19. https://doi.org/10.1016/j.engfailanal.2025.109959

Mouyiannou A, Rota M, Penna A, Magenes G (2014) Identification of suitable limit states from nonlinear dynamic analyses of masonry structures. J Earthq Eng 18:231–263. https://doi.org/10.1080/13632469.2013.842190

Nale M, Minghini F, Chiozzi A, Tralli A (2021) Fragility functions for local failure mechanisms in unreinforced masonry buildings: a typological study in Ferrara, Italy. Springer Netherlands

NTC (2008) Norme tecniche per le costruzioni (Technical Code for Constructions). Minist Infrastructures Transp

Okail H, Abdelrahman A, Abdelkhalik A (2016) Experimental and analytical investigation of the lateral load response of confined masonry walls. HBRC J 12:33–46. https://doi.org/10.1016/j.hbrcj.2014.09.004

Onescu I, Lo Monaco A, Grillanda N, et al (2025) Simplified Vulnerability Assessment of Historical Churches in Banat Seismic Region , Romania. Int J Archit Herit 19:825–838. https://doi.org/10.1080/15583058.2024.2341054

Onutu C, Ungureanu D, Taranu N, Isopescu DN (2024) Managing Intervention Works for Conservation and Revitalization: A Case Study of the Bârnova Monastery, Iasi. Buildings 14:. https://doi.org/https://doi.org/10.3390/buildings14072005

Pacheco M, Cachão M (2024) The Natural and Cultural Legacy of Stone Pavements from Selected Palaces and Churches of Lisbon (Portugal). Geoheritage 16:. https://doi.org/10.1007/s12371-024-01007-y

Page AW (1979) FINITE ELEMENT MODEL FOR MASONRY. J Struct Div

104:1267–1285. https://doi.org/https://doi.org/10.1061/JSDEAG.0004969

Palazzi NC, Favier P, Rovero L, et al (2020) Seismic damage and fragility assessment of ancient masonry churches located in central Chile. Bull Earthq Eng 18:3433–3457. https://doi.org/10.1007/s10518-020-00831-1

Pantò B, Caliò I (2021) Numerical modeling for the seismic assessment of masonry structures

Parisi F, Augenti N (2013) Seismic capacity of irregular unreinforced masonry walls with openings. Pacific Conf Earthq Eng 1–6. https://doi.org/DOI: 10.1002/eqe.2195

Pastor M, Binda M, Harčarik T (2012) Modal assurance criterion. Procedia Eng 48:543–548. https://doi.org/10.1016/j.proeng.2012.09.551

Peña F, Chávez MM (2016) Seismic Behavior of Mexican Colonial Churches Seismic Behavior of Mexican Colonial Churches. Int J Archit Herit 10:332–345. https://doi.org/10.1080/15583058.2015.1113341

Penna A, Calderini C, Sorrentino L, et al (2019) Damage to churches in the 2016 central Italy earthquakes. Bull Earthq Eng 17:5763–5790. https://doi.org/10.1007/s10518-019-00594-4

Pianigiani M, Careccia C, Montone C (2020) Correlation analysis between churches and their artistic content in terms of damage. A damage map of Italian Cultural Heritage through four Regions after the 2016 earthquake. Procedia Struct Integr 29:103–110. https://doi.org/10.1016/j.prostr.2020.11.145

Pirchio D, Walsh KQ, Kerr E, et al (2021a) Seismic risk assessment and intervention prioritization for Italian medieval churches. J Build Eng 43:103061. https://doi.org/10.1016/j.jobe.2021.103061

Pirchio D, Walsh KQ, Kerr E, et al (2021b) Integrated framework to structurally model unreinforced masonry Italian medieval churches from photogrammetry to finite element model analysis through heritage building information modeling. Eng Struct 241:112439. https://doi.org/10.1016/j.engstruct.2021.112439

Preciado A, Pena F, Colmenero Fonesca F, Silva C (2022) Damage description and schematic crack propagation in Colonial Churches and old masonry buildings by the 2017 Puebla-Morelos. Eng Fail Anal 141:. https://doi.org/10.1016/j.engfailanal.2022.106706

Preciado A, Santos JC, Silva C, et al (2020) Seismic damage and retrofitting identification in unreinforced masonry Churches and bell towers by the

september 19, 2017 (Mw = 7.1) Puebla-Morelos earthquake. Eng Fail Anal 118:104924. https://doi.org/10.1016/j.engfailanal.2020.104924

Pulatsu B, Bretas EM, Lourenço PB (2016) Discrete element modeling of masonry structures: Validation and application. Earthq Struct 11:563–582. https://doi.org/10.12989/eas.2016.11.4.563

Pulatsu B, Erdogmus E, Lourenço PB, et al (2020) Discontinuum analysis of the fracture mechanism in masonry prisms and wallettes via discrete element method. Meccanica 55:505–523. https://doi.org/10.1007/s11012-020-01133-1

Pulatsu B, Gonen S, Lourenço PB, et al (2023) Computational investigations on the combined shear–torsion–bending behavior of dry-joint masonry using DEM. Comput Part Mech 10:249–260. https://doi.org/10.1007/s40571-022-00493-7

Puncello I, Caprili S (2023) Seismic Assessment of Historical Masonry Buildings at Different Scale Levels: A Review. Appl Sci 13:. https://doi.org/10.3390/app13031941

Quagliarini E, Maracchini G, Clementi F (2017) Uses and limits of the Equivalent Frame Model on existing unreinforced masonry buildings for assessing their seismic risk: A review. J Build Eng 10:166–182. https://doi.org/10.1016/j.jobe.2017.03.004

Ramirez R, Mendes N, Lourenço PB (2019) Diagnosis and Seismic Behavior Evaluation of the Church of São Miguel de Refojos (Portugal). Buildings 9:. https://doi.org/10.3390/buildings9060138

Ravichandran N, Losanno D, Parisi F (2021) Comparative assessment of finite element macro-modelling approaches for seismic analysis of non-engineered masonry constructions. Springer Netherlands

Roca P (2006) Assessment of masonry shear-walls by simple equilibrium models. Constr Build Mater 20:229–238. https://doi.org/10.1016/j.conbuildmat.2005.08.023

Rosti A, Rota M, Penna A (2021) Empirical fragility curves for Italian URM buildings. Bull Earthq Eng 19:3057–3076. https://doi.org/10.1007/s10518-020-00845-9

Ruggieri S, Tosto C, Rosati G, et al (2022) Seismic Vulnerability Analysis of Masonry Churches in Piemonte after 2003 Valle Scrivia Earthquake: Post-event Screening and Situation 17 Years Later. Int J Archit Herit 16:717–745. https://doi.org/10.1080/15583058.2020.1841366

Salzano P, Casapulla C, Ceroni F, Prota A (2022) Seismic Vulnerability and

Simplified Safety Assessments of Masonry Churches in the Ischia Island (Italy) after the 2017 Earthquake. Int J Archit Herit 16:136–162. https://doi.org/10.1080/15583058.2020.1759732

Sandoli A, Pacella G, Cordasco EA, Calderoni B (2021) PROS and CONS of linear and nonlinear seismic analyses for existing URM structures: Application to a historical building. Structures 32:532–547. https://doi.org/10.1016/j.istruc.2021.03.021

Sangiorgio V, Uva G, Adam JM (2021) Integrated Seismic Vulnerability Assessment of Historical Masonry Churches Including Architectural and Artistic Assets Based on Macro-element Approach. Int J Archit Herit 15:1609–1622. https://doi.org/10.1080/15583058.2019.1709916

Sangirardi M, Liberatore D, Addessi D (2019) Equivalent Frame Modelling of Masonry Walls Based on Plasticity and Damage. Int J Archit Herit 13:1098–1109. https://doi.org/10.1080/15583058.2019.1645240

Sarhosis V, Lemos J V. (2018) A detailed micro-modelling approach for the structural analysis of masonry assemblages. Comput Struct 206:66–81. https://doi.org/10.1016/j.compstruc.2018.06.003

Schiavoni M, Giordano E, Roscini F, Clementi F (2023) Numerical modeling of a majestic masonry structure: A comparison of advanced techniques. Eng Fail Anal 149:107293. https://doi.org/10.1016/j.engfailanal.2023.107293

Silva ABF De, Parisi APF, Silvestri SSF (2021) Numerical simulation of the seismic response and soil – structure interaction for a monitored masonry school building damaged by the 2016 Central Italy earthquake. Springer Netherlands

Singh MP (1988) Seismic design of secondary systems. Probabilistic Eng Mech 3:151–158

Singh MP, Burdisso RA (1987) MULTIPLY SUPPORTED SECONDARY SYSTEMS PART II: SEISMIC INPUTS. Earthq Eng Struct Dyn 15:

Sisti R, Argiento L, Casapulla C, et al (2023a) Empirical fragility curves for macro-elements and single mechanisms of churches damaged during the 2016-2017 Central Italy seismic sequence. Procedia Struct Integr 44:1380–1387. https://doi.org/10.1016/j.prostr.2023.01.177

Sisti R, Argiento LU, Ceroni F, et al (2023b) Empirical fragility curves for masonry churches and their macro-elements using a large database: Proposal of a new likelihood function. Structures 57:105164. https://doi.org/10.1016/j.istruc.2023.105164

Sorrentino L, Liberatore L, Decanini LD, Liberatore D (2014) The performance of churches in the 2012 Emilia earthquakes. Bull Earthq Eng 12:2299–2331. https://doi.org/10.1007/s10518-013-9519-3

Spiridon IA, Ungureanu D, Țăranu N, et al (2023) Structural Assessment and Strengthening of a Historic Masonry Orthodox Church. Buildings 13:1–18. https://doi.org/10.3390/buildings13030835

Suppapitnarm A, Seffen KA, Parks GT, Clarkson PJ (2000) A SIMULATED ANNEALING ALGORITHM FOR MULTIOBJECTIVE OPTIMIZATION. Eng Optim 59–85

Tomazevic M (1978) The computer program POR. Rep ZRMK

Valente M, Barbieri G, Biolzi L (2017) Damage assessment of three medieval churches after the 2012 Emilia earthquake. Bull Earthq Eng 15:2939–2980. https://doi.org/10.1007/s10518-016-0073-7

Valente M, Brandonisio G, Milani G, De Luca A (2020) Seismic response evaluation of ten tuff masonry churches with basilica plan through advanced numerical simulations. Int J Mason Res Innov. https://doi.org/https://doi.org/10.1504/IJMRI.2020.104849

Valente M, Milani G (2019) Damage survey, simplified assessment, and advanced seismic analyses of two masonry churches after the 2012 Emilia earthquake. Int J Archit Herit 13:901–924. https://doi.org/10.1080/15583058.2018.1492646

Valente M, Milani G (2016) Non-linear dynamic and static analyses on eight historical masonry towers in the North-East of Italy. Eng Struct 114:241–270. https://doi.org/10.1016/j.engstruct.2016.02.004

Valluzzi MR, Modena C, Felice G De (2014) Current practice and open issues in strengthening historical buildings with composites. Mater Struct 1971–1985. https://doi.org/10.1617/s11527-014-0359-7

van der Pluijm R (1993) Shear behaviour of bed joints. In: 6th North American Masonry Conference. pp 125–136

Vanin F, Penna A, Beyer K (2020a) A three-dimensional macroelement for modelling the in-plane and out-of-plane response of masonry walls. Earthq Eng Struct Dyn 49:1365–1387. https://doi.org/10.1002/eqe.3277

Vanin F, Penna A, Beyer K (2020b) Equivalent-Frame Modeling of Two Shaking Table Tests of Masonry Buildings Accounting for Their Out-Of-Plane Response. 6:1–18. https://doi.org/10.3389/fbuil.2020.00042

Vecchio D, Vlachakis G, Menon A, Lourenço PB (2025) Seismic vulnerability assessment against rocking and sliding failure using nonlinear dynamic analysis : Application to the temples of Bagan , Myanmar. Structures 74:108584. https://doi.org/10.1016/j.istruc.2025.108584

Vlachakis G, Vlachaki E, Lourenço PB (2020) Learning from failure: Damage and failure of masonry structures, after the 2017 Lesvos earthquake (Greece). Eng Fail Anal 117:104803. https://doi.org/10.1016/j.engfailanal.2020.104803

Vuoto A, Ortega J, Lourenço PB, et al (2022) Safety assessment of the Torre de la Vela in la Alhambra, Granada, Spain: The role of on site works. Eng Struct 264:. https://doi.org/10.1016/j.engstruct.2022.114443

Wang C, Sarhosis V, Nikitas N (2018) Strengthening / Retrofitting Techniques on Unreinforced Masonry Structure / Element Subjected to Seismic Loads : A Literature Review. Open Constr Build Technol J 251–268. https://doi.org/10.2174/1874836801812010251

Wang P, Milani G (2023) Seismic vulnerability prediction of masonry aggregates : Iterative Finite element Upper Bound limit analysis approximating no tensile resistance. Eng Struct 293:

Yavartanoo F, Kang TH (2022) Retrofitting of unreinforced masonry structures and considerations for heritage-sensitive constructions. J Build Eng 49:103993. https://doi.org/10.1016/j.jobe.2022.103993

Zhang Z, Davis L, Malomo D (2024) Distinct Element macro-crack networks for expedited discontinuum seismic analysis of large-scale URM structures. J Build Eng 97:. https://doi.org/10.1016/j.jobe.2024.110962

(2023) Prezzario Regione Liguria - Year 2023 - Aggiornamento al 28/12/2022. 1–888

Appendix A